12-2017

Estimating Evapotranspiration Using the Complementary Relationship and the Budyko Framework

Homin Kim
Utah State University

ESTIMATING EVAPOTRANSPIRATION USING THE COMPLEMENTARY RELATIONSHIP AND THE BUDYKO FRAMEWORK

by

Homin Kim

A dissertation submitted in partial fulfillment
of the requirements for the degree

of

DOCTOR OF PHILOSOPHY

in

Civil and Environmental Engineering

Approved:

_____	_____
Jagath J. Kaluarachchi, Ph.D. Major Professor	Mac McKee, Ph.D. Committee Member
_____	_____
Richard C. Peralta, Ph.D. Committee Member	Ronald C. Sims, Ph.D. Committee Member
_____	_____
Robert Gillies, Ph.D. Committee Member	Mark McLellan, Ph.D. Vice President for Research and Dean of the School of Graduate Studies

UTAH STATE UNIVERSITY
Logan, Utah

2017

ABSTRACT

Estimating Evapotranspiration Using the Complementary Relationship and the Budyko Framework

by

Homin Kim, Doctor of Philosophy

Utah State University, 2017

Major Professor: Dr. Jagath J. Kaluarachchi
Department: Civil and Environmental Engineering

Evapotranspiration is the single most important mechanism of mass and energy exchange between atmosphere, biosphere, and hydrosphere. Among the common approaches to estimating evapotranspiration, the complementary relationship has been the subject of many recent studies given its simplicity and the use of meteorological data only. Recently, a modified version of the complementary relationship, Modified GG, was developed using meteorological data only and had been successfully applied at 34 diverse global sites to provide more accurate information of evapotranspiration. However, the complementary relationship including Modified GG showed weak performance under dry conditions. This dissertation addressed this limitation of the complementary relationship using the Budyko hypothesis and extended its application to drought monitoring. For this purpose, Fu equation was used as the relative evaporation parameter in the complementary relationship on the basis that the Budyko hypothesis is consistent with the

complementary relationship through the Fu equation. The proposed approach, Adjusted GG-NDVI, was applied at 75 eddy covariance sites in the United States from AmeriFlux and validated by comparing with other methods including a remote sensing method. Moreover, this study addressed the use of evapotranspiration data as a proxy for drought monitoring. This dissertation explored, for the first time, to bring the vegetation cover into the complementary relationship, and the proposed process is a simple and reliable approach to estimate evapotranspiration. The most obvious finding of this study was that evapotranspiration can be used as a complementary tool to monitor vegetation conditions and for drought monitoring.

(161 pages)

PUBLIC ABSTRACT

Estimating Evapotranspiration Using the Complementary Relationship and the Budyko Framework

Homin Kim

Land surface actual evapotranspiration (ET) is an important process in terrestrial water balance and reliable estimates of ET are necessary to improve water resources management. In this regard, there is a growing body of literature that recognizes the importance of an accurate ET model. Among them, the complementary relationship between ET and potential ET (ETP) has been the subject of many studies because it uses only meteorological data as inputs. However, there is an increasing concern that some complementary relationship models perform poorly under dry conditions. To overcome this limitation, this dissertation was designed to extend the latest complementary relationship model, Modified GG, using both meteorological data and vegetation information, NDVI, which is readily available from remote sensing data. The proposed model, Adjusted GG-NDVI, was validated by comparing to other ET models and measured ET data. With Adjusted GG-NDVI, this dissertation addressed the applicability of using ET as a proxy for drought monitoring. As a result, the drought patterns from the proposed drought index, EWDI, were consistent with commonly used USDM in the United States. More importantly, this study described drought conditions by comprehensively considering both precipitation and vegetation conditions. Taken together, these findings have significant implications for the understanding of how ET can assist in water resources management.

ACKNOWLEDGMENTS

I would like to thank my advisor, Dr. Jagath J. Kaluarachchi. I am so happy that I have him as my advisor during my graduate studies. His consistent and insightful guidance and continual support have helped me to conquer all barriers that I had during my studies. His knowledge as well as passion will continue to inspire me in my future career. I would especially like to thank my committee members, Dr. Mac McKee, Richard C. Peralta, Ronald C. Sims, and Robert Gillies for their support and assistance through- out the entire process. I also give special thanks to my colleagues for valuable discussions and friendships.

Finally, I would like to thank my family who always support me in the direction where I want to go with love and my wife who has made my life a very enjoyable time. I deeply acknowledge these people and I could not have done it without all of you.

Homin Kim

CONTENTS

Page

LIST OF TABLES

Table Page

LIST OF FIGURES

CHAPTER 1

INTRODUCTION

The fifth Assessment Report of the Intergovernmental Panel on Climate Change (IPCC) stated that the world has experienced significant droughts during the past 25 years and that climate projections indicate an increased frequency in the future. In agriculture, drought is the most critical factor affecting sustainable crop productivity and food security. Recent studies have shown the importance of remotely sensed data in improving drought and vegetation monitoring (Tadesse et al., 2014; Rojas et al., 2011). Yet, there is still an increasing demand to improve and integrate existing satellite-derived products using ground observations of climate data to address drought (Rojas et al., 2011; Vicente-Serrano et al., 2012). Recent state-of-the-art drought monitoring tools, such as the vegetation drought response index (VegDRI), Vegetation Outlook (VegOut), and Atmosphere-Land Exchange Inverse (ALEXI) were developed to address vegetation stress using remote sensing data. However, remote sensing models still need to calibrate and validate with ground based measurements because of the limitation of remote sensing data such as cloud cover. Moreover, these studies focused on the use of evapotranspiration (ET) data as a proxy for drought monitoring in a limited manner. According to U.S. Geological Survey (USGS) Famine Early Warning Systems Network (FEWSNET, 2014), the knowledge of rate and amount of ET are essential components in the monitoring of agricultural and environmental systems. Up to now, several lines of evidence suggest that the knowledge of rate and amount of ET are essential components in the monitoring of agricultural and environmental systems (Allam et al., 2016;

FEWSNET, 2014; Senay et al., 2013; Velpuri et al., 2013), and many studies have attempted to develop accurate ET model (Anayah and Kaluarachchi, 2014; Bastiaanssen et al., 2014; Liu et al., 2016). Among the recently developed models, Anayah and Kaluarachchi (2014) proposed a modified version of the complementary relationship model and it showed excellent performance compared to other published work of Han et al., (2011), Mu et al. (2011), Szilagyi and Kovacs (2010), and Thompson et al. (2011). While the model of Anayah and Kaluarachchi (2014) showed good ET estimations, the results also showed that further refinements can improve performance under dry conditions. Taking this point into account, this dissertation will focus on the complementary relationship method to develop an enhanced ET predicting method using historical precipitation data, potential evaporation, and the Normalized Difference Vegetation Index (NDVI). The proposed approach will be validated by comparing with other ET methods including a remote sensing model. Finally, we will evaluate the potential use of the proposed ET model for drought monitoring to support agricultural risk management and food security.

The goal of this dissertation is to develop a simple and improved model to estimate ET using remote sensing and meteorological data. The specific objectives are (1) to extend the modified GG model by combining the complementary relationship and the Budyko framework, (2) to validate and provide accurate estimates for both the proposed approach and the state-of-art remote sensing ET products over the United States, and (3) to address the possibility of using ET as a proxy for drought monitoring through a new and reliable drought index than using potential ET.

The dissertation is comprised of three main sections; development, validation, and

application in accordance with the three objectives mentioned earlier. The model development section is described in Chapter 2, the validation section is presented in Chapter 3, and the proposed model application is addressed in Chapter 4. Finally, Chapter 5 summarizes all the findings and brings together the final conclusions discussed in the three previous chapters.

Literature Cited

Allam, M. M., Jain-Figueroa, A., McLaughlin, D. B., and Eltahir, E. A. B. (2016). "Estimation of evaporation over the Upper Blue Nile basin by combining observations from satellites and river flow gauges." Water Resour. Res., 52.

Anayah, F. M., and Kaluarachchi, J. J. (2014). "Improving the complementary methods to estimate evapotranspiration under diverse climatic and physical conditions." Hydrology and Earth System Sciences, 18, 2049-2064.

Bastiaanssen, W. G. M., Karimi, P., Rebelo, L-M., Duan, Z., Senay, G.B., Muttuwatte, L., and Smakhtin, V. (2014). "Earth Observation-based Assessment of the Water Production and Water Consumption of Nile Basin Agro-Ecosystems." Remote Sensing, 6, 10306-10334.

FEWSNET. (2014). "Famine Early Warning Systems Network." <http://earlywarning.usgs.gov/fews> (Oct. 10, 2014).

Han, S., Hu, H., and Yang, D. (2011). "A complementary relationship evaporation model referring to the Granger model and the advection-aridity model." Hydrol. Processes, 25(13), 2094–2101.

Liu, X., Liu, C., and Brutsaert, W. (2016). "Regional evaporation estimates in the eastern

monsoon region of China: Assessment of a nonlinear formulation of the complementary principle." Water Resour. Res., 52, 9511-9521.

Mu, Q., Zhao, M., and Running, S. W. (2011). "Improvements to a MODIS global terrestrial evapotranspiration algorithm." Remote Sens. Environ., 115, 1781-1800.

Rojas, O., Vrieling, A., and Rembold, F. (2011). "Assessing drought probability for agricultural areas in Africa with coarse resolution remote sensing imagery." Remote Sens. Environ, 115, 343–352.

Senay, G. B., Bohms, S., Singh, R. K., Gowda, P. H., Velpuri, N.M., Alemu, H., and Verdin, J.P. (2013). "Operational evapotranspiration mapping using remote sensing and weather datasets: A new parameterization for the SSEB approach." Journal of the American Water Resources Association 49, 577–591.

Szilagyi, J., and Kovacs, A. (2010). "Complementary-relationship-based evapotranspiration mapping (cremap) technique for Hungary." Per. Pol. Civil Eng., 54(2), 95-100.

Tadesse, T., Demisse, G.B., Zaitchik, B., and Dinku, T. (2014). "Satellite-based hybrid drought monitoring tool for prediction of vegetation condition in Eastern Africa: a case study for Ethiopia." Water Resour. Res., 50, 2176–2190.

Thompson, S. E., Harman, C. J., Konings, A. G., Sivapalan, M., Neal, A., and Troch, P. A. (2011). "Comparative hydrology across AmeriFlux sites: The variable roles of climate, vegetation, and groundwater." Water Resour. Res., 47, W00J07.

Velpuri, N. M., Senay, G. B., Singh, R. K., Bohms, S., and Verdin, J. P. (2013). "A comprehensive evaluation of two MODIS evapotranspiration products over the conterminous United States: Using point and gridded FLUXNET and water

balance ET.” Remote Sensing of Environment, 139, 35-49.

Vivente-Serrano, S. M., Begueria, S., Lorenzo-Lacruz, J., Camarero, J. J., Lopez-Moreno, J. I., Azorin-Molina, C., Revuelto, J., Moran-Tejeda, E., and Sanchez-Lorenzo, A. (2012). “Performance of drought indices for ecological, agricultural, and hydrological applications.” Earth Interactions, 16, 10, 1-27.

CHAPTER 2

ESTIMATING EVAPOTRANSPIRATION USING THE COMPLEMENTARY RELATIONSHIP AND THE BUDYKO FRAMEWORK

Abstract

Several models have been developed to estimate evapotranspiration. Among those, the complementary relationship has been the subject of many recent studies because it relies on meteorological data only. Recently the modified Granger and Gray (GG) model showed its applicability across 34 diverse global sites. While the modified GG model showed better performances compared to the recently published studies, it can be improved for dry conditions and the relative evaporation parameter in original GG model needs to be further investigated. This parameter was empirically derived from limited data from wet environments in Canada – a possible reason for decreasing performance with dry conditions. This study proposed a refined GG model to overcome the limitation using the Budyko framework and vegetation cover to describe relative evaporation. This study used 75 Eddy Covariance sites in the US from AmeriFlux representing 36 dry and 39 wet sites. The proposed model produced better results with decreasing monthly mean root mean square error of about 30% for dry sites and 15 % for wet sites compared to the modified GG model. The proposed model in this study maintains the characteristics of the Budyko framework and the complementary relationship and produced improved evapotranspiration estimates under dry conditions.

Introduction

Estimating evapotranspiration (E_T) is an essential part of agricultural water

management and there are many classical methods available for E_T estimation based on data availability and required accuracy. The original models include the Penman (1948) and Penman-Monteith (Monteith 1965) equations that combine energy balance and aerodynamic water vapor mass transfer principles. In the recent years, the Food and Agriculture Organization (FAO) version of the Penman-Monteith equation (Allen et al. 1998) is widely used to estimate E_T. According to Morton (1994), the Penman-Monteith equation is limited for hydrologic purposes. For example, meteorological data are not measured at 2 m elevation from ground level and not at crop elevation as required by the Penman-Monteith equation (Shuttleworth 2006). Also, the FAO method is primarily used to estimate crop E_T from agricultural lands using crop coefficients which are estimated under specific environmental conditions and at specific times of the growing cycle. According to Shuttleworth and Wallace (2009), this extrapolation is questionable while information of crop coefficients and growing cycles are not readily available worldwide.

Another approach to estimate E_T directly is the complementary relationship developed by Bouchet (1963). This approach proposed the first complementary function of potential evapotranspiration (E_P) and wet environment evapotranspiration (E_W) for a wide range of available energy to estimate regional E_T. Bouchet (1963) postulated that as a wet surface dries, the decrease in evapotranspiration is matched by an equivalent increase in potential evapotranspiration. E_P is evaporation from a saturated surface while energy and atmospheric conditions do not change. E_w is the value of potential evaporation when actual evaporation is equals to the potential rate. Bouchet's idea has been widely tested in conjunction with the models of Priestley and Taylor (1972) and

Penman (1948). Examples of widely known models using the complementary relationship are the Advection-Aridity (AA) model of Brutsaert and Stricker (1979), the Complementary Relationship Areal Evapotranspiration (CRAE) model of Morton (1983), and the complementary relationship model proposed by Granger and Gray (1989) which is named as the GG model hereafter. In these three models, E_T is usually calculated by Eq. (1) developed by Bouchet (1963).

$$E_T + E_P = 2E_W \quad (1)$$

The procedure to calculate E_T, which requires only meteorological data, was proposed by Brutsaert and Stricker (1979).

In the AA model, E_P is estimated by combining information from the energy budget and water vapor transfer in the Penman (1948) equation. The partial equilibrium evapotranspiration equation of Priestley and Taylor (1972) was used to calculate E_W. In the CRAE model of Morton (1983), the Penman equation is divided into two separate terms representing the energy balance and the vapor transfer process to calculate E_P. A refinement to this approach is proposed through the definition of 'equilibrium temperature', T_P which is the temperature at which the energy budget method and the mass transfer method for a moist surface yields same E_P. In the calculation of E_W, Morton (1983) modified the Priestley and Taylor equilibrium evapotranspiration to explain the temperature dependence of both net radiation and the slope of the saturated vapor pressure curve. In the GG model of Granger and Gray (1989), they proposed a revised version of the Penman's equation for estimating E_T from different saturated and non-saturated surfaces using a dimensionless relative evaporation parameter for a given

set of atmospheric and surface conditions. Later they showed that relative evaporation, the ratio of actual to potential evapotranspiration, has a unique relationship with a parameter which they called relative drying power using 158 measurement data points from Canada. This relationship is independent of surface parameters (temperature and vapor pressure). The primary advantage of the GG model is that E_T can be directly estimated without the surface parameters or prior estimates of E_P. The original GG model has been successfully applied to a wide range of physical and surface conditions (Hobbins et al. 2001; Szilagyi & Jozsa, 2008).

Although Eq. (1) of Bouchet (1963) has been widely used in conjunction with Penman (1948) and Priestly-Taylor (1972) (Brutsaert & Stricker 1979; Morton 1983; Hobbins et al. 2001), Bouchet (1963) assumed that E_P decreases by the same amount as E_T increases. Granger (1989) argued that the symmetrical relationship of Eq. (1) lacked a theoretical background and showed the symmetrical relationship only occurs near a temperature of 6 ˚C. This earlier study showed that E_T and E_P contribute to E_W with different coefficients that depend on the psychrometric constant and the slope of the saturation vapor pressure curve. Later Crago and Crowley (2005) evaluated the Granger (1989) equation by comparing to measured latent heat fluxes and determined that the radiometric surface temperature measurements can be successfully incorporated into a complementary approach of Granger (1989). Kahler and Brutsaert (2006) incorporated a constant parameter, b, into the energy balance equation. The parameter b is dependent on the response of natural evaporation from the surrounding landscape. They showed that 'b' values around 5 may be appropriate for the complementary relationship. Venturini et

al. (2008) and Venturini et al. (2011) evaluated the approach of Granger and Gray (1989) along with the Priestly and Taylor equation. In their studies, the relative evaporation parameter in the GG model was derived from surface temperature of MODIS data and produced errors of about 15 % compared to observed E_T. In essence, these studies support the complementary relationship, but confirmed that it requires improvements to better predict E_T.

Recently, Anayah and Kaluarachchi (2014) developed a modified method using the complementary method proposed by the GG model with meteorological data from 34 global Eddy Covariance (EC) sites. These sites were distributed as follows: North America (17), Europe (11), Asia (5), and Africa (1). The results of this modified GG model showed that the average root mean square error decreased from 20 % to as much as 80 % compared to the recently published work of Suleiman and Crago (2004), Mu et al. (2007), Szilagyi and Kovacs (2010), Han et al. (2011), Mu et al. (2011), and Thompson et al. (2011). While the results of Anayah and Kaluarachchi (2014) were very good, the results also showed that further refinements can improve performance under dry conditions. A probable reason for this limitation is that the relative evaporation equation of the original GG model was empirically derived from 158 sites under wet environments in Canada. Thus, the complementary relationship in the GG model still needs improvements under dry conditions. The purpose of this study is therefore to extend the modified GG model of Anayah and Kaluarachchi (2014) to propose refinements to the relative evaporation equation in original GG model to better predict regional E_T especially under dry conditions and different land cover conditions. In

addressing this goal, this work is still committed to use minimal data such as meteorological data and other readily accessible information with no local calibration.

Other classical approaches for estimating long-term E_T assumes that evaporation is controlled by availability of both energy and water (Budyko 1974; Pike 1964). For example, the Budyko hypothesis (1974) and the corresponding Budyko curve has been broadly used for estimating annual E_T as a function of the ratio of E_P to precipitation. Usually, E_P which measures the availability of energy and precipitation is a measure of available of water. According to the Budyko hypothesis (1974), actual evapotranspiration in humid regions is controlled by potential evapotranspiration, while in arid regions, it is controlled by precipitation. However, the Budyko hypothesis (1974) makes no attempt to consider the impact of land surface characteristics such as vegetation cover. Later, other authors attempted to incorporate these characteristics to the Budyko hypothesis (1974). Examples of such widely used studies are Fu (1981) and Choudhury (1999). Choudhury (1999) developed an empirical equation by introducing water equivalent of annual net radiation and an adjustable parameter which was estimated from field observations at eight locations with different vegetation types. Fu (1981) developed differential forms of the Budyko hypothesis (1974) through a dimensional analysis and introduced a single parameter that determine the shape of the Budyko curve. This parameter can be calibrated from local data and represents the land surface conditions such as vegetation cover, soil properties, and topography (Yang et al., 2006). This also supports the Penman hypothesis (1948) that E_T is proportional to E_P. Furthermore, Yang et al. (2008) derived the corresponding equivalence of Fu (1981) and Choudhury (1999) equations. While these

expressions were not identical, their numerical values are same. Thereafter, several studies used land surface characteristics including vegetation, soil types, and topography in the Budyko hypothesis using the work of Choudhury (1999) and Fu (1981) (Zhang et al. 2001, 2004; Yang et al. 2006, 2007, 2009; Li et al. 2013).

According to Zhang et al. (2004), the Fu equation can be restated that any change in evapotranspiration is a function of potential evapotranspiration and precipitation when precipitation is the only source of water. When there is no precipitation, evapotranspiration becomes zero and the atmospheric conditions are dry allowing potential evapotranspiration to reach the maximum. As precipitation increases, evapotranspiration increases and the atmosphere becomes cooler allowing potential evapotranspiration to decrease. This statement is similar to the complementary relationship introduced by Bouchet (1963). Yang et al. (2006) examined the complementary relationship using the long-term water balance data from 108 dry regions in China, and attempted to explain the consistency between the Budyko hypothesis and Bouchet hypothesis.

Recently, Li et al. (2013) focused on the vegetation impact and examined the conditions under which the vegetation index plays a major role in controlling the parameter ϖ which represents the land surface characteristics and climate seasonality, and they proposed a simple process to estimate ϖ using remote sensing vegetation information. Using data from 26 major global river basins, the basin-specific ϖ was found to be a linear relationship with the long-term average annual vegetation cover. Vegetation cover is derived from the Normalized Difference Vegetation Index (NDVI).

As a result, the new parameterization of ω reduces the root mean square error (E_{RMS}) by approximately 40 % compared to the original Budyko framework.

As discussed earlier, the Budyko frameworks provide an opportunity to consider land surface characteristics especially the vegetation cover to improve E_T prediction. In this work, we proposed to upgrade the modified GG model of Anayah and Kaluarachchi (2014) to better predict ET under dry conditions using the Budyko framework. As mentioned before, one possible reason for poor performance of the original GG model is the use of data from wet regions of Canada thus the GG model not properly capturing the prevailing dry conditions in arid regions. This work will use the approach in line with the earlier studies of Yang et al. (2006) and Zhang et al. (2004).

Methodology and Data

Methodology

Modified GG Model

Anayah and Kaluarachchi (2014) developed their universal model using a three-step approach. First, they evaluated the original complementary methods under a variety of physical and climate conditions and developed 39 different model combinations. Second, three models variations were identified based on performance compared to observed data from a set of global sites. Third, a statistical analysis was conducted to contrast and compare the three models to identify the best. The results showed that average E_{RMS}, mean absolute bias, and R^2 across the 34 global sites were 20.6 mm/month, 10.6 mm/month and 0.64, respectively. More importantly, the performance

of this modified GG model increased partly due to the use of the Priestley and Taylor (1972) equation shown in Eq. (2) to calculate E_W instead of the Penman (1948) equation.

$$E_W = \alpha \frac{\Delta}{\gamma+\Delta}(R_n - G_{soil}) \quad (2)$$

where E_W is in mm/d, α is a coefficient equal to 1.28, R_n is net radiation (mm/d), γ is the psychrometric constant (kPa/˚C), Δ is the rate of change of saturation vapor pressure with temperature (kPa/˚C), and G_{soil} is soil heat flux density (mm/d).

Also, two parameters were considered similar to the original GG (Granger & Gray 1989); relative drying power (D) and relative evaporation (G). D and G are described in Eqs. (3) and (5), respectively.

$$D = \frac{E_a}{E_a+(R_n-G_{soil})} \quad (3)$$

where E_a is drying power of air (mm/d) given in Eq. (4).

$$E_a = 0.35(1 + 0.54U)[(e_s - e_a)] \quad (4)$$

where U is wind speed at 2 m above ground level (m/s) that needs adjustments, and conducted using the procedure described by Allen et al. (1998), e_s is saturation vapor pressure (mmHg), e_a is vapor pressure of air (mmHg).

$$G = \frac{E_T}{E_P} = \frac{1}{c_1+c_2 e^{c_3 D}} \quad (5)$$

where $c_1 = 1.0, c_2 = 0.028$, and $c_3 = 8.045$. The effect of G_{soil} is negligible compared to R_n when calculated at monthly or higher timescale (e.g. Hobbins et al. 2001).

Solving Eq. (5) for E_P and substituting in Eq. (1), the modified GG model is given in Eq. (6).

$$E_T = \frac{2G}{G+1} E_W \quad (6)$$

Therefore, the modified GG model of Anayah and Kaluarachchi (2014) can estimate E_T directly without calculating E_P.

Budyko framework

Fu (1981) proposed the differential forms of the Budyko framework through a dimensional analysis. The corresponding analytical solution of the Budyko framework is given in Eq. (7) or (8).

$$\frac{E_T}{P} = 1 + \frac{E_P}{P} - \left[1 + \left(\frac{E_P}{P}\right)^{\varpi}\right]^{1/\varpi} \quad (7)$$

$$\frac{E_T}{E_P} = 1 + \frac{P}{E_P} - \left[1 + \left(\frac{P}{E_P}\right)^{\varpi}\right]^{\frac{1}{\varpi}} \quad (8)$$

where P is precipitation (mm) and E_P is estimated using the Priestly and Taylor equation (1972). Parameter ϖ is a constant and represents the land surface conditions of the basin, especially the vegetation cover (Li et al. 2013). Li et al. (2013) showed that ϖ is linearly correlated with the long-term average annual vegetation cover and a model using NDVI can improve the estimation of E_T. In that study, vegetation cover defined by M is calculated as (Yang et al. 2009).

$$M = \frac{NDVI - NDVI_{min}}{NDVI_{max} - NDVI_{min}} \quad (9)$$

where $NDVI_{min}$ is minimum NDVI and $NDVI_{max}$ is maximum NDVI. The values of $NDVI_{min}$ and $NDVI_{max}$ are constants at 0.05 and 0.8, respectively (Yang et al. 2009). Then, an optimal ϖ value for the basin can be derived through a curve fitting procedure that minimizes the mean squared error between the measured and predicted

evaporation ratio (Li et al. 2013). The objective function used to find optimal ϖ is

$$\text{Obj}_{\omega} = min \sum_i \left\{ \frac{(E_T)_i}{P_i} - \left\{ 1 + \frac{(E_P)_i}{P_i} - \left[1 + \left(\frac{(E_P)_i}{P_i} \right)^{\omega} \right]^{1/\omega} \right\} \right\}^2 \quad (10)$$

where i is year. Li et al. (2013) proposed parameterization that is simply a linear regression between optimal ϖ and long-term average M given as

$$\varpi = a \times M + b \quad (11)$$

where a and b are constants that are found for each site.

Proposed GG model refinements

Figure 2-1 illustrates a schematic of the complementary relationship and the Budyko framework. Figure 2-1(a) shows the original complementary relationship proposed by Bouchet (1963) which translates to Fig. 2-1(b) if all variables are divided by E_P. Figure 2-1(c) is the original curve describing the Budyko hypothesis on the basis of Eq. (7) where ϖ is the curve shape factor of the Fu equation. Figure 2-1(d) shows the other form of the Fu equation as given in Eq. (8). Comparing Figs. 2-1(b) and 2-1(d), it can be concluded that the complementary relationship is consistent with the Budyko hypothesis through the Fu equation.

In the modified GG model (Anayah & Kaluarachchi 2014), the ratio of E_T to E_P is defined as relative evaporation (G) as shown in Eq. (5). Parameter G was empirically derived using limited data from wet environments in western Canada (Granger & Gray 1989). As discussed earlier, this bias towards wet region data may be the reason for relatively poor predictions with the GG model under dry conditions. In order to improve the E_T predictions of the modified GG model (Anayah & Kaluarachchi 2014) given by

Eq. (6), parameter G needs improvements. If this ratio can be improved and used appropriately in the modified GG model with the Fu equation, it would bring the Budyko framework which works well in dry conditions and maintains the complementary relationship. For this purpose, we use the theoretical framework of Fu equation developed by Li et al. (2013) on the basis of the work of Yang et al. (2006) and Zhang et al. (2004). Eq. (12) shows the Fu equation where the ratio of E_T/E_P is now defined as G_{new}.

$$G_{new} = \frac{E_T}{E_P} = 1 + \frac{P}{E_P} - \left[1 + \left(\frac{P}{E_P}\right)^{\varpi}\right]^{\frac{1}{\varpi}} \quad (12)$$

Note G_{new} in Eq. (12) is the new (updated) definition of relative evaporation, G, which includes the Budyko hypothesis and vegetation index. To estimate G_{new}, E_P is required and can be estimated using the equation from Penman (1948) given in Eq. (13).

$$E_P = \frac{\Delta}{\gamma+\Delta}(R_n - G_{soil}) + \frac{\gamma}{\gamma+\Delta}E_a \quad (13)$$

Having found G_{new} from Eq. (12) and estimating E_W from Eq. (2), we can estimate E_T of the proposed model from Eq. (14).

$$E_T = \frac{2G_{new}}{G_{new}+1}E_W \quad (14)$$

Hereafter, this proposed model will be referred as the GG-NDVI model. Essentially, GG-NDVI is a combination of the complementary relationship through the modified GG model and the Budyko hypothesis that uses NDVI to describe the vegetation cover.

Data

The complementary method requires meteorological data for estimating E_T and these include temperature, pressure or elevation, net radiation, and wind speed. As seen

from Table 2-1, the GG-NDVI model require two additional data strings, precipitation and NDVI, compared to the modified GG model proposed by Anayah and Kaluarachchi (2014). FLUXNET is a global network of micrometeorological tower sites. A flux tower uses the Eddy Covariance (EC) method to measure ecosystems-scale mass and energy fluxes. This study proposes to use data from AmeriFlux EC tower sites in the United States, a part of FLUXNET, because the U.S. sites have wide variety of climatic and physical conditions and land cover especially in dry regions. At present, there are over 110 sites where data are collected at 30-minute intervals. In some cases, data are not available at monthly intervals and for such instances mean monthly data were aggregated from 30-minute time-scale that are available from Level 2 data of AmeriFlux. This study selected 75 sites with less than 50 % missing data and the selected sites are shown in Fig. 2-2. These data were obtained from the Oak Ridge National Laboratory's AmeriFlux website (http://ameriflux.ornl.gov/, last accessed: Nov, 2015). These sites provide 10 land cover types and a wide range of climates. The land cover types developed by the International Geosphere-Biosphere Programme (IGBP) include Evergreen Needleleaf Forests (ENF), Evergreen Broadleaf Forests (EBF), Deciduous Broadleaf Forests (DBF), Mixed Forests (MF), Closed Shrublands (CSH), Open Shrublands (OSH), Woody Savannas (WSA), Grasslands (GRA), Permanent Wetlands (WET), and Croplands (CRO). Table 2-2 shows that the largest portion of land cover in the dry sites is GRA at 31 % and the wet sites have ENF at 44 %. The observed E_T to validate the proposed model was calculated from measured latent heat flux (LE) data from EC towers using the equation $E_T = LE/\lambda$ where λ is latent heat of vaporization (J/kg).

To classify the climatic conditions, the ratio of P/E_P, which is called the aridity index of the United Nations Environment Program (AIU) was used (Barrow, 1992). AIU divides climatic conditions into six classes; hyper-arid regimes (AIU < 0.05), arid ($0.05 \leq$ AIU < 0.20), semi-arid ($0.20 \leq$ AIU < 0.50), dry sub-humid ($0.50 \leq$ AIU < 0.65), wet sub-humid ($0.65 \leq$ AIU < 0.75), and humid (AIU $\geq$ 0.75). Similar to Anayah and Kaluarachchi (2014), this work simplified the climatic class definitions to two classes, simply combining hyper-arid regimes, arid, semi-arid, and dry sub-humid to define as the dry class and wet sub-humid and humid as the wet class. Using this simplified and updated definition, 36 sites fall to the dry class and 39 sites fall to the wet class. Mean AIU of the dry and wet sites are 0.41 and 0.92, respectively. The details of AIU values and additional details of 75 sites are given in Tables 2-3.

There are two methods available to compute net radiation; Morton (1983) and Allen et al. (2005). Morton (1983) proposed net radiation for soil-plant surfaces at an equilibrium temperature that is derived from the solution to the water vapor transfer and energy-balance equations under a small moist surface. On the other hand, Allen et al. (2005) predicted net radiation from observed short wave radiation, vapor pressure, and air temperature; this method is routine and generally accurate. Anayah and Kaluarachchi (2014) found that the method described by Allen et al. (2005) is better than that of Morton (1983). In this study, we used mean of daily maximum and minimum temperatures to define mean daily air temperature in order to standardize air temperature. For NDVI, we retrieved 16-Day L3 Global 250 m SIN Grid (http://daac.ornl.gov/MODIS/modis.shtml) of MODIS. Generally, NDVI values are between -1 and 1, with values > 0.5 indicating dense vegetation and < 0 indicating water

surface. The NDVI values of this study varied between 0.18 and 0.76. The mean NDVI is 0.44 for dry sites and 0.60 for wet sites and the distribution of NDVI is shown in Fig. 2-3(a). The average annual precipitation varied from 249 mm to 1312 mm with a mean of 703.1 mm for dry sites and from 494 mm to 2452 mm with a mean of 1033.3 mm for wet sites and the distribution of precipitation is shown in Fig. 2-3(b). Data were available from 1995 to 2013. The shortest data available period is 3 years at one of the sites and the longest period is 19 years.

Results and Discussion

This study used two scenarios to evaluate the performance of the proposed GG-NDVI model. In Scenario 1, the modified GG model of Anayah and Kaluarachchi (2014) is used for direct comparison and this scenario used all 75 AmeriFlux sites (36 dry and 39 wet sites). In Scenario 2, the original GG model described by Han et al. (2012) (also called the normalized complementary method) and the CRAE method of Morton (1983) are used for comparison. Scenario 2 used only 59 sites (29 dry and 30 wet sites) since only these 59 sites have incident global radiation data required by the CRAE model.

Scenario 1: Comparison with the modified GG model

Table 2-4 shows the comparison of results between the proposed GG-NDVI and the modified GG models. The GG-NDVI model reduces the mean E_{RMS} by about 32 % and 15 % for dry and wet sites, respectively. In the dry sites, the GG-NDVI model showed higher maximum E_{RMS} values compared to the modified GG model but the mean is much lower at 13.9 mm/month compared to 20.5 mm/month. On the other hand, the wet class values are comparable. Although the maximum increased with GG-NDVI for

the dry sites, the lower mean value indicates more occurrence of lower values with GG-NDVI. Figure 2-4 confirms this observation where the occurrences of less than 10 mm/month is more frequent than the modified GG model. Similar results are seen with the wet sites as well except even higher occurrences of low E_{RMS} values. The results also show that E_T estimates of both models improve with wetness similar to other previous studies discussed earlier.

The major difference between the two models is the use of vegetation to estimate E_T in the GG-NDVI model. To assess the contribution of NDVI on GG-NDVI, the variation of NDVI with E_{RMS} was studied but not shown here. The E_{RMS} distribution of the GG-NDVI model that uses NDVI is consistently below 25 mm/month with 92 % (33 sites) of the dry sites compared to 58 % (21 sites) with the modified GG model that does not account for NDVI.

Most dry sites used in this work have hot summer and warm winter seasons with low vegetation density (low NDVI). For instance, the mean annual temperature at the Freeman Ranch in Texas is 20 ˚C and there is significant precipitation during summer. The minimum, maximum, and mean E_{RMS} of the GG-NDVI model were 0.01, 48.4, and 14.0 mm/month, respectively. Figure 2-5 shows a comparison of monthly E_T of the modified GG and GG-NDVI models with observed E_T from 2005 to 2008. The mean E_{RMS} of the modified GG model is 20.6 mm/month. While the modified GG model showed a regular and periodic performance and significant deviation from observed E_T, the pattern of GG-NDVI is similar to the observed values. We observe similar results at the Goodwin Creek site in Mississippi as shown in Fig. 2-6. A reasonable conclusion

would be that GG-NDVI is improved by using the vegetation cover information in the model. On the other hand, the method that uses only climatic data seems incomplete in estimating E_T. This conclusion is supported by Bethenod et al. (2000) and Potter et al. (2005). Even under low vegetation cover (low NDVI) conditions, plant transpiration accounts for most E_T from 20 % to as much as 80 %. Moreover, hot summer and warm winter months are producing high fluctuation of plant transpiration and therefore high fluctuation of E_T (Hsiao and Henderson, 1985). In this regard, the GG-NDVI model can be expected to be more accurate than the modified GG model due to the use of NDVI to better represent plant transpiration whereas meteorological data alone may not be sufficient to estimate E_T under dry conditions.

Meanwhile, the simulated patterns of E_T from the modified GG model may be representing the principles of the complementary relationship. First, the complementary relationship assumes a homogeneous surface layer that assumes the mixing of the effects of surface environmental discontinuities. When surface discontinuities are prevalent such as in the western United States where vegetation is less flourishing than other regions, this assumption may not be valid. Second, given the heterogeneity of surface conditions, the approaches used in identifying and calculating the various input data may not be perfect in the modified GG model. For these reasons, the modified GG model probably showed a regular and periodic performance in estimated E_T and therefore the differences with observed E_T.

Among the results of GG-NDVI, it should be noted that there are two sites with relatively large E_{RMS} (higher than 40 mm/month). One is Brookings in South Dakota and

the other is Florida Shark River in Florida. The IGBP land cover class of Brookings site is Grassland which is representative of north central United States. The mean annual precipitation from 2005 to 2009 is 586 mm at this site. The mean NDVI of Brookings is 0.41 and this site has a large seasonal vegetation cover as shown in Fig. 2-7. Although not shown here, the Florida Shark River site has a mean annual precipitation of 1259 mm from 2007 to 2010 and the annual rainfall is high during the summer season. This site has a high dense vegetation cover with NDVI of 0.75.

A possible reason for high E_{RMS} could be that NDVI is not the best index to represent the vegetation cover in this site given the large seasonal variation and dense vegetation cover. According to Pettorelli et al. (2005), the Soil-Adjusted Vegetation Index (SAVI) is recommended instead of NDVI for areas with Leaf Area Index (LAI) less than 3. It should be noted that LAI of Brookings and Florida sites are 2.5 and 2.9, respectively. However, a limitation of SAVI is it requires soil brightness correction with local calibration (Huete et al., 1988). Mu et al. (2007) modified their algorithm to include vapor pressure deficit, minimum air temperature, and LAI, and replaced NDVI with Enhanced Vegetation Index (EVI) to represent dense vegetation conditions. Prior studies have also demonstrated that NDVI is insufficient to account for transpiration under a dense vegetation cover conditions (Pettorelli et al. 2005; Yuan et al. 2010; Mu et al. 2011). For these reasons, the modified GG model showed better performance than GG-NDVI at both sites; E_{RMS} of the modified GG for the Brookings site is 33 mm/month compared to 44 mm/month with GG-NDVI and 15 mm/month for the Florida site compared to 56 mm/month with GG-NDVI.

These results suggest that models using the complementary relationship may not

predict E_T accurately as the vegetation cover becomes dense. Beyond a given level of vegetation cover density and seasonality, NDVI is not capturing plant transpiration correctly as seen with the Florida Shark River site. In essence, these results suggest that a different vegetation index such as EVI may be needed to better predict E_T.

Scenario 2: Comparison with other complementary methods

The CRAE method is considered to be simple, practical and a reliable method to estimate monthly E_T (Hobbins et al. 2001). Han et al. (2012) developed the normalized complementary method which is based on the CRAE method. This study found that the method performed better than the AA model in predicting E_T under dry and wet conditions. However, the normalized complementary method was tested using only four sites with different land covers. Therefore, this study provides the opportunity to test both models, CRAE and GG models, compared to the proposed GG-NDVI model. This comparison used only 59 sites from the 75 sites due to the reason described earlier.

The results of the comparison are given in Table 2-4. Again, all models showed high maximum E_{RMS} values in dry sites in the order of more than 40 mm/month. However, the GG-NDVI model showed the lowest mean E_{RMS} across all models at 14.7 mm/month for the dry and 11.6 mm/month for the wet sites. The modified GG models was the third best for mean values for the dry sites. The GG-NDVI model performed much better in the wet category too. The GG-NDVI model produced the lowest mean E_{RMS} for the dry sites and lowest mean and maximum E_{RMS} for the wet sites. The results in general indicate that GG-NDVI can perform well in the dry regions and even better in the wet sites. These results also confirm the observation of Xu and Singh (2005) that

showed the estimation capability of E_T reduces with increased aridity.

The CRAE model assumes that the vapor transfer coefficient is independent of wind speed and this may lead to errors in calculating E_T. The complementary relationship driven models do not directly use soil moisture information and hence may overestimate E_T as aridity increases (Xu & Singh 2005). This reason may cause decreased predictive power of these methods using the complementary method. To evaluate this concern, this study used the 59 sites and simulated E_T using the CRAE method, modified GG model of Anayah and Kaluarachchi (2014), original GG model, and the proposed GG-NDVI model. Figure 2-8 presents a comparison of the E_{RMS} distribution of these four models and the corresponding boxplots are shown in Fig 2-9. The results indicate better performance of the GG-NDVI model compared to the other models. For example, most values of E_{RMS} of the GG-NDVI model are at less than 20 mm/month interval. The number of less than 20 mm/month contributed 72 % of the 29 dry sites in the GG-NDVI model in comparison with 48 % with GG, 55 % with CRAE, and 45% with the modified GG. Figure 2-9 shows that the GG-NDVI model has the lowest mean error across all four methods especially in the dry sites while maintaining a low range of E_{RMS} values.

GG-NDVI underestimates E_T in most dry sites during the rainy months. For example, the Audubon Research Ranch site in Arizona is considered dry with an annual precipitation of about 438 mm. About 70 % of annual precipitation is present in the rainy months from July to September. In this period, the GG-NDVI model underestimated E_T as shown in Fig. 2-10. A possible explanation was mentioned by Budyko (1974) and Gerrits et al. (2009). They found that locations where monthly E_P and precipitation are

out of phase, for example in a dry site, E_T is generally underestimated. Similarly, E_T decreases with increasing E_P on the basis of the complementary relationship and E_P is overestimated in regions of decreasing moisture availability. According to Hobbins et al. (2001), a negative relationship between wind speed and E_P and the mean monthly values of wind speed are the lowest in the summer months. Hence, higher E_P estimates and correspondingly lower E_T estimates should be expected for these summer months with higher precipitation.

Although not shown here, we plotted monthly E_{RMS} and precipitation to evaluate the relationship between model accuracy and wetness. The results showed a weak relationship for dry sites. Figure 2-11(a) shows the relationship between the correlation coefficient between precipitation and E_{RMS} versus mean annual precipitation. Results indicate that GG-NDVI produce errors that increase in variability with increasing precipitation and this trend decreases with increasing precipitation based on the negative slope of least fit (dashed-line in Fig. 2-11(a)). Accordingly, the R-square for this relationship from GG-NDVI across all 75 sites is 0.322. While this value is not high, it is still better than the results obtained from the CRAE and AA models by Hobbins et al. (2001) which were 0.148 and 0.314, respectively.

Figure 2-11(b) shows the relationship between the correlation coefficient between AIU and E_T, and AIU. The correlation coefficients for the wet sites are mostly negative and ranged from -0.68 to -0.11. On the contrary, many dry sites have positive correlation coefficients. This implies that increasing AIU decreased E_T for most wet sites but increased for most dry sites. These trends are the characteristics of the complementary

relationship and have been observed by Roderick et al. (2009) and Han et al. (2014).

For a clear relationship between vegetation cover and E_T, Figure 2-12 displays the estimated E_T with NDVI for all 75 sites. In a linear regression analysis between both, NDVI explains 51 % of the variance in the estimated E_T and similar observations have been made by Hsiao and Henderson (1985), Bethenod et al. (2000), and Hsiao and Xu (2005).

Comparison with other published studies

Table 2-5 shows a comparison between the results of the proposed GG-NDVI model and the results from recently published studies. The mean E_{RMS} of GG-NDVI across the 75 sites produced the lowest E_{RMS} of 12.3 mm/month compared to 25.6 mm/month from a remote sensing method and 20.6 mm/month from the modified GG. It should be noted both studies by Han et al. (2011, 2012) have only four sites. Although these studies evaluated other methods and applied at different study sites, Mu et al. (2011) used the same data from AmeriFlux similar to this study and Li et al. (2013) used the Fu equation across 26 global river basins. A comparison of GG, Fu equation, CRAE, and remote sensing methods with the GG-NDVI model shows that the proposed GG-NDVI is an enhancement to the modified GG model providing improved predictions of E_T especially under dry conditions.

We plotted the GG-NDVI estimates of E_T against observed E_T and the same with the modified GG estimates for dry sites. The results are shown in Fig. 2-13. In a linear regression analysis, the GG-NDVI model has more strong agreement ($R^2 = 0.60$) with observed E_T than modified GG model ($R^2 = 0.46$). The GG-NDVI is therefore shown to

be a reasonably good predictor of E_T and the R^2 of 60 % is much better than the recently published study of Allam et al. (2016) which is about 37 %. In essence, the results show that GG-NDVI can improve performance under dry conditions.

Summary and Conclusions

Models using the complementary method to estimate E_T are simple, practical and provide valuable estimates of regional E_T using point meteorological data only. The methods do not require data such as soil moisture, stomatal resistance properties of vegetation, or any other aridity measures. After the original work of Bouchet (1963), the complementary relationship has been the subject of many studies. Among the recent methods, Anayah and Kaluarachchi (2014) developed the modified GG model that is an enhanced version of the original GG method. It can be universally applied under a variety of climatic conditions without local calibration. While that study showed excellent results compared to the recently published work, the accuracy could be improved under dry conditions.

The Budyko framework has been successfully used to predict the long-term annual water balance as a function of E_P and precipitation. According to Yang et al. (2006), the Budyko hypothesis through the Fu equation is consistent with the Bouchet hypothesis which is based on the complementary relationship. Also, the Fu equation works well in dry conditions and it can be improved by using the vegetation cover represented by NDVI.

Given the limitation of not accurately predicting E_T under dry conditions, the goal of this work is to extend the modified GG model (Anayah & Kaluarachchi, 2014) to

combine the complementary relationship and the Budyko approach for improved estimation of E_T. The expectation is that this enhanced version of the GG model to produce better performance especially under dry conditions.

For the purpose of model development and application, 75 sites from the AmeriFlux database covering the United States were selected. These sites were divided based on an aridity index from UNEP (Barrow 1992) where 39 sites fall into the dry class and the remaining 36 to the wet class. The GG-NDVI model shows better performance with both dry and wet sites compared to other methods. In general, the GG-NDVI model reduces mean E_{RMS} by about 24 % compared to the modified GG model while increasing wetness leads to increasing accuracy with the GG-NDVI model. Lastly, E_T is directly proportional to the aridity index of dry sites. On the other hand, increasing of aridity index leads to decreasing E_T in wet sites. These trends were seen in recent studies from Roderick et al. (2009) and Han et al. (2014). The GG-NDVI model is more correlated with observed E_T than the modified GG model at values better than the work of Allam et al. (2016). Although this study applied the Budyko framework to the modified GG model, the GG-NDVI model shows similar results with other complementary relationship studies as well. We may therefore conclude that the GG-NDVI model maintains the characteristics of both the complementary relationship and Budyko hypothesis. We also observed that E_T estimates of GG-NDVI have a good correlation coefficient with NDVI confirming conclusions from several previous studies (Hsiao & Henderson 1985; Bethenod et al. 2000; Hsiao & Xu 2005). However, when the vegetation cover is very dense or has a seasonal fluctuation, the proposed GG-NDVI model did not perform well.

As a result, NDVI seems insufficient to represent plant transpiration, which suggests that other vegetation indices might be more suitable.

It is also noted that the GG-NDVI model requires NDVI and more computation than the modified GG model proposed by Anayah and Kaluarachchi (2014). However, NDVI data are readily available from satellite data from MODIS or similar outlets. On a positive note, both GG-NDVI and modified GG require no local calibration. Reference E_T of FAO (Allen et al. 2005) is considered to be the best method and is widely used globally. Unfortunately, this method requires crop coefficients that vary depending on the growing season and crop type for different regions or countries. Lastly, this study will be the first to incorporate the vegetation cover to the complementary relationship through the Budyko framework to improve E_T predictions especially under dry conditions. Consequently, the GG-NDVI model can be used as a powerful tool to estimate E_T with meteorological and remote sensing data at monthly time scale without local calibration.

Literature Cited

Allam, M. M., Jain-Figueroa, A., McLaughlin, D. B., and Eltahir, E. A. B. (2016). "Estimation of evaporation over the Upper Blue Nile basin by combining observations from satellites and river flow gauges." Water Resour. Res., 52.

Allen, R. G., Pereira, L. S., Raes D., and Smith, M. (1998). "Crop evapotranspiration: Guidelines for computing crop water requirements." FAO Irrig. and Drain. Paper No. 56. Food and Agric. Orgn. of the United Nations, Rome.

Allen, R. G., Walter, I. A., Elliot, R., Howell, T., Itenfisu, D., and Jensen, M. (2005). *The ASCE Standardized Reference Evapotranspiration Equation*, American Society of

Civil Engineers Environmental and Water Resource Institute (ASCE-EWRI), American Society of Civil Engineers, Virginia.

Anayah, F. M., and Kaluarachchi, J. J. (2014). "Improving the complementary methods to estimate evapotranspiration under diverse climatic and physical conditions." Hydrology and Earth System Sciences, 18, 2049-2064.

Barrow, C. J. (1992). *World atlas of desertification (United Nations Environment Programme)*, edited by N. Middleton and D. S. G. Thomas. Edward Arnold, London.

Bethenod, O., Katerji, N., Goujet, R., Bertolini, J. M., and Rana, G. (2000). "Determination and validation of corn crop transpiration by sap flow measurement under field conditions." Theoretical and Applied Climatology, 67, 153-160.

Bouchet, R. J. (1963). "Evapotranspiration reelle et potentielle, signification climatique (Actual and Potential Evapotranspiration Climate Service)." Int. Assoc. Sci. Hydrol., 62: 134-142, France.

Brutsaert, W., and Stricker, H. (1979). "An advection-aridity approach to estimate actual regional evapotranspiration." Water Resour. Res., 15(2), 443-450.

Budyko, M. I. (1974). *Climate and Life,* Xvii, Academic Press, New York.

Choudhury, B. J. (1999). "Evaluation of an empirical equation for annual evaporation using field observations and results from a biophysical model". J. Hydrol., 216, 99-110.

Crago, R., and Crowley, R. (2005). "Complementary relationship for near-instantaneous evaporation". Journal of Hydrology, 300, 199-211.

Fu, B. P. (1981). "On the calculation of the evaporation from land surface (in Chinese). SCI." Atmos. Sin, 5(1), 23-31.

Gerrits, A. M. J., Savenije, H. H. G., Veling, E. J. M., and Pfister L. (2009). "Analytical derivation of the Budyko curve based on rainfall characteristics and a simple evaporation model." Water Resources Research, 45, W04403.

Granger, R. J. (1989). "A complementary relationship approach for evaporation from nonsaturated surfaces." Journal of Hydrology, 111, 31-38.

Granger, R. J., and Gray, D. M. (1989). "Evaporation from natural non-saturated surface." J. Hydrol., 111, 21-29.

Han, S., Hu, H., and Yang, D. (2011). "A complementary relationship evaporation model referring to the Granger model and the advection-aridity model." Hydrol. Processes, 25(13), 2094–2101.

Han, S., Hu, H., and Tian, F. (2012). "A nonlinear function approach for the normalized complementary relationship evaporation model." Hydrol. Processes, 26(26), 3973–3981.

Han, S., Tian, F., and Hu, H. (2014). "Positive or negative correlation between actual and potential evaporation? Evaluating using a nonlinear complementary relationship model." Water Resour. Res., 50, 1322-1336.

Hobbins, M. T., Ramirez, J. A., Brown, T. C., and Classens L. H. J. M. (2001). "The complementary relationship in estimation of regional evapotranspiration: The complementary relationship areal evapotranspiration and advection-aridity models." Water Resour. Res., 37(5), 1367-1387.

Hsiao, T. C., and Henderson, D. W. (1985). *Improvement of crop coefficients for*

evapotranspiration, Final Report. California Irrigation Management Information System project, Vol. 1 Land, Air & Water Resources Papers 10013-A, University of California Davis, III3-III35.

Hsiao, T. C., and Xu, L. (2005). "Evapotranspiration and relative contribution by the soil and the plant." California water plan update 2005, UC Davis.

Huete, A. R. (1988). "A soil-adjusted vegetation index (SAVI)." Remote Sens. Environ., 25, 295-309.

Kahler, D. M., and Brutsaert, W. (2006). "Complementary relationship between daily evaporation in the environment and pan evaporation." Water Resources Research, 42, W05413.

Li, D., Pan, M., Cong, Z., Zhang, L., and Wood, E. (2013). "Vegetation control on water and energy balance within the Budyko framework." Water Resour. Res., 49, 969-976.

Morton, F. I. (1983). "Operational estimates of areal evapotranspiration and their significance to the science and practice of hydrology." J. Hydrol., 66, 1-76.

Morton, F. I. (1994). "Evaporation research - a critical review and its lessons for the environmental sciences." Critical Reviews in Environmental Science and Technology, 24(3), 237-280.

Mu, Q., Zhao, M., and Running, S. W. (2007). "Development of a global evapotranspiration algorithm based on MODIS and global meteorological data." Remote Sens. Environ., 111(4), 519-536.

Mu, Q., Zhao, M., and Running, S. W. (2011). "Improvements to a MODIS global terrestrial evapotranspiration algorithm." Remote Sens. Environ., 115, 1781-1800.

Penman, H. L. (1948). "Natural evaporation from open water, bare and grass." Proceedings of the Royal Society A: Mathematical, Physical and Engineering Sciences, 193(1032), 120-145.

Pettorelli, N., Vik, J. O., Mysterud, A., Gaillard, J. M., Tucker, C. J., and Stenseth, N. C. (2005). "Using the satellite-derived NDVI to assess ecological responses to environmental change." TRENDS in Ecology and Evolution, 20(9), 503-510.

Pike, J. G. (1964). "The estimation of annual runoff from meteorological data in a tropical climate." J. Hydrol., 2, 116-123.

Potter, N. J., Zhang, L., Milly, P. C. D., McMahon, T. A., and Jakeman A. J. (2005). "Effects of rainfall seasonality and soil moisture capacity on mean annual water balance for Australian catchments." Water Resour. Res., 41, W06007.

Priestley, C. H. B., and Taylor, R. J. (1972). "On the assessment of surface heat fluxes and evaporation using large-scale parameters." Monthly Wather Rev., 100, 81-92.

Roderick, M. L., Hobbins, M. T., and Farquhar, G. D. (2009). "Pan evaporation trends and the terrestrial water balance. II: Energy balance and interpretation." Geogr. Compass, 3(2), 761–780.

Rojas, O., Vrieling, A., and Rembold, F. (2011). "Assessing drought probability for agricultural areas in Africa with coarse resolution remote sensing imagery." Remote Sens. Environ, 115, 343–352.

Shuttleworth, W. J. (2006). "Towards one-step estimation of crop water requirements. Trans." ASABE, 49(4), 925-935.

Shuttleworth, W. J., and Wallace, J. S. (2009). "Calculating the water requirements of irrigated crops in Australia using the Matt-Shuttleworth approach." Trans.

ASABE, 52(6), 1895-1906.

Suleiman, A., and Crago, R. (2004). "Hourly and daytime ET from grassland using radiometric surface temperatures." Agron. J., 96, 384-390.

Szilagyi, J., and Jozsa, J. (2008). "New findings about the complementary relationship based evaporation estimation methods." J. Hydrol., 354, 171-186.

Szilagyi, J., and Kovacs, A. (2010). "Complementary-relationship-based evapotranspiration mapping (cremap) technique for Hungary." Per. Pol. Civil Eng., 54(2), 95-100.

Thompson, S. E., Harman, C. J., Konings, A. G., Sivapalan, M., Neal, A., and Troch, P. A. (2011). "Comparative hydrology across AmeriFlux sites: The variable roles of climate, vegetation, and groundwater." Water Resour. Res., 47, W00J07.

Venturini, V., Islam, S., and Rodríguez, L. (2008). "Estimation of evaporative fraction and evapotranspiration from MODIS products using a complementary based model." Remote Sensing of Environment, 112, 132-141, ISSN 0034-4257.

Venturini, V., Rodriguez, L., and Bisht, G. (2011). "A comparison among different modified Priestley and Taylor´s equation to calculate actual evapotranspiration." International Journal of Remote Sensing, 32(5), 1319-1338.

Xu, C. Y., and Singh, V. P. (2005). "Evaluation of three complementary relationship evapotranspiration models by water balance approach to estimate actual regional evapotranspiration in different climate regions." Journal of Hydrology, 308, 105-121, ISSN 0022-1694.

Yang, D., Sun, F., Liu, Z., Cong, Z., and Lei, Z. (2006). "Interpreting the complementary relationship in non-humid environments based on the Budyko and Penman

hypotheses." Geophysical Research Letters, 33, L18402.

Yang, D., Sun, F., Liu, Z., Cong, Z., Ni, G., and Lei, Z. (2007). "Analysing spatial and temporal variability of annual water energy balance in nonhumid regions of China using the Budyko hypothesis." Water Resour. Res., 43, W04426.

Yang, H. B., Yang, D. W., Lei, Z. D., and Sun, F. B. (2008). "New analytical derivation of the mean annual water-energy balance equation." Water Resour. Res., 44(3), W03410.

Yang, D., Shao, W., Yeh, P. J. F., Yang, H., Kanae, S., and Oki, T. (2009). "Impact of vegetation coverage on regional water balance in the nonhumid regions of China." Water Resour. Res., 45, W00A14.

Yuan, W. P., Liu, S. G., Yu, G. R., Bonnefond, J. M., Chen, J. Q., Davis, K., Desai, A. R., Goldstein, A. H., Gianelle, D., Rossi, F., Suyker, A. E., and Verma, S. B. (2010). "Global estimates of evapotranspiration and gross primary production based on MODIS and global meteorology data." Remote Sensing of Environment, 114(7), 1416-1431.

Zhang, L., Dawes, W. R., and Walker, G. R. (2001). "Response of mean annual evapotranspiration to vegetation changes at catchment scale." Water Resour. Res., 37(3), 701–708.

Zhang, L., Hickel, K., Dawes, W. R., Chiew, F. H. S., Western, A. W., and Briggs P. R. (2004). "A rational function approach for estimating mean annual evapotranspiration." Water Resour. Res., 40, 02502.

Table 2-1. Required meteorological data for different E_T estimation methods including the GG-NDVI model in this study.

	CRAE	Modified GG[1]	GG-NDVI[2]	ASCE[3]
Temperature (min, max)	●	●	●	●
Pressure (or elevation)	●	●	●	●
Net radiation	●	●	●	●
Wind speed		●	●	●
Precipitation			●	
NDVI			●	
C_n, C_d[4]				●

[1] From Anayah & Kaluarachchi (2014)
[2] Proposed in this work
[3] From Allen et al. (2005)
[4] C_n and C_d are constants that change with reference crop and time step

Table 2-2. Land cover class distribution of the 75 EC sites from the AmeriFlux database used in this study with IGBP (International Geosphere-Biosphere Program).

IGBP Land Cover Class	Dry (36 sites)	Wet (39 sites)
Evergreen Needleleaf Forests (ENF)	11% (4 sites)	44% (17 sites)
Evergreen Broadleaf Forests (EBF)	3% (1 site)	-
Deciduous Broadleaf Forests (DBF)	-	28% (11 sites)
Mixed Forests (MF)	8% (3 sites)	3% (1 site)
Closed Shrublands (CSH)	14% (5 sites)	5% (2 sites)
Open Shrublands (OSH)	11% (4 sites)	-
Woody Savannas (WSA)	6% (2 sites)	3% (1 site)
Grasslands (GRA)	31% (11 sites)	10% (4 sites)
Permanent wetlands (WET)	3% (1 site)	-
Croplands (CRO)	14% (5 sites)	8% (3 sites)

Table 2-3. Details of the 75 AmeriFlux EC sites selected for this study; P is mean annual precipitation, T is mean annual temperature, AIU is aridity index of UNEP, and EL is elevation.

#	Site ID	T (°C)	P (mm)	AIU	EL. (m)	#	Site ID	T (°C)	P (mm)	AIU	EL. (m)
Dry											
1	US-Seg	13.4	250	0.15	1622	19	US-Ne3	10.1	784	0.45	363
2	US-Ses	17.7	250	0.16	1593	20	US-Kon	12.8	867	0.46	330
3	US-Ctn	9.7	278	0.16	744	21	US-Ne2	10.1	789	0.46	362
4	US-Wjs	12.1	249	0.16	1926	22	US-Ivo	-8.3	304	0.47	568
5	US-Whs	17.1	355	0.20	1372	23	US-Wlr	13.5	881	0.49	408
6	US-FPe	5.5	335	0.22	364	24	US-PFa	4.3	823	0.49	470
7	US-SRM	17.9	380	0.22	1120	25	US-Blk	6.2	574	0.50	1718
8	US-Wkg	15.6	407	0.24	1531	26	US-Syv	3.8	826	0.50	540
9	US-Mpj	10.4	330	0.25	2138	27	US-FR2	19.5	864	0.51	272
10	US-Aud	14.9	438	0.26	1469	28	US-KUT	8.0	701	0.52	301
11	US-SP1	20.1	1310	0.26	50	29	US-FR3	19.6	869	0.52	232
12	US-SO4	14.7	484	0.34	1429	30	US-Skr	23.8	1259	0.53	0
13	US-SO3	13.3	576	0.37	1429	31	US-KFS	12.0	1014	0.58	310
14	US-SO2	13.6	553	0.39	1394	32	US-Ro1	6.9	806	0.60	260
15	US-Bkg	6.0	586	0.41	510	33	US-Bo1	11.0	991	0.61	219
16	US-LWW	16.1	805	0.43	365	34	US-Me3	7.1	719	0.61	1005
17	US-GMF	6.1	1259	0.44	380	35	US-KS2	21.7	1294	0.64	3
18	US-Ne1	10.1	790	0.45	361	36	US-SP3	20.3	1312	0.64	50
Wet											
1	US-IB1	9.0	929	0.65	227	21	US-Ced	11.0	1138	0.83	58
2	US-Ton	15.8	559	0.65	177	22	US-LPH	7.0	1071	0.87	378
3	US-Var	15.8	559	0.65	129	23	US-NC2	16.0	1294	0.89	12
4	US-Moz	12.0	986	0.65	220	24	US-Me4	8.0	1039	0.9	922
5	US-Oho	9.0	843	0.66	230	25	US-Me5	6.0	591	0.91	1188
6	US-IB2	9.0	930	0.66	227	26	US-Vcm	6.0	646	0.91	3003
7	US-UMB	6.0	803	0.68	234	27	US-Ho2	5.0	1064	0.93	91
8	US-Vcp	7.0	693	0.68	2542	28	US-Ho1	5.0	1070	0.94	60
9	US-Bo2	11.0	991	0.69	219	29	US-Goo	16.0	1426	0.94	87
10	US-Los	4.0	828	0.69	480	30	US-Ho3	5.0	1072	0.94	61
11	US-WCr	4.0	787	0.71	520	31	US-Ha1	7.0	1071	0.97	340
12	US-Me6	7.6	494	0.71	998	32	US-ChR	14.0	1359	1.00	286
13	US-Me2	6.3	523	0.71	1253	33	US-WBW	14.0	1372	1.09	283
14	US-Pon	14.9	866	0.74	310	34	US-Blo	11.0	1226	1.06	1315
15	US-MMS	11.0	1032	0.75	275	35	US-Bar	6.0	1246	1.14	272
16	US-NC1	16.0	1282	0.81	5	36	US-CaV	8.0	1317	1.15	994
17	US-Dix	11.0	1127	0.81	48	37	US-MRf	10.0	1820	1.75	263
18	US-SP2	20.0	1314	0.81	43	38	US-GLE	1.0	525	2.08	3190
19	US-Slt	11.0	1152	0.82	30	39	US-Wrc	9.0	2452	2.31	371
20	US-NR1	2.0	800	0.82	3050						

Table 2-4. Comparison of performance using E_{RMS} (mm/month) of GG-NDVI compared to other models described in Scenarios 1 and 2.

Method	Min	Mean	Max	Min	Mean	Max
		Dry sites			Wet sites	
Scenario 1: All 75 sites (36 dry and 39 wet sites)						
Modified GG	0.3	20.5	42.7	0.6	12.5	36.0
GG-NDVI	0.4	13.9	56.6	0.3	10.7	31.5
Scenario 2: 59 sites only (29 dry and 30 wet sites)						
Modified GG	1.7	21.4	42.7	0.6	12.9	36.0
GG-NDVI	0.4	14.7	56.6	0.3	11.6	28.5
CRAE	0.5	18.9	53.9	0.8	22.3	62.3
GG	0.1	32.3	75.1	1.1	19.6	60.1

Table 2-5. Comparison of performance using E_{RMS} (mm/month) between GG-NDVI and recently published results.

Study	# of sites	Method	E_{RMS} [mm/month]			R^2		
			Min	Max	Mean	Min	Max	Mean
This study	75	GG-NDVI	0.3	56.6	12.3	0.01	0.94	0.60
This study	75	Modified GG[1]	0.3	42.7	16.4	0.01	0.94	0.64
Mu et al. (2011)	46	MODIS[2]	9.4	52.0	25.6	0.02	0.93	0.65
Anayah & Kaluarachchi (2014)	34	Modified GG	10.3	59.9	20.6	0.01	0.94	0.64
Anayah & Kaluarachchi (2014)	34	CRAE	7.4	50.0	18.3	0.02	0.94	0.67
Han et al. (2011)	4	GG	3.7	16.0	10.7	0.82	0.98	0.92
Han et al. (2012)	4	GG	11.8	18.3	14.8			
Li et al. (2013)	26	Budyko	1.8	18.8	-			

[1] Anayah & Kaluarachchi (2014)
[2] Remote Sensing method

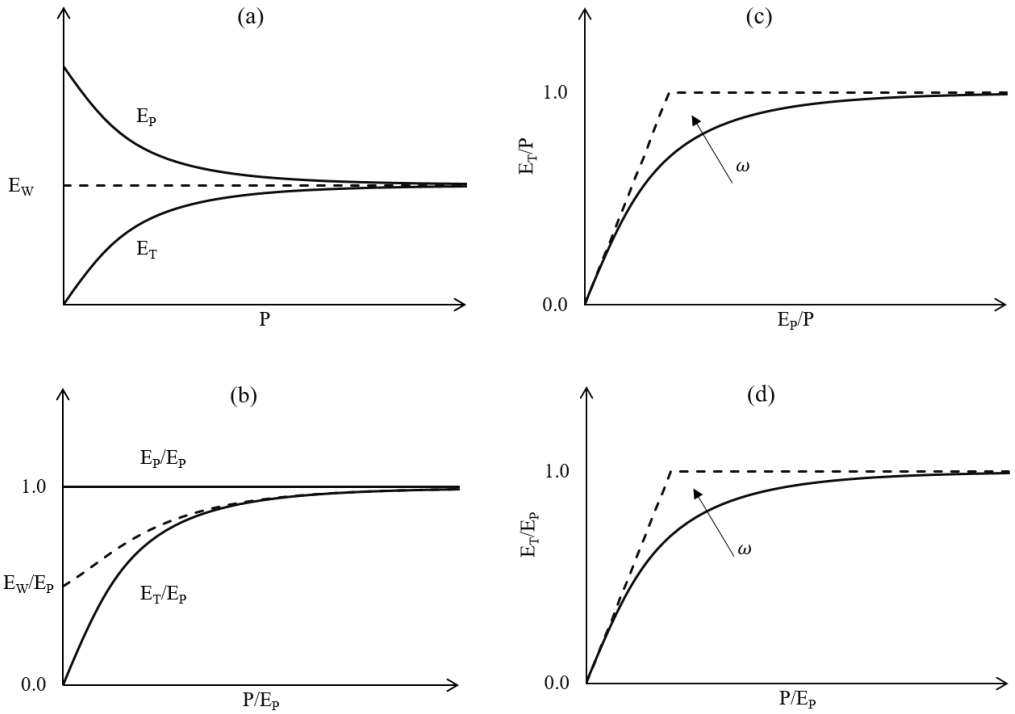

Figure 2-1. A schematic of the complementary relationship and the Fu equation; (a) Original complementary relationship of Bouchet (1963), (b) Updated complementary relationship with division by E_P, (c) Budyko hypothesis on the basis of Eq. (7), and (d) Budyko hypothesis on the basis of Eq. (8).

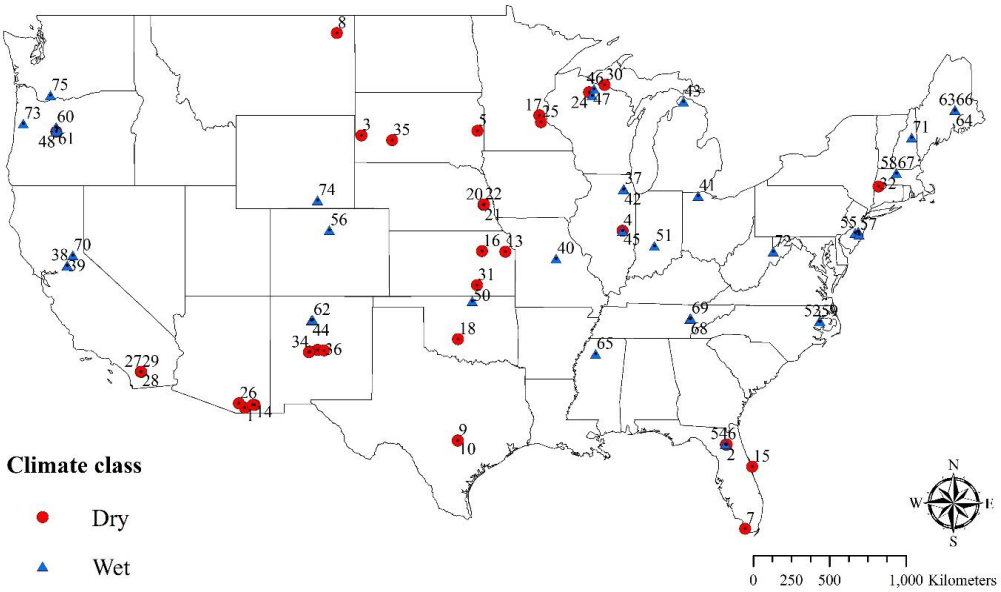

Figure 2-2. Locations of 75 AmeriFlux EC towers used in this study.

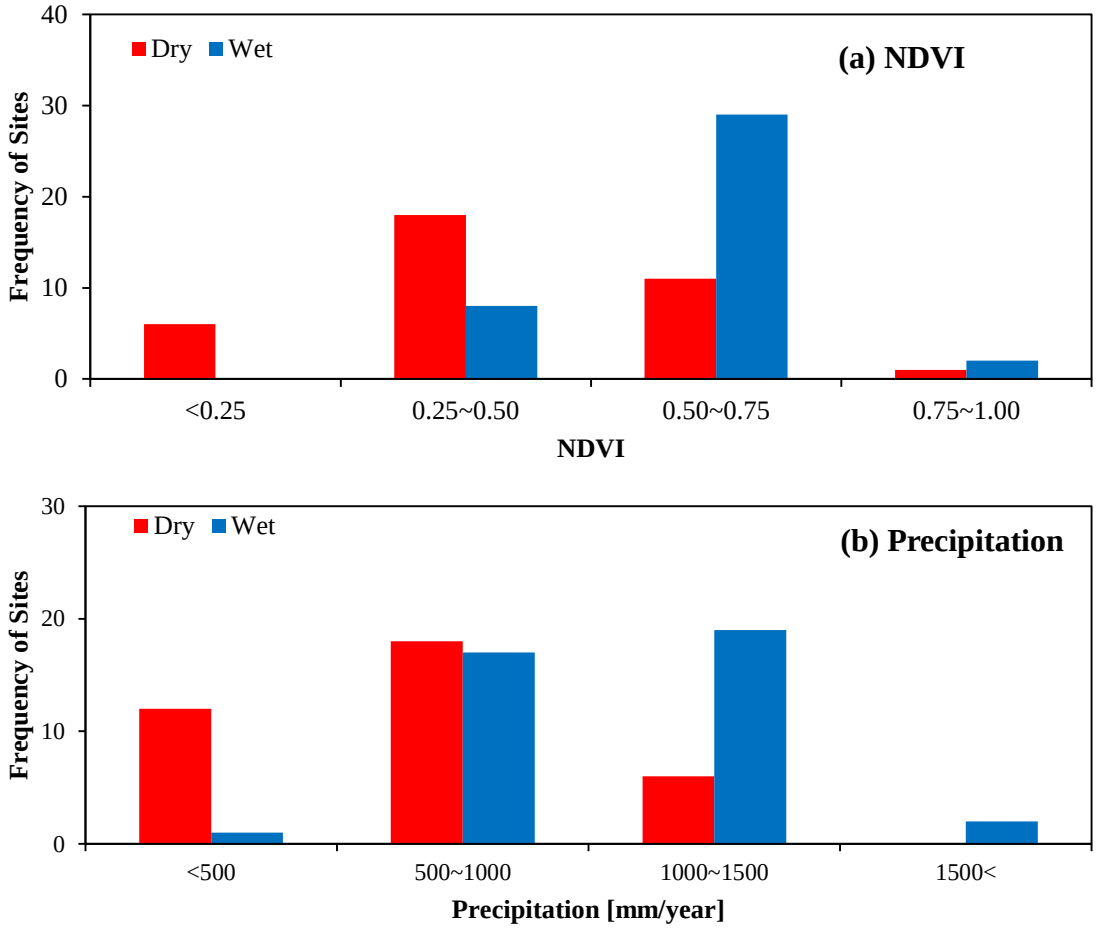

Figure 2-3. Distribution of (a) NDVI and (b) precipitation for dry and wet sites.

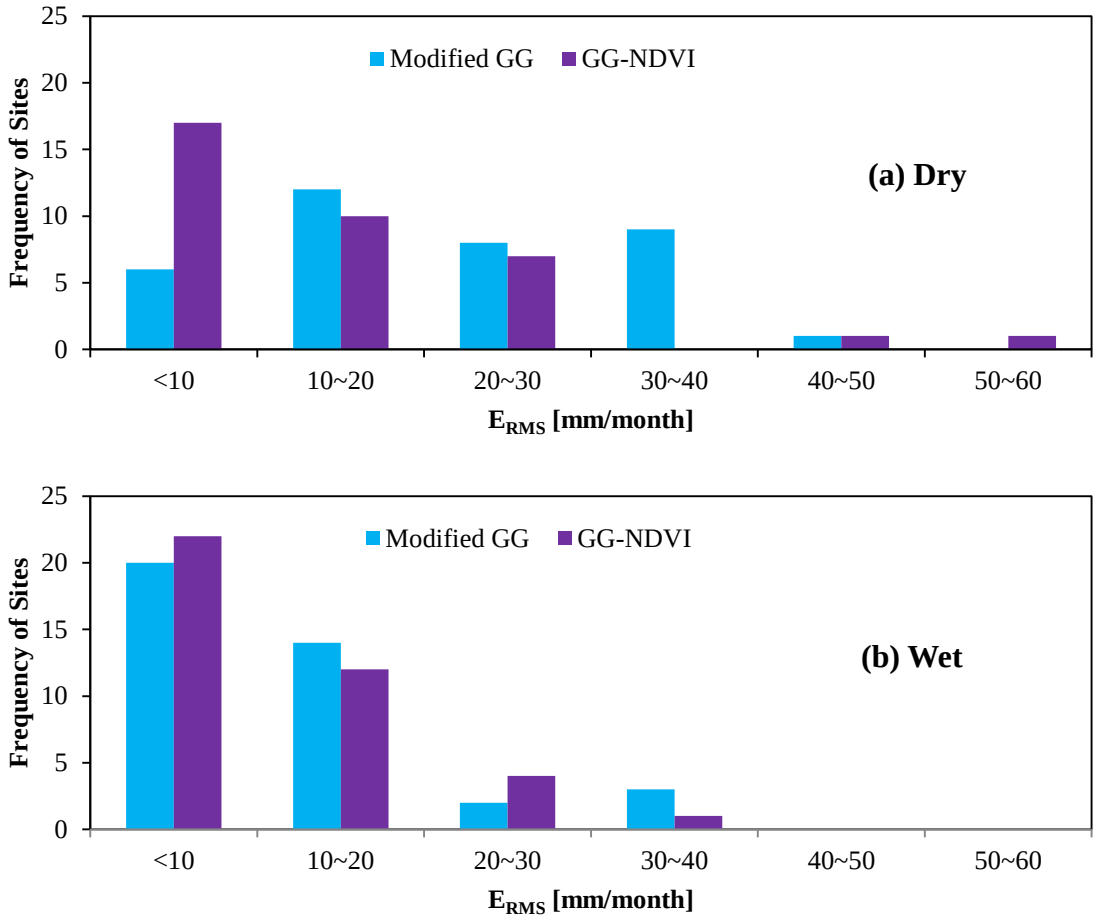

Figure 2-4. Histogram of E_{RMS} of GG-NDVI and the modified GG models for (a) dry and (b) wet sites.

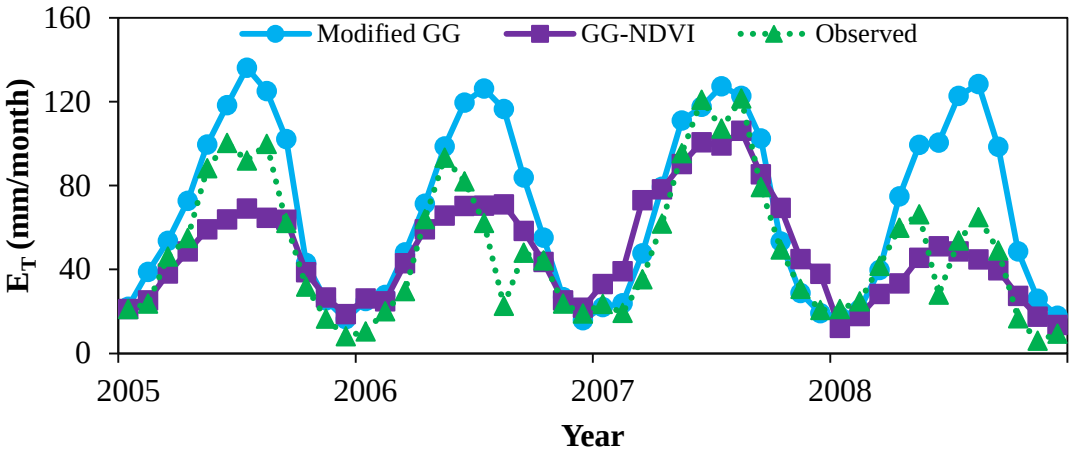

Figure 2-5. Comparison of monthly E_T distribution and observed E_T at Freeman Ranch in Texas for the period 2005-2008.

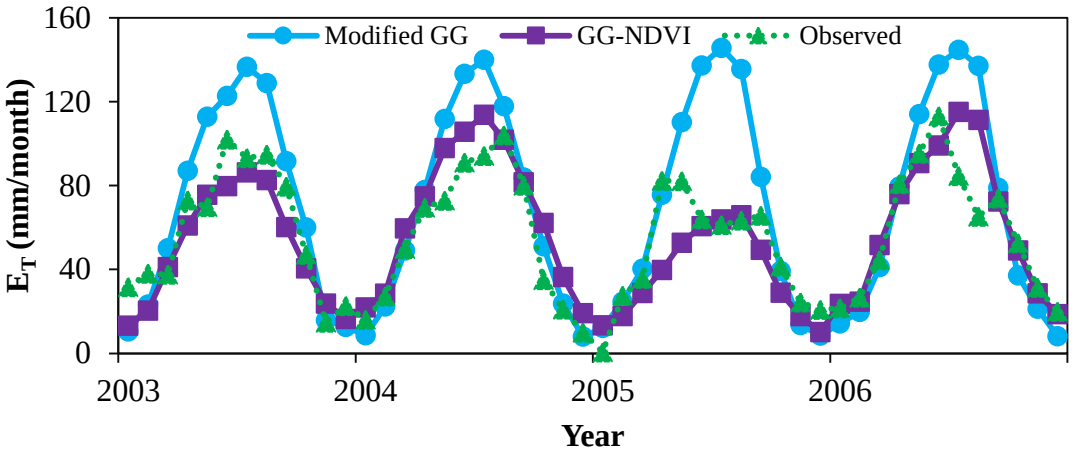

Figure 2-6. Comparison of monthly E_T distribution and observed E_T at Goodwin Creek in Mississippi for the period 2003-2006.

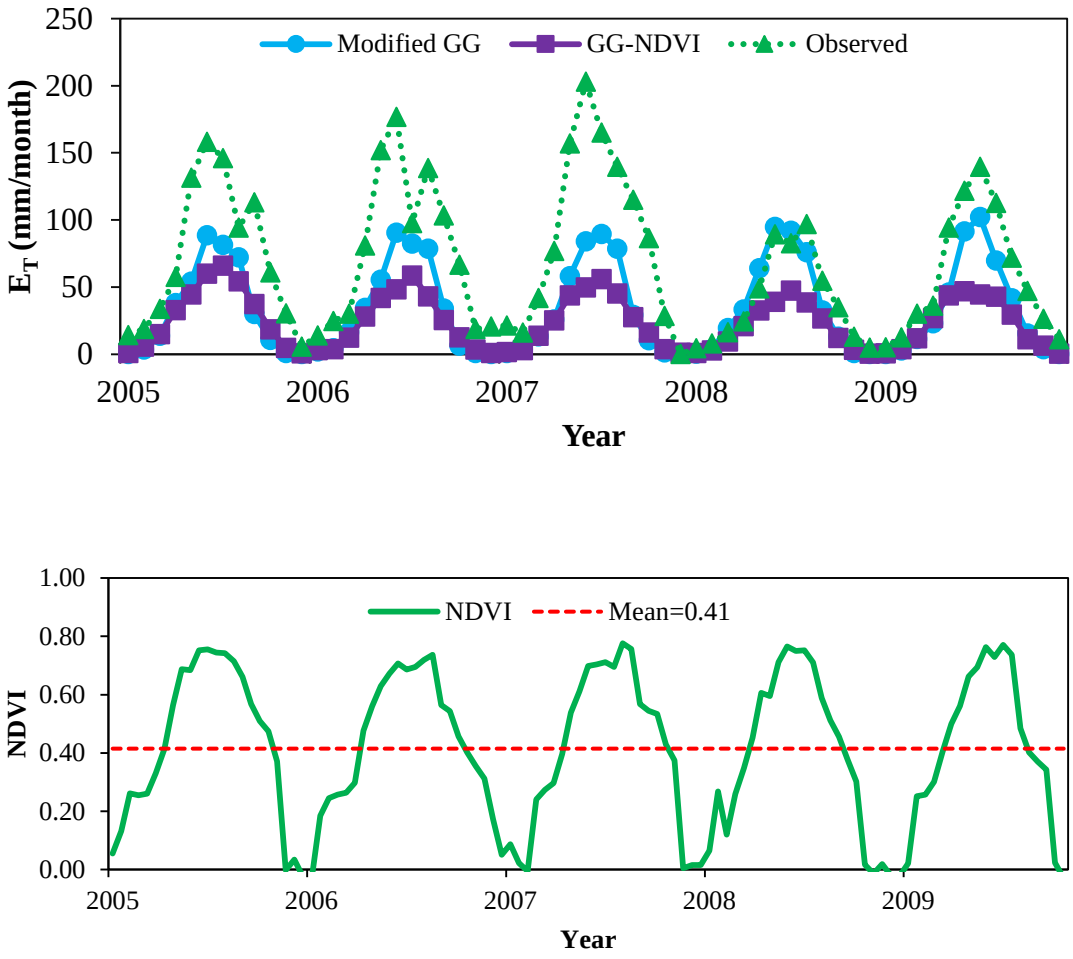

Figure 2-7. Comparisons of monthly E_T and observed E_T and corresponding time-series of NDVI at the Brookings site in South Dakota.

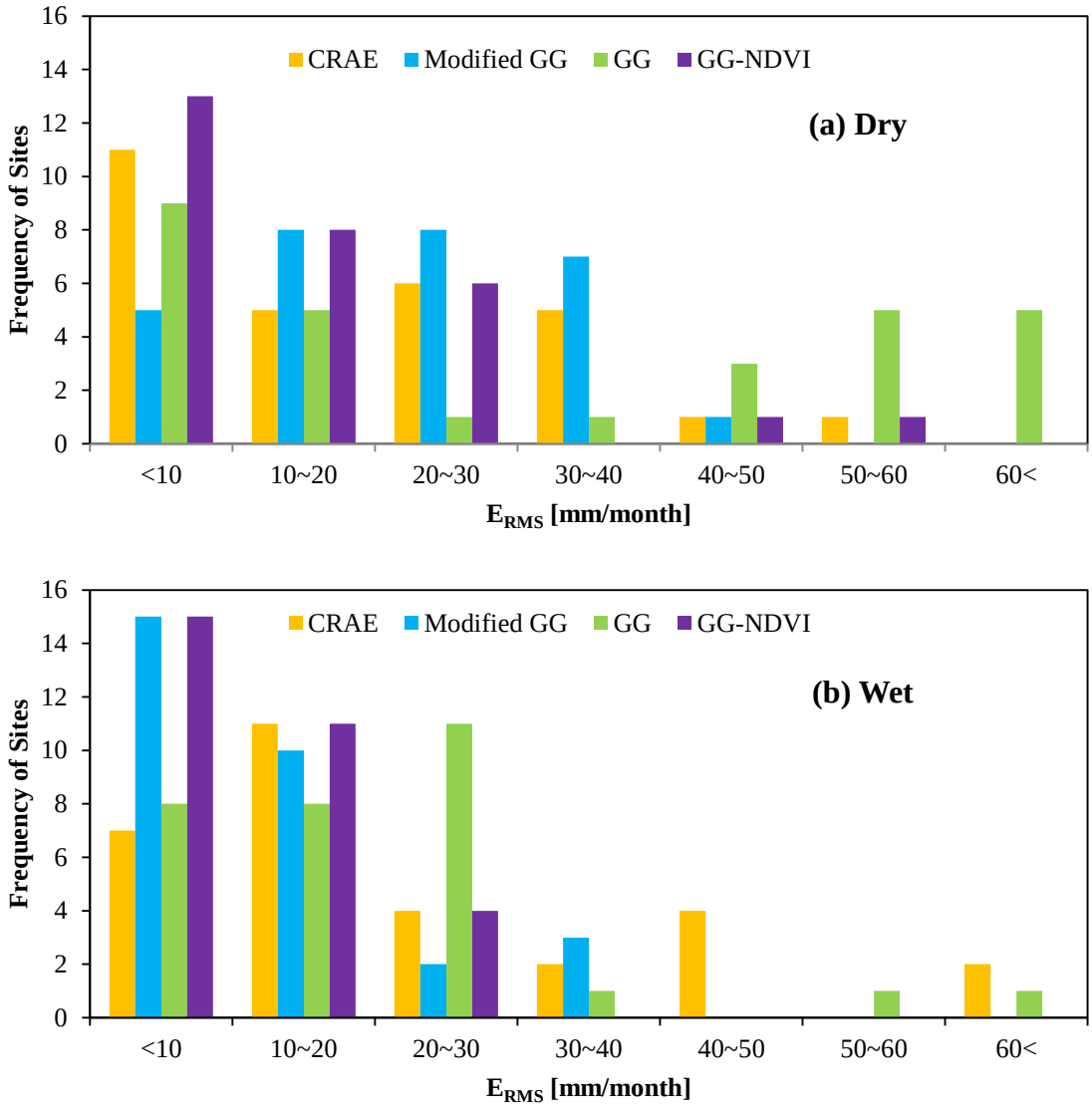

Figure 2-8. Histogram of E_{RMS} for GG-NDVI and other complementary methods. GG refers to the normalized complementary method of Han et al. (2012).

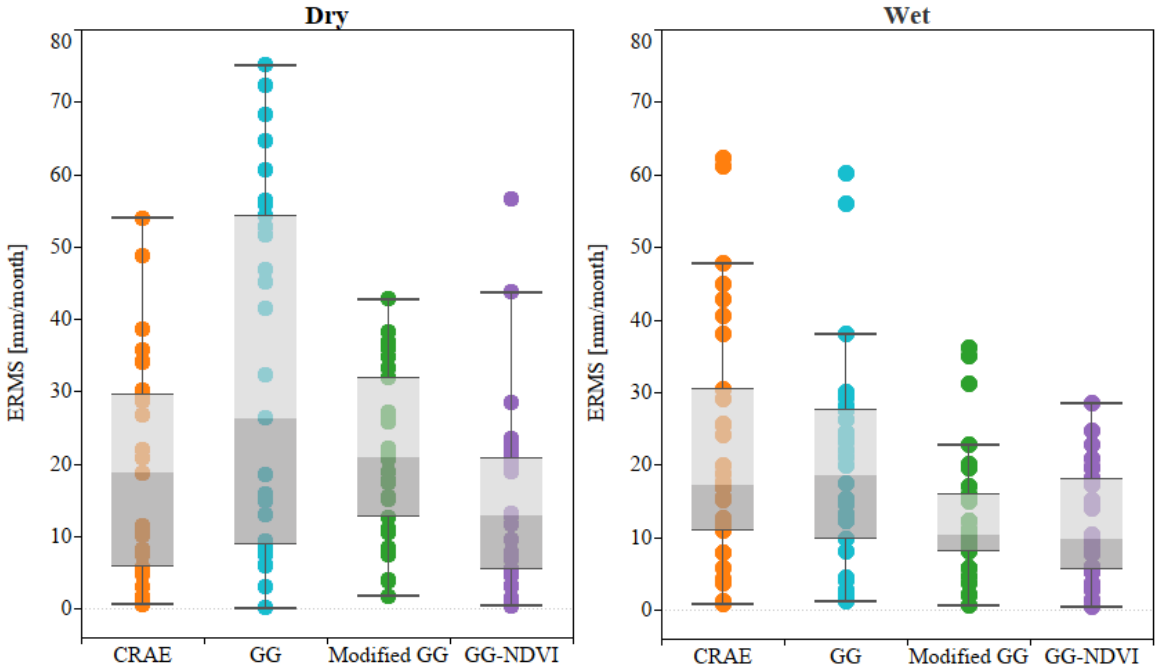

Figure 2-9. Boxplots of E_{RMS} between different complementary methods of Scenario 2. GG refers to the normalized complementary method of Han et al. (2012).

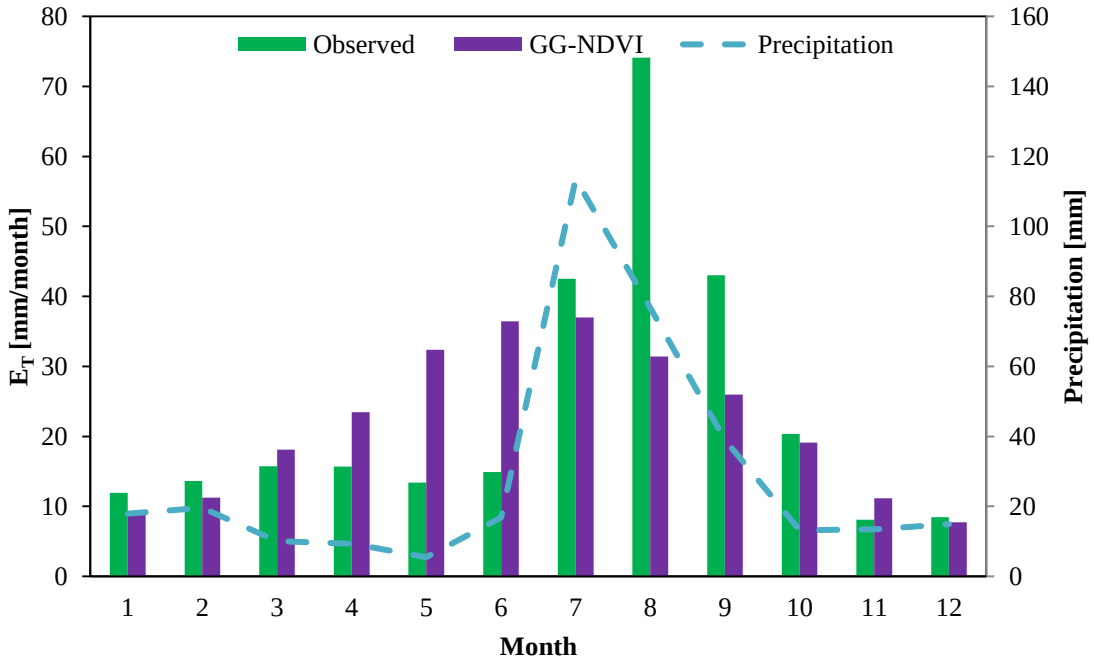

Figure 2-10. Comparison of mean monthly E_T of GG-NDVI and observed E_T values at the Audubon site in Arizona.

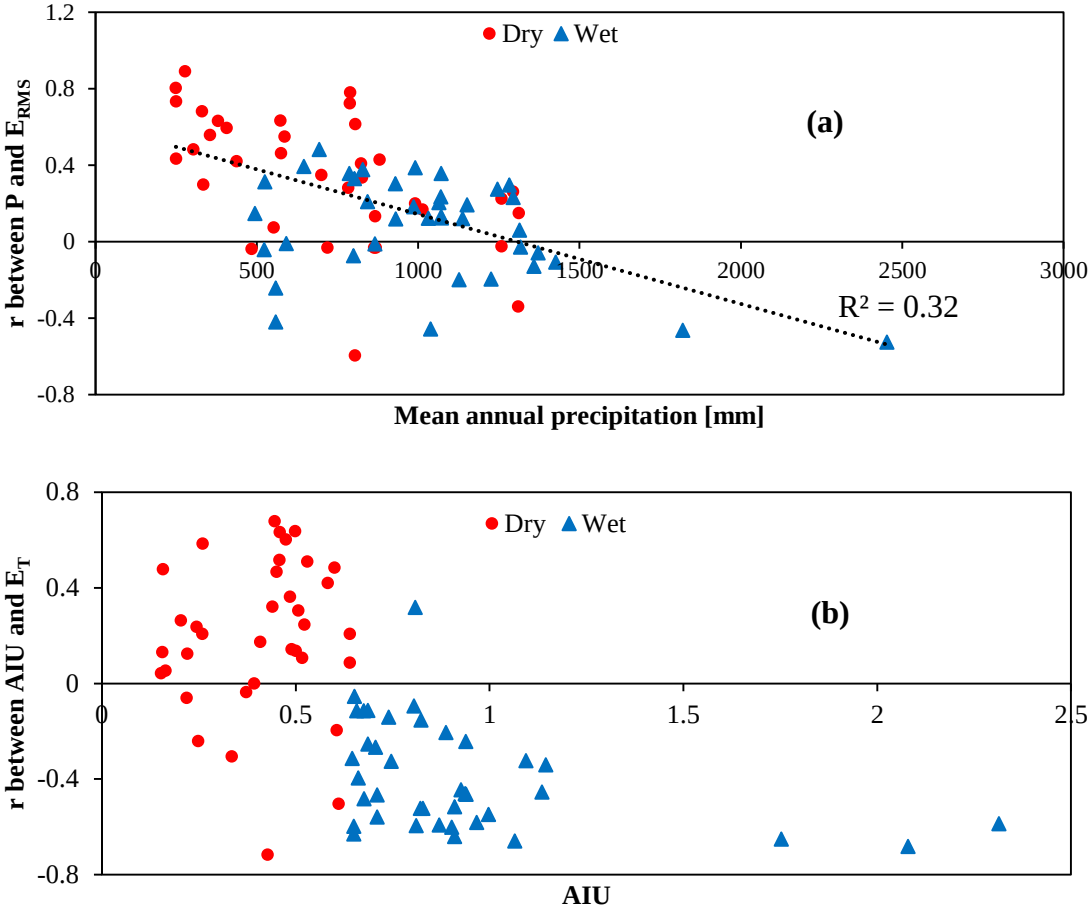

Figure 2-11. (a) Correlation coefficient between precipitation and E_{RMS} versus mean annual precipitation. (b) Correlation coefficient between AIU and E_T versus AIU.

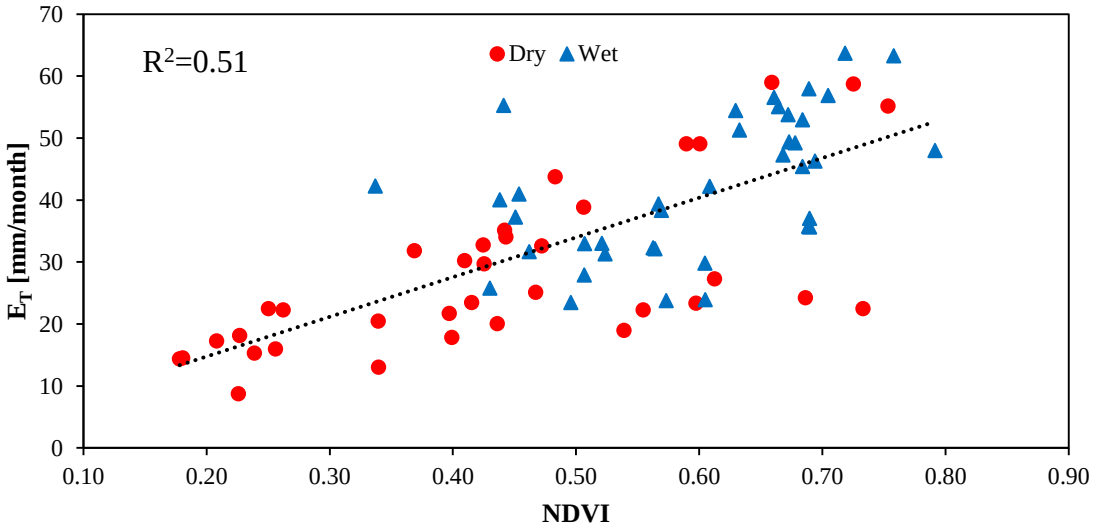

Figure 2-12. Scatter plot of monthly GG-NDVI E_T and NDVI from all 75 sites. The dashed line indicates a linear fit to the data.

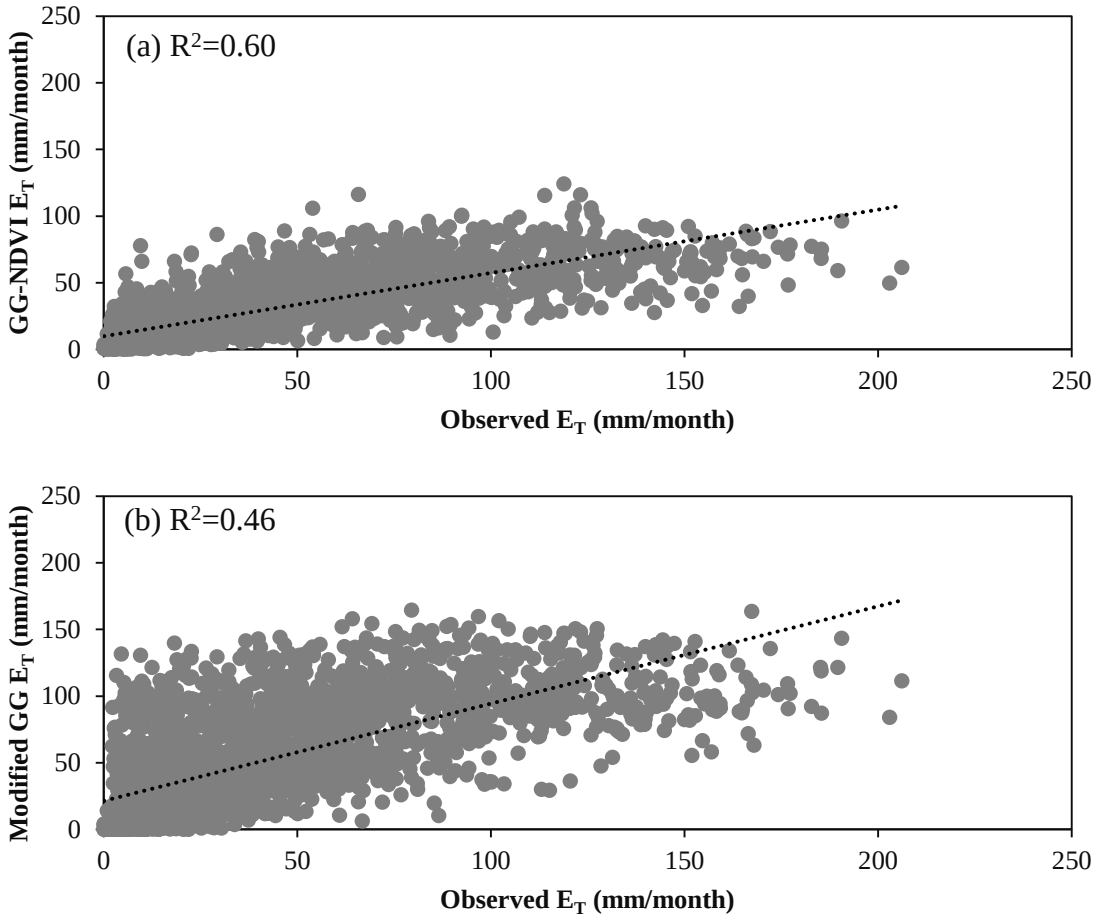

Figure 2-13. Scatter plot of monthly observed E_T and estimated E_T across 36 dry sites; (a) GG-NDVI and (b) modified GG. The dashed line indicates a linear fit to the data.

CHAPTER 3

COMPLEMENTARY RELATIONSHIP FOR ESTIMATING EVAPOTRANSPIRATION USING THE GRANGER-GRAY MODEL: IMPROVEMENTS AND COMPARISON WITH A REMOTE SENSING METHOD

Abstract

The Granger and Gray (GG) model, which uses the complementary relationship for estimating evapotranspiration (ET), is a simple approach requiring only commonly available meteorological data; however, most complementary relationship models decrease in predictive power with increasing aridity. In this study, a previously developed modified GG model using the vegetation index is further improved to estimate ET under a variety of climatic conditions. This updated GG model, GG-NDVI, includes Normalized Difference Vegetation Index (NDVI), precipitation, and potential evapotranspiration using the Budyko framework. The Budyko framework is consistent with the complementary relationship and performs well under dry conditions. We validated the GG-NDVI model under operational conditions with the commonly used remote sensing-based Operational Simplified Surface Energy Balance (SSEBop) model at 60 Eddy Covariance AmeriFlux sites located in the USA. Results showed that the Root Mean Square Error (RMSE) for GG-NDVI ranged between 15 and 20 mm/month, which is lower than for SSEBop every year. Although the magnitude of agreement seems to vary from site to site and from season to season, the occurrences of RMSE less than 20 mm/month with the proposed model are more frequent than with SSEBop in both dry and wet sites. This study also found an inherent limitation of the complementary relationship

under moist conditions, indicating the relationship is not symmetrical as previously suggested. A nonlinear correction function was incorporated into GG-NDVI to overcome this limitation. The resulting Adjusted GG-NDVI produced much lower RMSE values, along with lower RMSE across more sites, as compared to measured ET and SSEBop.

Introduction

According to the U.S. Geological Survey (USGS) Famine Early Warning Systems NETwork (FEWSNET, 2015), the rate and amount of evapotranspiration (ET) plays a considerable role in the monitoring of water loss from agricultural lands. As noted by Senay et al. (2013), ET may be used to show the current vegetation condition compared to the historical records. This comparison has the potential to help identify vegetation stress in time and space. ET estimation methods can be divided into two types: (1) ground-based ET methods that use standard meteorological data; and (2) ET models that use remote sensing data that must be combined with retrieval algorithms to estimate ET.

McMahon et al. (2016) classified the ground-based ET methods into six classes on the basis of application: (1) potential evapotranspiration (ETP); (2) reference evapotranspiration; (3) actual evapotranspiration; (4) open water evaporation; (5) lake/storage evaporation; and (6) pan evaporation. We have focused on actual ET in this study because it can be representative of actual conditions, whereas reference evapotranspiration would require a vegetation resistance parameter and deep lakes would require water temperature data. In addition, we use the term ‘evapotranspiration (ET)’ in this paper to include actual evapotranspiration except in places where the term ‘reference (crop) evapotranspiration’ is used by other authors.

One approach to estimating ET with ground-based methods is the complementary relationship proposed by Bouchet (1963). The primary advantage of the complementary relationship is that it generally requires only meteorological data. Bouchet (1963) suggested that as a surface dries, the decrease in ET is matched with an increase in potential evapotranspiration (ETP). Such a relationship offers a simple and attractive approach for estimating ET using ETP without the detailed knowledge of surface properties. Examples of widely known models using this concept are the Advection-Aridity (AA) model by Brutsaert and Stricker (1979), the Complementary Relationship Areal Evapotranspiration (CRAE) by Morton (1983), and the GG model proposed by Granger and Gray (1989). These three models have been widely applied to a broad range of surface and atmospheric conditions (Crago et al., 2016; Hobbins et al., 2001; Kahler and Brutsaert, 2006; Szilagyi and Jozsa, 2008; Xu and Singh, 2005).

Granger (1989), however, argued that the symmetric relationship in Bouchet (1963) lacked a theoretical background and proved that the symmetric condition is only true when the temperature is near 6 ˚C. Hence, the author developed a new complementary relationship with the psychrometric constant and the slope of the saturation vapor pressure curve. Later, Cargo and Crowley (2005) showed that the radiometric surface temperature measurements can be successfully incorporated into the Granger (1989) equation. Similar to Cargo and Crowley (2005), Anayah and Kaluarachchi (2014) proposed a modified version of the GG model using the Priestley and Taylor (1972) equation instead of the Penman (1948) equation. The model proposed by Anayah and Kaluarachchi (2014) is hereafter called the modified GG model. The results of the modified GG model showed a decrease in Root Mean Square Error (RMSE)

from 20 % to as much as 80 % compared to the recent studies of Mu et al. (2007, 2011), Han et al. (2011), and Thompson et al. (2011). On the other hand, Kahler and Brutsaert (2006) proposed an empirical constant, b, in the Bouchet (1963) hypothesis and demonstrated that b is generally greater than 1, based on their theoretical and experimental evidence, while the symmetric condition of the Bouchet (1963) hypothesis requires $b = 1$. More recently, Aminzadeh et al. (2016) extended the asymmetric complementary relationship with an analytical prediction of b for Kahler and Brutsaert (2006). Furthermore, Venturini et al. (2008; 2011) applied surface temperature of Moderate Resolution Imaging Spectroradiometer (MODIS) data into the GG model and showed a good agreement between their approach and measured ET. Especially, Szilagyi et al. (2017) developed a calibration free version of the complementary relationship.

Prior studies show that the complementary relationship is not symmetric with ETW and that the GG model can be successfully applied to a wide range of physical and surface conditions. Specially, the modified GG model (Anayah and Kaluarachchi, 2014) provided more reliable ET estimates than other models. Although the modified GG model demonstrated excellent performance across 34 global sites, the authors suggested that additional refinements could further improve performance under dry conditions. The low performance in dry conditions may be due to relative evaporation (the ratio of ET to ETP) in the original GG model (Granger and Gray, 1989), which was empirically derived from 158 sites under wet conditions in Canada. Therefore, models based on the original GG may have difficulty predicting ET under dry conditions. To improve relative evaporation, Kim and Kaluarachchi (2017) used the Budyko model equation described by

Li et al., (2013) to represent relative evaporation instead of using the original equation. The basis for this change is that the concept of relative evaporation is consistent and similar to that described in the Budyko framework (Yang et al., 2006; Zhang et al., 2004). Kim and Kaluarachchi (2017) selected 75 Eddy Covariance (EC) flux tower sites across the USA and compared them with measured ET and with other complementary relationship models. The Kim and Kaluarachchi (2017) model reduced mean RMSE by 32 % compared to the Anayah and Kaluarachchi (2014) modified GG model across 36 dry sites. Using the Kim and Kaluarachchi (2017) model, the mean RMSE across the 59 sites was shown to be 14 mm/month, compared to 21 mm/month with CRAE, 28 mm/month with AA, 27 mm/month with GG, and 17 mm/month with the modified GG model. Moreover, the predicted ET values were more correlated with estimated ET, showing a correlation coefficient of 60 % compared to 37 % in the Allam et al. (2016) study.

Figure 3-1 presents the results obtained from the previous Kim and Kaluarachchi (2017) study. These results are in agreement with Anayah and Kaluarachchi (2014), which showed that the modified GG model needs further improvements in dry conditions, and showed the lowest mean RMSE in both dry and wet sites. Overall, these results indicate that, among the ground-based methods, the Kim and Kaluarachchi (2017) model can be used as a powerful methodology to estimate ET.

While these findings are good within the realm of complimentary methods (or ground-based methods), some of the more commonly used ET estimation methods now use remote sensing data. If the complementary relationship and the corresponding methods, such as the model proposed by Kim and Kaluarachchi (2017), are to be

accepted as operational models in field conditions, then the results should be compared and validated with remote sensing-based ET estimation methods. Taking into consideration of the improvements made with complementary relationship-based methods, this study examines the work of Kim and Kaluarachchi (2017) in comparison with a commonly used remote sensing method and measured ET data from 60 EC flux tower sites located across the USA.

Biggs et al. (2016) grouped the remote sensing-based methods into three classes: vegetation-based methods, radiometric land surface temperature-based methods, and triangle/trapezoid or scatterplot inversion methods. Among them, the radiometric land surface temperature-based methods have several attractive features compared to the other classes: minimal ground data, ease of implementation, and operational application over large areas.

Radiometric land surface temperature-based methods use the fact that ET is a change of state in water that uses energy in the environment for vaporization and reduces surface temperature (Su et al., 2005). A subset of these methods is often called energy balance methods since they solve the energy balance equation. Moreover, these methods do not directly measure ET but must be combined with retrieval algorithms since data and technical requirements to solve the full energy balance equation can be challenging, especially in large regions. For example, the Surface Energy Balance Algorithm for Land (SEBAL) model (Bastiaanssen et al., 1998; 2005) requires the measurements of wind speed, iterative calibration, and review by an expert operator. Mapping EvapoTranspiration at high Resolution with Internalized Calibration (METRIC) (Allen et al., 2011) needs high-quality meteorological data such as net radiation, air temperature,

wind speed, and humidity. According to Allen et al. (2011), METRIC has higher accuracy for hourly reference ET than SEBAL, but the processing cost of METRIC is high.

As an alternative, FWESNET (USGS) has produced ET measurements from MODIS using the operational Simplified Surface Energy Balance (SSEBop) model (Senay et al., 2013). The SSEBop setup uses the Simplified Surface Energy Balance (SSEB) approach developed by Senay et al. (2007). The SSEB approach estimates ET using ET fraction scaled from thermal imagery in combination with a spatially explicit maximum reference ET. SSEB has an advantage in that it does not require air temperature and the knowledge of land cover types. Instead, the method uses the 'hot' and 'cold' pixel approach of Bastiaanssen et al. (1998) to calculate the ET fraction. Gowda et al. (2009) found a strong correlation of 0.84 between SSEB results and lysimeter data. Later, Senay et al. (2011a) enhanced SSEB to accommodate diverse vegetation and topographic conditions using a lapse rate correction factor. They successfully evaluated the results by comparing with METRIC and ET values computed from the water balance approach. As a result of the work by Senay et al. (2011a), the enhanced SSEB model increased the correlation with METRIC from 0.83 to 0.90. Furthermore, Senay et al. (2011b) proposed a revised SSEB to handle both elevation and latitude effects on surface temperature using the difference between Land Surface Temperature (LST) and air temperature. Recently, Senay et al. (2013) proposed an operational SSEB, renamed as SSEBop, that uses predefined boundary conditions for hot and cold reference pixels so that ET can be calculated as a function of LST and reference ET. The SSEBop approach has been validated comprehensively by comparing with 45

EC flux tower observations (Senay et al., 2013) and then with both MOD16 and 60 EC flux tower observations (Velpuri et al., 2013). Later, Bastiaanssen et al. (2014) applied SSEBop to determine ET in the Nile Basin, Ethiopia, for mapping water production and consumption zones. SSEBop ET data is now freely available through the USGS Geo Data Portal.

Despite the general consensus of using SSEBop for estimating ET, a detailed study of SSEBop conducted by Senay et al. (2013) showed that the use of reference ET can introduce a significant difference of up to 20 % in the magnitude of ET. They also showed that the use of constant pre-defined differential temperature between the hot and cold boundary conditions can also create an inherent inaccuracy. Thus, it is important that SSEBop ET be validated and calibrated with available data such as EC flux tower data before using it to model ET.

The facts provided in the previous discussion indicate a need to further validate both the Kim and Kaluarachchi (2017) and SSEBop models in the operational application of the complementary relationship in estimating ET. Therefore, the objectives of this study are: (1) assess the validity of the ET estimation model of Kim and Kaluarachchi (2017) through a direct comparison with remote sensing methodology, which in this case is the SSEBop model; and (2) use the results of the first objective to identify the potential improvements required in the complementary relationship for estimating ET under diverse climate conditions.

Methodology and Data

Methodology

For the base model, we used the model proposed by Kim and Kaluarachchi (2017) called the GG-NDVI model in the original publication. GG-NDVI is the most updated model using the original GG model. GG-NDVI uses historical annual Normalized Difference Vegetation Index (NDVI) data and precipitation to improve the ET estimates of the modified GG model proposed by Anayah and Kaluarachchi (2014). We then used the SSEBop model (Senay et al. 2013) to further validate GG-NDVI in comparison to an operational remote sensing model.

GG-NDVI model

The first complementary relationship was proposed by Bouchet (1963), who postulated that, as a surface dries, the actual ET decrease is matched by an equivalent increase in ETP. In spite of the fact that ET is negatively correlated with ETP, Morton (1983) showed that the relationship has no defined shape. Granger (1989) showed that the symmetrical relationship between ET and ETP only occurs when the temperature is near 6 ˚C and suggested the following complementary relationship formulation:

$$\mathrm{ET} + \frac{\gamma}{\Delta}\mathrm{ETP} = \left(1 + \frac{\gamma}{\Delta}\right)\mathrm{ETW} \quad (1)$$

where ET, ETP, and ETW are in mm/day, γ is the psychrometric constant (kPa/˚C), and Δ is the slope of saturation vapor pressure-temperature (kPa/˚C) relationship. Thereafter, Granger and Gray (1989) developed the GG model based on Eq. (1) using the concept of relative evaporation. Recently, Anayah and Kaluarachchi (2014)

developed the modified GG model using the work of Granger and Gray (1989). The performance of the modified GG model improves when the Priestley and Taylor (1972) equation shown in Eq. (2) is used to calculate ETW instead of the Penman (1948) model.

$$\text{ETW} = \alpha \frac{\Delta}{\gamma+\Delta}(R_n - G_{soil}) \quad (2)$$

where α is a coefficient equal to 1.28, R_n is net radiation (mm/day), and G_{soil} is soil heat flux density (mm/day). Note that soil heat flux density is negligible compared to net radiation when calculated at daily or monthly time-scale (Gavilana et al., 2007; Hobbins et al., 2001).

ET is then estimated as a fraction of ETW using Eq. (3):

$$\text{ET} = \frac{2G}{G+1}\text{ETW} \quad (3)$$

where G is the relative evaporation parameter derived from Granger and Gray (1989). They proposed a unique relationship with a parameter called relative drying power (D). The unique relationship between G and D are described in Eqs. (4) and (5), respectively.

$$G = \frac{\text{ET}}{\text{ETP}} = \frac{1}{1+0.028e^{8.045D}} \quad (4)$$

$$D = \frac{E_a}{E_a+R_n} \quad (5)$$

where E_a is drying power of air (mm/day) given in Eq. (6).

$$E_a = 0.35(1 + 0.54U)(e_s - e_a) \quad (6)$$

where U is wind speed at 2 m above ground level (m/s), which is adjusted using the work of Allen et al. (1998); e_s is saturation vapor pressure (mm Hg); and e_a is vapor pressure of air (mm Hg).

The performance of the GG model, including the modified GG model proposed later, decreased with increasing aridity. A possible reason is G in Eq. (4), which was empirically derived from 158 sites representing wet environments in Canada. To improve the parameter G, the Kim and Kaluarachchi (2017) GG-NDVI model used the latest version of the Fu equation (Li et al., 2013). In particular, the Fu (1981) equation is one of the formulations of the Budyko curve (Budyko, 1974) and it is consistent with the complementary relationship (Yang et al., 2006; Zhang et al., 2004). The corresponding analytical formulation of the Fu equation is given in Eq. (7).

$$\frac{\mathrm{ET}}{\mathrm{ETP}} = 1 + \frac{\mathrm{P}}{\mathrm{ETP}} - \left[1 + \left(\frac{\mathrm{P}}{\mathrm{ETP}}\right)^{\varpi}\right]^{\frac{1}{\varpi}} \tag{7}$$

where P is precipitation (mm) and ETP is estimated using Penman (1948). Parameter ϖ is a constant and represents the land surface conditions of the basin, especially the vegetation cover (Li et al., 2013). Furthermore, Li et al. (2013) showed that ϖ is linearly correlated with the long-term average annual vegetation cover that can help improve ET estimates. Yang et al. (2009) showed that vegetation cover defined by M is calculated using Eq. (8).

$$M = \frac{\mathrm{NDVI} - \mathrm{NDVI}_{\mathrm{min}}}{\mathrm{NDVI}_{\mathrm{max}} - \mathrm{NDVI}_{\mathrm{min}}} \tag{8}$$

where $NDVI_{min}$ and $NDVI_{max}$ are chosen to be 0.05 and 0.8, respectively. An optimal ϖ value for the basin can be derived through a curve fitting procedure that minimizes RMSE between the measured and predicted evaporation ratio (Li et al., 2013).

Li et al. (2013) proposed parameterization that is simply a linear regression between optimal ϖ and the long-term average M given as

$$\varpi = a \times M + b \tag{9}$$

where a and b are constants that are found for each site.

To incorporate Eq. (7) into the modified GG model, Kim and Kaluarachchi (2017) used the work of Zhang et al. (2004) and Yang et al. (2006). According to Zhang et al. (2004), the Fu equation showed that the rate of change of ET with precipitation increases with ETP but decreases with precipitation. This is similar to the complementary relationship proposed by Bouchet (1963). Later, Yang et al. (2006) derived the consistency between the Fu equation and the complementary relationship using 108 dry regions in China. With this theoretical background, Kim and Kaluarachchi (2017) used the Fu equation to calculate G in the modified GG model instead of Eq. (4). Equation (10) shows the Fu equation with the updated G now defined as G_{new}.

$$G_{new} = \frac{\mathrm{ET}}{\mathrm{ETP}} = 1 + \frac{\mathrm{P}}{\mathrm{ETP}} - \left[1 + \left(\frac{\mathrm{P}}{\mathrm{ETP}}\right)^{\varpi}\right]^{\frac{1}{\varpi}} \tag{10}$$

Note G_{new} is the updated definition of relative evaporation, G, which includes the Budyko hypothesis and the vegetation index. To estimate G_{new}, ETP is required and can be estimated using the Penman equation given by Eq. (11).

$$\mathrm{ETP} = \frac{\Delta}{\gamma+\Delta}(R_n - G_{soil}) + \frac{\gamma}{\gamma+\Delta}E_a \tag{11}$$

Having found G_{new} from Eq. (11) and estimated ETW from Eq. (2), we can estimate ET of the proposed model from Eq. (12).

$$\mathrm{ET} = \frac{2G_{new}}{G_{new}+1}\mathrm{ETW} \tag{12}$$

SSEBop model

The SSEBop algorithm (Senay et al., 2013) does not solve the full energy balance

equation. This approach assumes that for a given time and location, the temperature difference between the hot and cold reference values of each pixel remains nearly constant throughout the year under clear sky conditions. Furthermore, the major simplification of SSEBop is based on the knowledge that the surface energy balance process is mostly driven by net radiation. With this simplification, the ET fraction, ETf, is calculated using Eq. (13).

$$\mathrm{E}Tf = \frac{Th - Ts}{\mathrm{d}T} = \frac{Th - Ts}{Th - Tc} \quad (13)$$

Here, ETf is between 0 and 1, with negative ETf values set to zero; Ts is surface temperature derived from MODIS LST; Th is hot reference value representing the temperature of hot conditions; and Tc is the cold reference value derived as a fraction of maximum air temperature (Senay et al., 2013). The difference between Th and Tc is dT with temperature units in Kelvin.

ET is estimated using Eq. (14) as a fraction of reference ET.

$$\mathrm{ET} = ETf \times k\, ET_o \quad (14)$$

where ET_o is reference ET, which is calculated from the Penman-Monteith equation (Allen et al., 2007; Senay et al., 2008), and k is a coefficient that scales ET_o into the level of maximum ET experienced by an aerodynamically rougher crop. A recommended value of k for the United States is 1.2.

Data

First, we used the SSEBop ET data set from the USGS Geo Data Portal (http://cida.usgs.gov/gdp/, last accessed on May 23, 2016) for the period 2000–2007 covering the United States. Second, ET data from GG-NDVI were generated using

meteorological data and NDVI. Meteorological data required are temperature, wind speed, precipitation, net radiation, and elevation (pressure). Among these, net radiation (R_n) was calculated using the equations recommended by Allen et al. (2007), similar to the SSEBop model. Air temperature, elevation, and precipitation data were obtained from the Parameter-elevation Regressions on Independent Slopes Model (PRISM) (http://www.prism.oregonstate.edu/, last accessed on Nov 23, 2015). As part of the input data for the GG-NDVI method, we used the 16-day Normalized Difference Vegetation Index (NDVI) data from MODIS (http://daac.ornl.gov/MODIS/modis.shtml, last accessed on Oct 23, 2015).

We collected the lever 4 meteorological data including latent heat flux (LE) from 76 AmeriFlux stations (Oak Ridge National Laboratory's AmeriFlux website, http://ameriflux.ornal.gov/, last accessed on Nov 23, 2015) then, we excluded those stations with actual vegetation type different from the MODIS global land cover product (MOD12) at any of surrounding 500 m by 500 m spatial resolution. Also, we further excluded those stations with fewer than half a year of measurements during 2000-2007. As a result, 60 AmeriFlux stations were used in this study. Level 4 data is gap-filled and quality-checked and does not require filling of the missing data. The measured monthly latent heat flux data were used to calculate the corresponding ET using latent heat of vaporization of water.

We defined the climate class of each site using the aridity index of the United Nations Environment Programme (UNEP) proposed by Barrow (1992). The aridity index divided climate conditions to six classes: hyper-arid, arid, semi-arid, dry sub-humid, wet sub-humid, and humid. However, this work simplified the climate class definition to two

classes, similar to the work of Anayah and Kaluarachchi (2014): dry and wet. Using this simplification, 24 sites were identified as dry, compared to 36 sites under the wet class.

Results and Discussion

This study was conducted in two phases. Phase 1 is the validation stage in which comparisons are made between the SSEBop model and measured ET to assess the accuracy of the remote sensing method to estimate ET. In Phase 2, a comparison of estimated ET from GG-NDVI with observed data will be performed to identify the weaknesses of the GG-NDVI model, especially relative to the complementary relationship, and appropriate corrections will be proposed.

Phase 1: Validation of GG-NDVI

Capturing inter-annual variations of ET estimates is important. Although such variations are not significant when water is unlimited, estimating these variations in water-limited conditions is essential for water resources management. In this phase, ET has been estimated from both SSEBop and GG-NDVI and compared against measured monthly ET data from 2000 to 2007.

Table 3-1 presents the yearly comparison of results between the SSEBop and GG-NDVI estimates. Compared with measured ET, the results indicate that the accuracy of SSEBop and GG-NDVI estimates show satisfactory R-square and RMSE values. R-square values for SSEBop and GG-NDVI are 0.65 and 0.61, respectively. The results demonstrate that the ET estimates from GG-NDVI ET at an annual time-scale are reasonable. Figure 3-3, however, shows the 1:1 scatter of yearly variability of both models with GG-NDVI showing a tendency to underestimate in the higher ET range. In

contrast, SSEBop tends to overestimate ET in the same higher ET range. Generally, higher ET occurs mostly in wet conditions, and underestimating ET in moist regions is a characteristic of the complementary relationship (Han et al., 2014; Hobbins et al., 2001; Roderick et al., 2009).

Figure 3-4 shows the poor results of SSEBop with the temporal variation in Th, Tc, and Ts on the left and the corresponding SSEBop, GG-NDVI, and measured ET values on the right. For example, at Austin Cary in Florida (Fig. 3-4(a)), RMSE ranged from 29 to 164 mm/month for SSEBop and 17 to 70 mm/month for GG-NDVI. Moreover, SSEBop showed significant deviations from measured ET throughout the year, and RMSE varied from 29 to 164 mm/month. Where SSEBop shows low RMSE values in Fig. 3-4(a) and 3-4(b), a possible reason for these significant deviations could be the concept of ET faction (ETf) in SSEBop. ETf is calculated using Th, Tc, and Ts, and the Ts curve lies mostly between the boundary conditions (Th and Tc). However, Ts in Fig. 3-4(a) is close to the predefined cold boundary (Tc), which brings ETf closer to 1.0, resulting in a corresponding ET that is close to the maximum ET.

According to Table 3-1 and Fig. 3-5, the mean RMSE of GG-NDVI ranged between 15 and 20 mm/month, and GG-NDVI showed lower RMSE than SSEBop every year. Although the magnitude of agreement (overestimation or underestimation) seems to vary from site to site and from season to season, Fig. 3-5 confirms that the occurrence of an RMSE less than 20 mm/month with GG-NDVI is more frequent than with SSEBop in both dry and wet sites. The averages of RMSE across 24 dry sites for GG-NDVI and SSEBop are 19 mm/month and 22 mm/month, respectively. For 36 wet sites, GG-NDVI

and SSEBop showed an average RMSE of 17 mm/month and 20 mm/month, respectively. These results indicate that GG-NDVI ET estimates improve with wetness, which is similar to the previous studies of Anayah and Kaluarachchi (2014), Hobbins et al. (2001), and Xu and Singh (2005).

Based on these results, we could conclude that GG-NDVI is a reliable approach for estimating ET, the novelty of GG-NDVI being that the Fu equation can be used to define relative evaporation in the original GG model using NDVI. This approach showed a reasonable match between GG-NDVI and the 60 AmeriFlux sites. However, GG-NDVI may not predict ET accurately when the vegetated cover changes significantly or is dense. For example, at Brooking in South Dakota, the mean RMSE of GG-NDVI was 42 mm/month, compared to 18 mm/month with all sites, and NDVI has a large seasonal vegetation cover as shown in Fig. 3-6. A possible reason is that the relationship between NDVI and vegetation can be biased in sparsely vegetated areas with a Leaf Area Index (LAI) of less than 3. According to Pettorelli et al. (2005), the Soil Adjusted Vegetation Index (SAVI) is recommended instead of NDVI when LAI is less than 3. It should be noted that the LAI of Brookings is about 2.5. Furthermore, prior studies of Mu et al. (2011) and Yuan et al. (2010) have demonstrated that NDVI is insufficient to represent vegetation under dense vegetation conditions. Recently, Zhang et al. (2016) introduced the fraction of absorbed photosynthetic active radiation absorbed by vegetation (or fPAR) under the Budyko framework to avoid the bias of NDVI. Thus, this inability of NDVI to represent vegetation under dense conditions may be the reason for the decreased performance of GG-NDVI. Another possible reason is that the relative infiltration capacity and the average topographic slope need to be taken into consideration when

using the Fu equation, especially in small catchments (Yang et al., 2009). Therefore, more work is needed to generalize the relationship for the use of NDVI with changing vegetation cover within the Budyko framework. The next section will discuss options to improve the GG-NDVI model.

Phase 2: Enhancements to GG-NDVI

As described earlier, GG-NDVI performed slightly better than SSEBop in both dry and wet climate conditions, and GG-NDVI increased the predictive power with increasing humidity. One interesting finding is that RMSE from GG-NDVI increases slightly with the relative evaporation parameter as shown in Fig. 3-7. Considering this observation, Phase 2 then focused on the relationship between the performance of GG-NDVI and Gin the context of using the complementary relationship.

Within the complementary relationship, increasing G means that climate is becoming wetter and ET is closer to ETW. When ET equals to ETW, surface has access to unlimited water as shown in Fig. 3-8. However, natural surfaces in even the wettest regions may not approach complete saturation, hence, ET can remain below its limiting value of ETW. Consequently, the magnitude of difference between ET and ETW is important in estimating ET, especially under highly moist conditions. A possible explanation may be that the complementary relationship between ET and ETP with respect to ETW is not symmetric. GG-NDVI has improved the performance of the original GG model, but Eq. (3) still contains the value of 2, which refers to a symmetric complementary relationship. As explained earlier, other authors (Aminzadeh et al., 2016; Kahler and Brutsaert, 2006) question the use of a symmetric relationship. Thus, the use of

a symmetric complementary relationship may have contributed to the decreased performance of GG models, both the modified GG model and GG-NDVI. In order to understand the relationships affecting model accuracy, a correction function as a function of G is required as shown in Eq. (17).

$$\mathrm{ET} = \frac{2G_{new}}{G_{new}+1} \times f(G) \times \mathrm{ETW} \tag{17}$$

where $f(G)$ is the correction function. We expect the correction function to be nonlinear, similar to an exponential function, since the magnitude of the difference between ET and ETW decreases exponentially. In this work, we fitted 2772 data points to an exponential function similar to Eq. (18). Multiple regression analysis was conducted to compute the values of the α and β coefficients.

$$f(G) = \alpha e^{\beta \cdot G} \tag{18}$$

Regression analysis found that α is 0.7895 and β is 0.9655. Hereafter, the GG-NDVI model with the proposed correction function given as Eq. (17) is called the Adjusted GG-NDVI model.

To assess the accuracy of Adjusted GG-NDVI, comparisons were made between the results from the Adjusted GG-NDVI and GG-NDVI and between measured ET data and ET values from SSEBop. These comparisons are shown in Fig. 3-9 and Table 3-2 across 60 sites. While ET from GG-NDVI at Mize in Florida (Fig. 3-9(a)) and Blodgett in California (Fig. 3-9(b)) showed deviations from measured ET, we can see that the Adjusted GG-NDVI produced ET estimates close to measured ET and reduced mean RMSE from 33 to 22 mm/month for Mize and 17 to 10 mm/month for Blodgett. In Table 3-2, overall RMSE across 60 sites for GG-NDVI and Adjusted GG-NDVI were found to

be 18 mm/month and 15 mm/month, respectively. Figure 3-10, which presents a histogram of RMSE from the different ET models, shows a significant improvement attributed to the Adjusted GG-NDVI model. With Adjusted GG-NDVI, 38 sites have less than 15 mm/month of RMSE, compared to 26 sites with GG-NDVI. These results suggest that the use of the correction function in GG-NDVI can significantly improve accuracy in estimating ET. In addition, Eq. (17) can be updated with the new definition of G as

$$\mathrm{ET} + \mathrm{ETP} = 2f(G)\mathrm{ETW} \tag{19}$$

where the value of $2f(G)$ can vary between 1.64 and 3.04 as G varies based on site-specific conditions. The new formulation of the Adjusted GG-NDVI model described in Eq. (19) clearly shows that the relationship between ET and ETP is not symmetric with respect to ETW, further confirming the earlier conclusions that the hypothesis of Bouchet (1963) needs to be extended and applied with appropriate corrections.

Summary and Conclusions

ET estimation models using the complementary relationship can estimate ET in most instances. In particular, the model proposed by Anayah and Kaluarachchi (2014) showed excellent performance compared to recently published studies. However, the predictive power of this model and other similar models decreases with increasing aridity (Anayah and Kaluarachchi 2014; Hobbins et al., 2001; Xu and Singh, 2005). In the case of the modified GG model proposed by Anayah and Kaluarachchi (2014), a reason may be that relative evaporation in the original GG model was derived using 158 sites in Canada under mostly humid conditions. To overcome this limitation, the previously

revised GG model, GG-NDVI (Kim and Kaluarachchi, 2017), used the Fu equation to describe relative evaporation on the basis that the Budyko framework can support the complementary relationship (Zhang et al., 2004; Yang et al., 2006). The results of GG-NDVI showed improved accuracy compared to other complementary relationship models but also showed the need for further refinements, especially under dense vegetation conditions. On the other hand, remote sensing methods are more common as operational models under field conditions. In order to determine whether complementary methods such as GG-NDVI can compete and deliver accuracy similar to remote sensing methods, it is important make appropriate comparisons. The objectives of this work were therefore twofold: (1) evaluate the recently developed ET estimation method, GG-NDVI, to see if it could deliver similar accuracy to the commonly used operational remote sensing method, SSEBop and (2) identify the inherent weaknesses of the original complementary relationship and make appropriate refinements to further improve the GG-NDVI model, especially under dense vegetation conditions. For this purpose, we selected 60 AmeriFlux sites located across the United States.

The first phase of the analysis showed that the GG-NDVI model with the Budyko framework and relative evaporation was found to work reasonably well. Validation with 60 AmeriFlux sites indicated similar levels of accuracy for both SSEBop and GG-NDVI. R-square between GG-NDVI and measured ET ranged from 0.40 to 0.79, overall RMSE of GG-NDVI ranged between 15 and 20 mm/month, and GG-NDVI showed lower RMSE than SSEBop every year. Furthermore, the occurrences of RMSE less than 20 mm/month with GG-NDVI were more frequent than SSEBop. Based on these results, we concluded that GG-NDVI is a reliable approach for estimating ET.

The second phase of the analysis showed that the predictive power of GG-NDVI decreased with relative evaporation possibly due to the use of the symmetric complementary relationship in estimating ET. In order to identify the true relationship between ET and ETP with respect to ETW, an exponential correction function was proposed. This phase demonstrated that the inclusion of relative evaporation with a correction function greatly improved the performance of the Adjusted GG-NDVI. For example, 68 % of Adjusted GG-NDVI sites had RMSE less than 15 mm/month compared 43 % with GG-NDVI.

In essence, this study strengthens the idea that the use of vegetation cover information in the complementary relationship has increased ET estimation power. More importantly, this work showed that the symmetric relationship typically assumed with the complementary relationship may not be valid. Instead, the results show that the symmetrical relationship needs to be updated with a nonlinear correction function as proposed here. A key strength of this study is that the latest proposed version of the GG model, Adjusted GG-NDVI, overcomes limitations of both relative evaporation as proposed by Granger and Gray (1989) and the assumption of a symmetric complementary relationship from the work of Bouchet (1963). Consequently, Adjusted GG-NDVI can lead to significantly increased accuracy of ET estimates under diverse climate conditions while producing comparable or even better results than the SSEBop operational remote sensing model.

Literature Cited

Allam, M. M., Jain Figueroa, A., McLaughlin, D. B., and Eltahir, E. A. B. (2016).

"Estimation of evaporation over the Upper Blue Nile basin by combining observations from satellites and river flow gauges." Water Resour. Res., 52.

Allen, R. G., Pereira, L. S., Raes, D., and Smith, M. (1998). "Crop evapotranspiration: Guidelines for computing crop water requirements." FAO Irrig. and Drain. Paper No. 56, Food and Agric. Orgn. of the United Nations; Rome.

Allen, R. G., Tasumi, M., Morse, A., and Trezza, R. (2007). "Satellite-Based Energy Balance for Mapping Evapotranspiration with Internalized Calibration (METRIC): Model." Journal of Irrigation and Drainage Engineering, 133 (4), 380-394.

Allen, R. G., Pereira, L. S., Howell, T. A., and Jensen, M. E. (2011). "Evapotranspiration information reporting: I." Factors governing measurement accuracy, Agricultural Water Management, 98, 899–920.

Anayah, F. M., and Kaluarachchi, J. J. (2014). "Improving the complementary methods to estimate evapotranspiration under diverse climatic and physical conditions." Hydrology and Earth System Sciences, 18, 2049-2064.

Aminzadeh, M., Roderick, M. L., and Or, D. (2016). "A generalized complementary relationship between actual and potential evaporation defined by a reference surface temperature." Water Resour. Res., 52, 385-406.

Bastiaanssen, W. G. M., Menenti, M., Feddes, R. A., and Holtslag, A. A. M. (1998). "The Surface Energy Balance Algorithm for Land (SEBAL): Part 1 Formulation." Journal of Hydrology, 198-212.

Bastiaanssen, W. G. M., Noordman, E. J. M., Pelgrum, H., Davids, G., Thoreson, B. P., and Allen, R. G. (2005). "SEBAL model with remotely sensed data to improve

water-resources management under actual field conditions." Journal of Irrigation and Drainage Engineering, 131, 85-93.

Bastiaanssen, W. G. M., Karimi, P., Rebelo, L-M., Duan, Z., Senay, G.B., Muttuwatte, L., and Smakhtin, V. (2014). "Earth Observation-based Assessment of the Water Production and Water Consumption of Nile Basin Agro-Ecosystems." Remote Sensing, 6, 10306-10334.

Barrow, C. J. (1992). *World atlas of desertification (United Nations Environment Programme)*, edited by N. Middleton and D. S. G. Thomas. Edward Arnold, London, 1992.

Biggs, T. W., Petropoulos, G. P., Velpuri, N. M., Marshall, M., Glenn, P., Nagler, P., and Messina, A. (2015). "Remote sensing of actual evapotranspiration from croplands." CRC Press 2015, 59-99.

Bouchet, R. J. (1963). "Evapotranspiration reelle et potentielle, signification climatique (Actual and Potential Evapotranspiration Climate Service)." Int. Assoc. Sci. Hydrol., 62, 134-142. France.

Brutsaert, W., and Stricker, H. (1979). "An advection-aridity approach to estimate actual regional evapotranspiration." Water Resour. Res., 15 (2), 443-450.

Budyko, M. I. (1974). *Climate and Life,* Xvii, Academic Press: New York.

Crago, R., and Crowley, R. (2005). "Complementary relationship for near-instantaneous evaporation." J. Hydrol., 300, 199-211.

Crago, R., Szilagyi, J., Qualls., and Huntington, J. (2016). "Rescaling the complementary relationship for land surface evaporation." Water Resources Research, 52, doi:10.1002/2016WR019753.

FEWSNET. (2015). “Famine Early Warning Systems Network.” http://earlywarning.usgs.gov/fews(Dec, 2015).

Fu, B. P. (1981). “On the calculation of the evaporation from land surface (in Chinese).” SCI. Atmos. Sin., 5 (1), 23-31.

Gavilána, P., Berengena, J., and Allen, R. G. (2007). “Measuring versus estimating net radiation and soil heat flux: Impact on Penman–Monteith reference ET estimates in semiarid regions.” Agricultural Water Management, 89, 275−286.

Granger, R. J. (1989). “A complementary relationship approach for evaporation from nonsaturated surfaces.” J. Hydrol., 111, 31-38.

Granger, R. J., and Gray, D. M. (1989). “Evaporation from natural nonsaturated surface.” J. Hydrol., 111, 21-29.

Han, S., Hu, H., and Yang, D. (2011). “A complementary relationship evaporation model referring to the Granger model and the advection aridity model.” Hydrol. Processes, 25 (13), 2094–2101.

Han, S, Tian, F., and Hu, H. (2014). “Positive or negative correlation between actual and potential evaporation? Evaluating using a nonlinear complementary relationship model.” Water Resour. Res., 50, 1322-1336.

Hobbins, M. T., Ramirez, J. A., Brown, T. C., and Classens, L. H. J. M. (2001). The complementary relationship in estimation of regional evapotranspiration: The complementary relationship areal evapotranspiration and advection-aridity models.” Water Resour. Res., 37 (5), 1367-1387.

Kahler, D. M., and Brutsaert, W. (2006). “Complementary relationship between daily evaporation in the environment and pan evaporation.” Water Resources Research,

42, W05413.

Kim, H., and Kaluarachchi, J. J. (2017). “Estimating evapotranspiration using the complementary relationship and the Budyko Framework.” Journal of Water and Climate Change, doi:10.2166/wcc.2017.148.

Li, D., Pan, M., Cong, Z., Zhang, L., and Wood, E. (2013). “Vegetation control on water and energy balance within the Budyko framework.” Water Resour. Res., 49, 969-976.

McMahon, T. A., Finlayson, B. L., and Peel, M. C. (2016). “Historical developments of models for estimating evaporation using standard meteorological data.” WIREs Water 2016.

Morton, F. I. (1983). “Operational estimates of areal evapotranspiration and their significance to the science and practice of hydrology.” J. Hydrol., 66, 1-76.

Mu, Q., Zhao, M., and Running, S. W. (2007). “Development of a global evapotranspiration algorithm based on MODIS and global meteorological data.” Remote Sens. Environ., 111(4), 519-536.

Mu, Q., Zhao, M., and Running, S. W. (2011). “Improvements to a MODIS global terrestrial evapotranspiration algorithm.” Remote Sens. Environ., 115, 1781-1800.

Penman, H. L. (1948). "Natural evaporation from open water, bare and grass.” Proceedings of the Royal Society A: Mathematical, Physical and Engineering Sciences, 193(1032), 120-145.

Pettorelli, N., Vik, J. O., Mysterud, A., Gaillard, J. M., Tucker, C. J., and Stenseth, N. C. (2005). “Using the satellite-derived NDVI to assess ecological responses to environmental change.” TRENDS in Ecology and Evolution, 20(9), 503-510.

Priestley, C. H. B., and Taylor, R. J. (1972). "On the assessment of surface heat fluxes and evaporation using large-scale parameters." Monthly Wather Rev. 100, 81-92.

Roderick, M. L., Hobbins, M. T., and Farquhar, G. D. (2009). "Pan evaporation trends and the terrestrial water balance. II: Energy balance and interpretation." Geogr. Compass, 3(2), 761–780.

Senay, G., Budde, M., Verdin, J., and Melesse, A. (2007). "A coupled remote sensing and simplified surface energy balance approach to estimate actual evapotranspiration from irrigated fields." Sensors 7, 979–1000.

Senay, G. B., Verdin, J. P., Lietzow, R., and Melesse, A. M. (2008). "Global daily reference evapotranspiration modelling and evaluation." J. Am. Water Res. Assoc., 44, 969-979.

Senay, G. B., Budde, M. E., and Verdin, J. P. (2011a). "Enhancing the simplified surface energy balance (SSEB) approach for estimating landscape ET: Validation with the METRIC model." Agricultural Water Management, 98, 606–618.

Senay, G.B., Leake, S., Nagler, P.L., Artan, G., Dickinson, J., Cordova, J. T., and Glenn, E. P. (2011b). "Estimating Basin Scale Evapotranspiration (ET) by Water Balance and Remote Sensing Methods." Hydrological Processes, 25, 4037-4049.

Senay, G. B., Bohms, S., Singh, R. K., Gowda, P. H., Velpuri, N.M., Alemu, H., and Verdin, J.P. (2013). "Operational evapotranspiration mapping using remote sensing and weather datasets: A new parameterization for the SSEB approach." Journal of the American Water Resources Association 49, 577–591.

Su, H., McCabe, M. F., Wood, E. F., Su, Z., and Prueger, J. H. (2005). "Modeling evapotranspiration during SMACEX: Comparing two approaches for local- and

regional-scale prediction.” Journal of Hydrometeorology, 6, 910-922.

Szilagyi, J., and Jozsa, J. (2008). “New findings about the complementary relationship based evaporation estimation methods.” J. Hydrol., 354, 171-186.

Szilagyi, J., Crago, R., and Qualls, R. J. (2017). “A calibration-free formulation of the complementary relationship of evaporation for continental-scale hydrology.” Journal of Geophysical Research Atmospheres, 122, doi:10.1002/2016JD025611.

Thompson, S. E., Harman, C. J., Konings, A. G., Sivapalan, M., Neal, A., and Troch, P. A. (2011). “Comparative hydrology across AmeriFlux sites: The variable roles of climate, vegetation, and groundwater.” Water Resour. Res., 47, W00J07.

Velpuri, N. M., Senay, G. B., Singh, R. K., Bohms, S., and Verdin, J. P. (2013). “A comprehensive evaluation of two MODIS evapotranspiration products over the conterminous United States: Using point and gridded FLUXNET and water balance ET.” Remote Sensing of Environment, 139, 35-49.

Venturini, V., Islam, S., and Rodríguez, L. (2008). “Estimation of evaporative fraction and evapotranspiration from MODIS products using a complementary based model.” Remote Sensing of Environment, 112, 132-141, ISSN 0034-4257.

Venturini, V., Rodriguez, L., and Bisht, G. (2011). “A comparison among different modified Priestley and Taylor´s equation to calculate actual evapotranspiration.” International Journal of Remote Sensing, In Press, ISSN 0143-1161.

Xu, C. Y., and Singh, V. P. (2005). “Evaluation of three complementary relationship evapotranspiration models by water balance approach to estimate actual regional evapotranspiration in different climate regions.” Journal of Hydrology, 308, 105-121, ISSN 0022-1694.

Yang, D., Sun, F., Liu, Z., Cong, Z., and Lei, Z. (2006). "Interpreting the complementary relationship in non-humid environments based on the Budyko and Penman hypotheses." Geophysical Research Letters, 33, L18402.

Yang, D., Shao, W., Yeh, P. J. F., Yang, H., Kanae, S., and Oki, T. (2009). "Impact of vegetation coverage on regional water balance in the nonhumid regions of China." Water Resour. Res., 45, W00A14.

Yuan, W. P., Liu, S. G., Yu, G. R., Bonnefond, J. M., Chen, J. Q., Davis, K., Resai, A. R., Goldstein, A. H., Gianelle, D., Rossi, F., Suker, A. E., and Verma, S. B. (2010). "Global estimates of evapotranspiration and gross primary production based on MODIS and global meteorology data." Remote Sensing of Environment, 114(7), 1416-1431.

Zhang, L., Hickel, K., Dawes, W. R., Chiew, F. H. S., Western, A. W., and Briggs, P. R. (2004). "A rational function approach for estimating mean annual evapotranspiration." Water Resour. Res., 40, 02502.

Zhang, S., Yang, H., Yang, D., and Jayawardena, A. W. (2016). "Quantifying the effect of vegetation change on the regional water balance within the Budyko framework." Geophys. Res. Lett., 43.

Table 3-1. Comparison of monthly ET estimates between SSEBop and GG-NDVI using AmeriFlux data from 2000 to 2007.

Year	AmeriFlux mean [mm/month]	R-square		RMSE [mm/month]	
		SSEBop	GG-NDVI	SSEBop	GG-NDVI
2000	43	0.82	0.79	16	15
2001	44	0.54	0.58	23	20
2002	41	0.73	0.67	19	16
2003	42	0.68	0.65	21	17
2004	42	0.68	0.60	18	18
2005	42	0.37	0.57	28	18
2006	41	0.61	0.55	20	18
2007	34	0.40	0.40	18	17
All years	44	0.65	0.61	19	18

Table 2. Comparison of RMSE between GG-NDVI, SSEBop, and Adjusted GG-NDVI across 60 sites.

ET Model	RMSE [mm/month]		
	Min	Mean	Max
GG-NDVI	7	18	48
SSEBop	8	20	48
Adjusted GG-NDVI	7	15	34

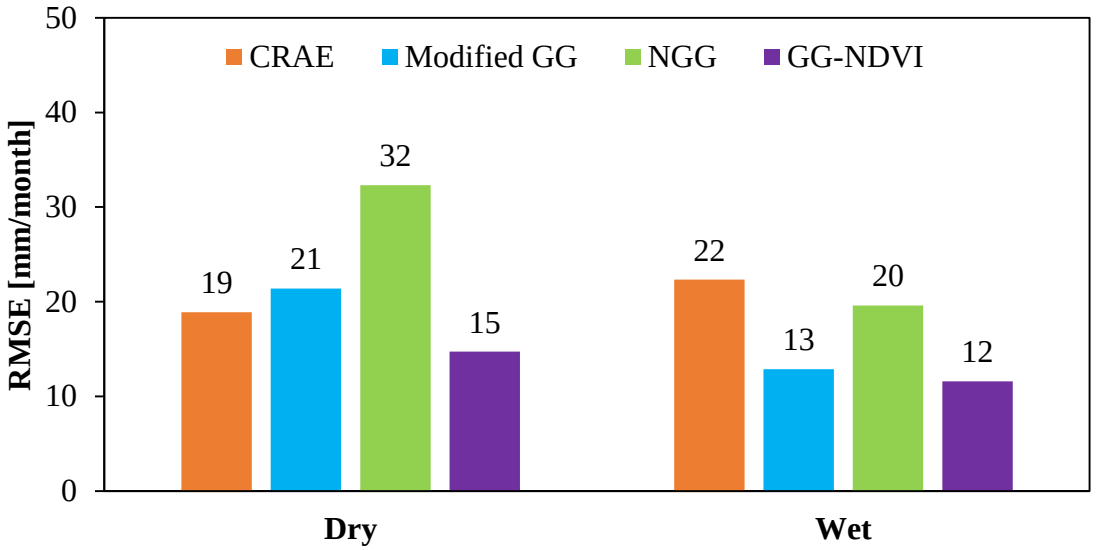

Figure 3-1. Comparison of RMSE between different complementary relationship models for 29 dry and 30 wet sites in the United States. NGG and GG-NDVI refer to the models of Han et al. (2011) and Kim and Kaluarachchi (2017), respectively.

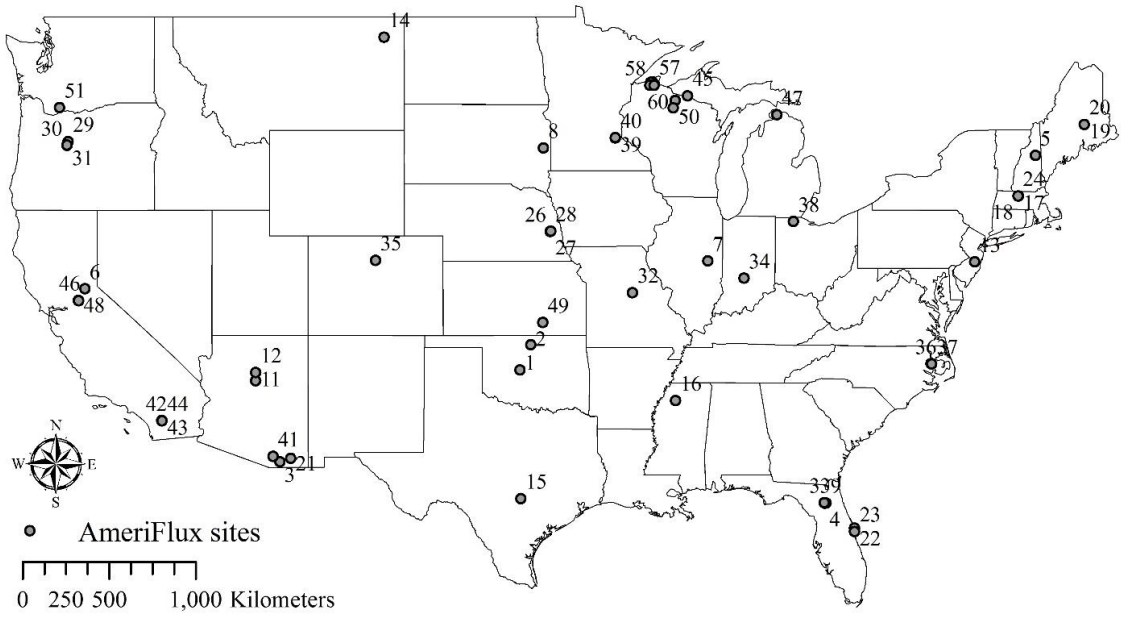

Figure 3-2. Locations of 60 AmeriFlux EC sites used in this study with number.

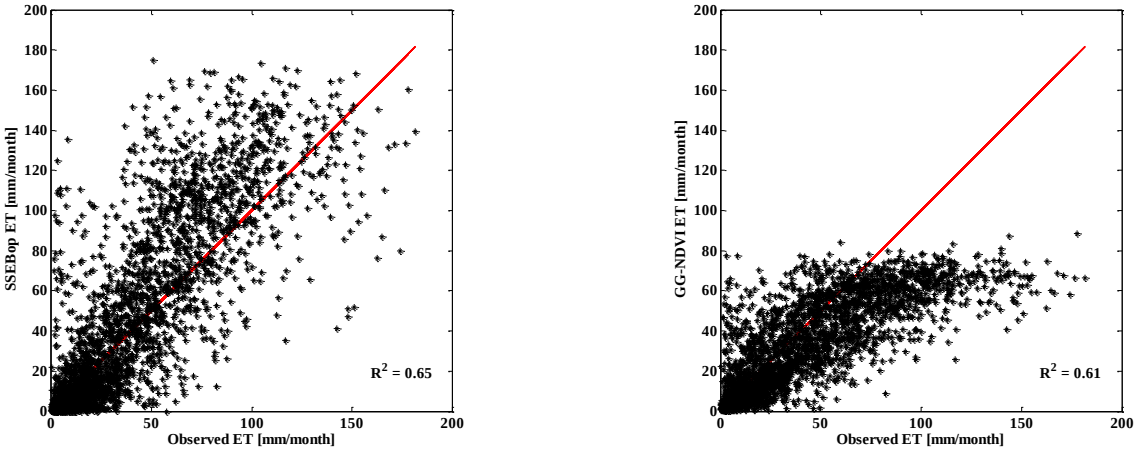

Figure 3-3. Validation results of monthly ET estimates from SSEBop and GG-NDVI against AmeriFlux ET data between 2000 and 2007.

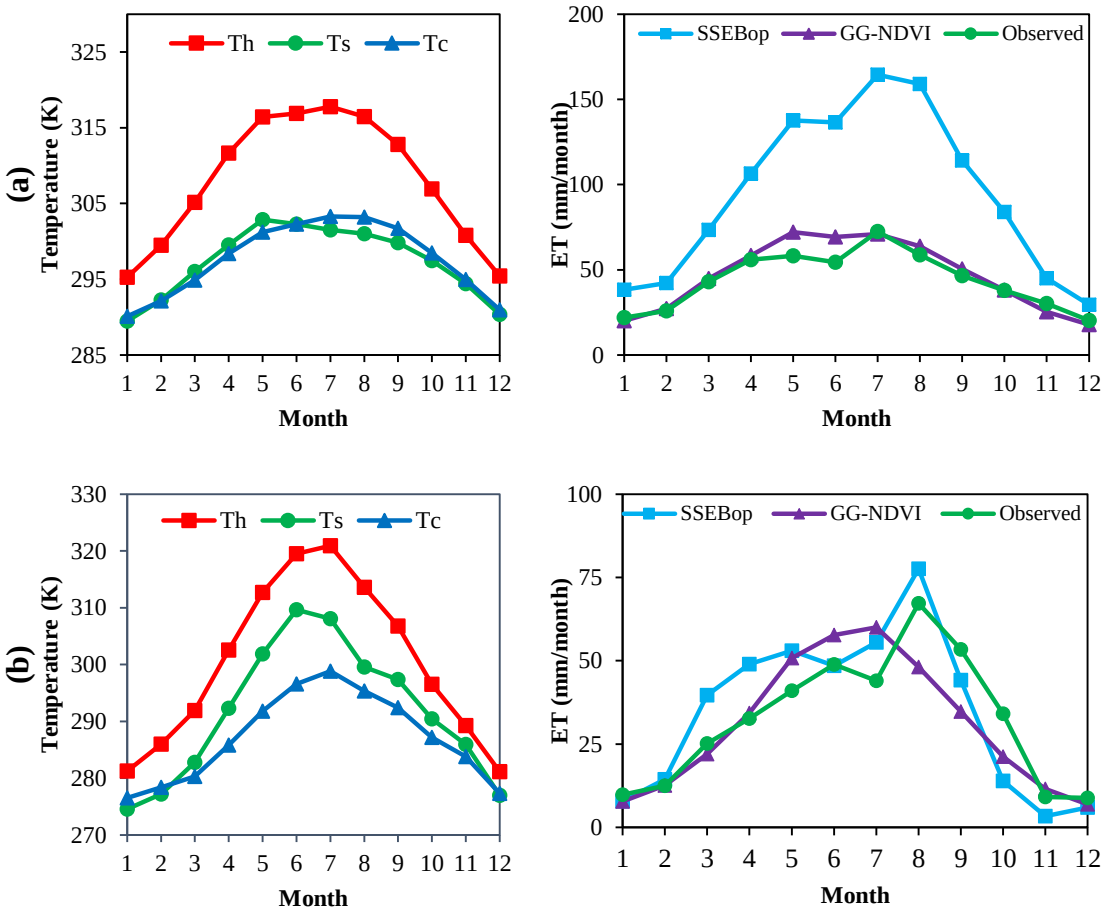

Figure 3-4. Temporal variation of 8-day average Ts, Th, Tc (left) and monthly ET estimates from SSEBop and GG-NDVI and measured ET at (a) Austin Cary in Florida and (b) Flagstaff in Arizona for 2005.

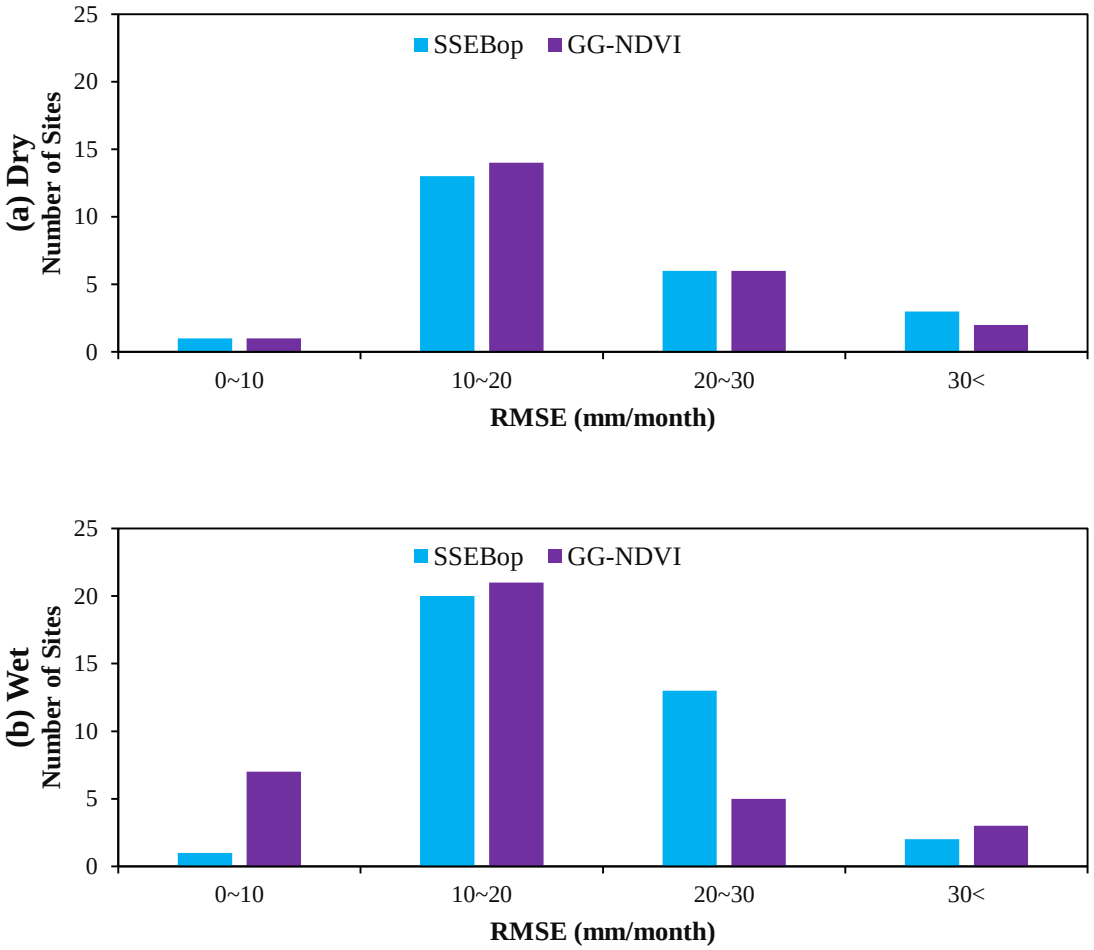

Figure 3-5. Histogram of RMSE values of SSEBop and GG-NDVI for (a) dry and (b) wet sites.

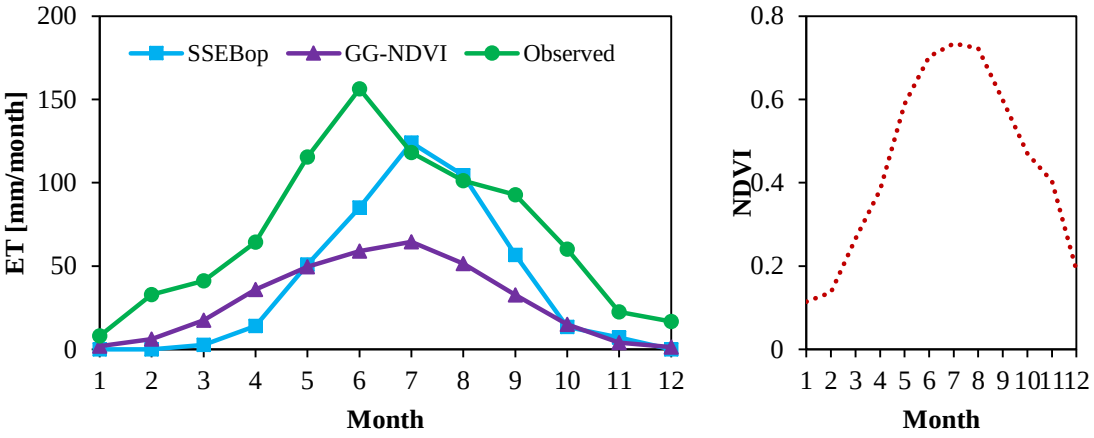

Figure 3-6. Comparisons of monthly ET between SSEBop and GG-NDVI against measured ET (left) and time-series of NDVI at Brookings in South Dakota (right).

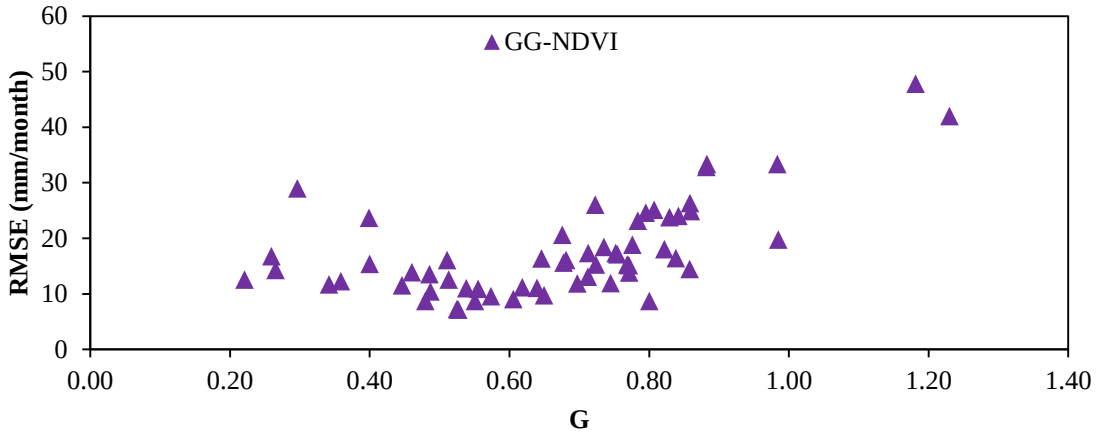

Figure 3-7. RMSE from GG-NDVI versus relative evaporation ($G = \mathrm{ET}/\mathrm{ETP}$).

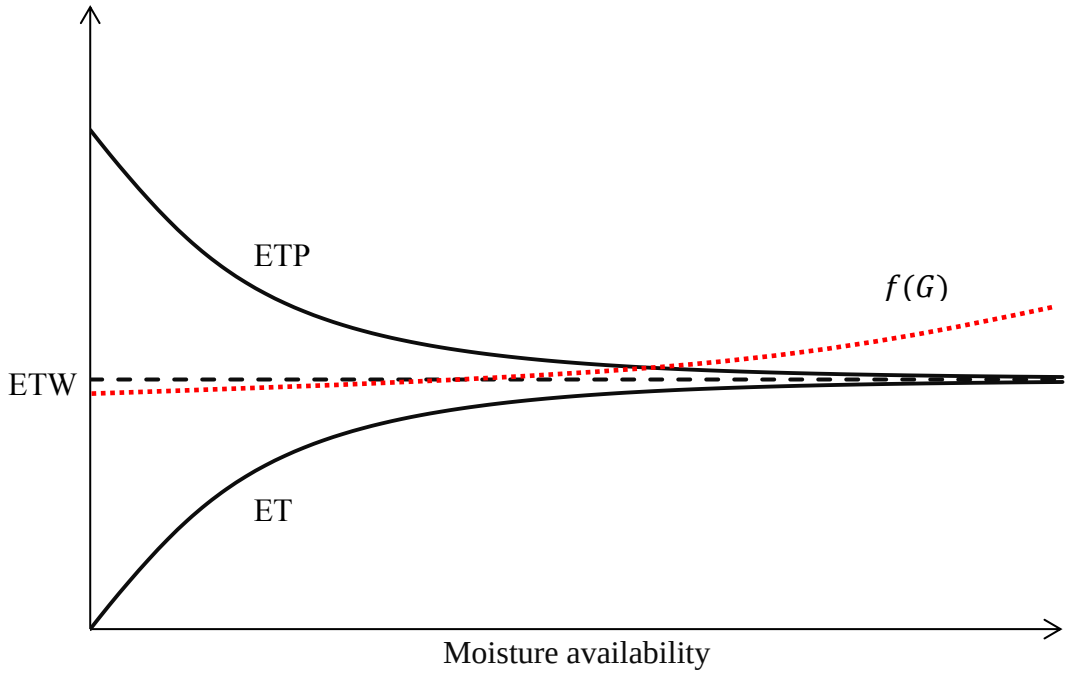

Figure 3-8. A schematic representation of the complementary relationship between ET, ETP, and ETW with the proposed correction function, $f(G)$.

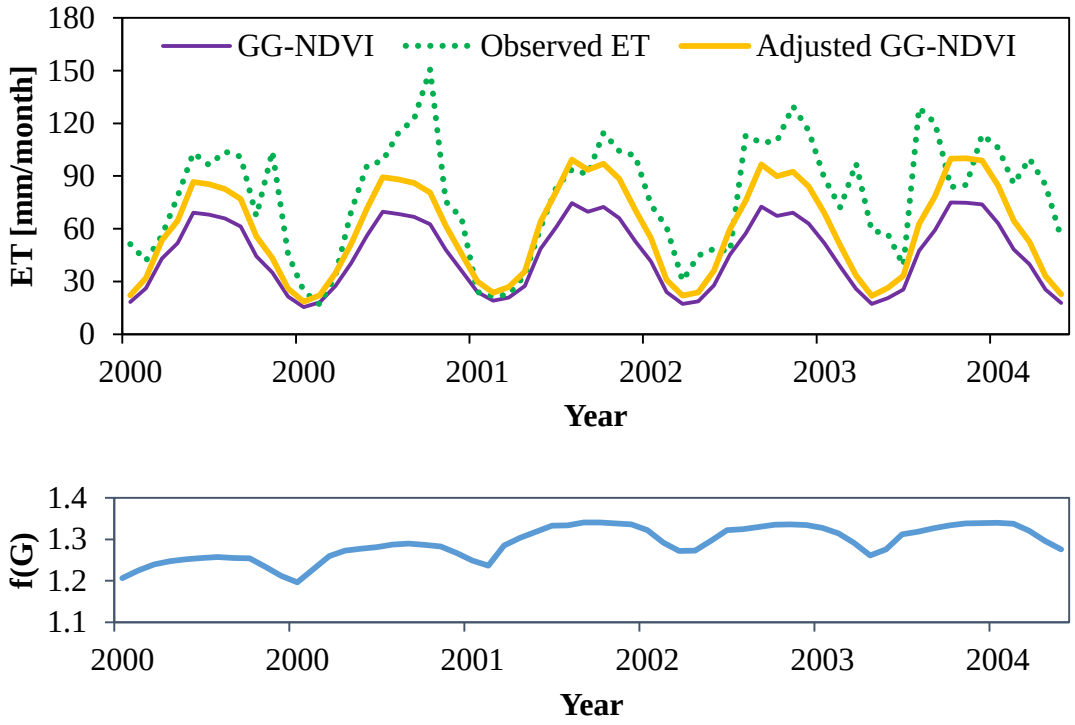

Figure 3-9(a). Comparison of monthly ET values of GG-NDVI and Adjusted GG-NDVI with measured ET and the corresponding $f(G)$ at Mize, Florida from 2000 to 2004.

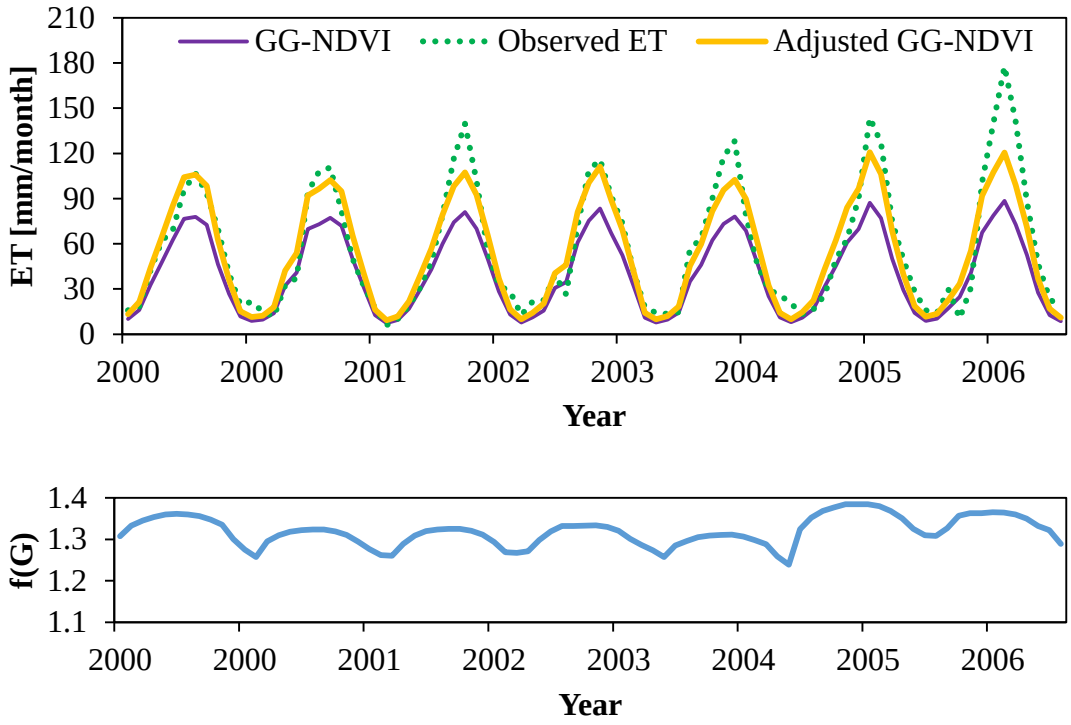

Figure 3-9(b). Comparison of monthly ET values of GG-NDVI and Adjusted GG-NDVI with measured ET and the corresponding $f(G)$ at Blodgett, California from 2000 to 2006.

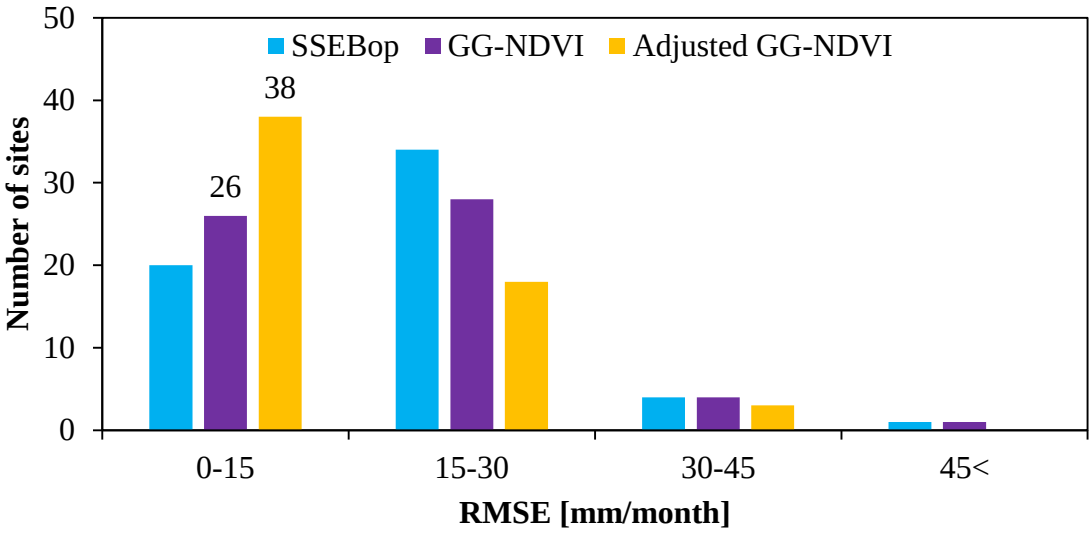

Figure 3-10. Comparison of RMSE values between different ET estimation models.

CHAPTER 4

DROUGHT MONITORING USING THE COMPLEMENTARY RELATIONSHIP AND LAND SURFACE INFORMATION

Abstract

Many operational drought indices focus on the effects of precipitation and temperature for drought monitoring, and the state-of-art drought monitoring indices were developed to address vegetation condition with advanced remote sensing technology. However, only a few are focused on the use of actual evapotranspiration (ET) when a drought index is defined. The Standardized Evapotranspiration Deficit Index (SEDI) was developed by using actual ET and the statistical approach. Although the results of SEDI demonstrated that the use of actual ET can provide a reliable measure for drought monitor, the SEDI did not address the effect of precipitation. Therefore, we brought the enhanced complementary relationship method to comprehensively consider precipitation and vegetation condition when depicting drought condition. We compared the proposed drought index with the U.S. Drought Monitor (USDM) which is widely used within the United States. The results of this study showed that the drought patterns from the proposed index were consistent with the USDM, and the use of accurate ET method improved its performance as a drought index. The key strengths of this study are that the proposed index can serve as an indicator of rapidly droughts developing over a few weeks, and uniquely describes drought conditions with vegetation condition which has large impacts on drought compared to other drought indices.

Introduction

Drought ranks fifth among the destructive natural disasters in the United States. Since 1996, drought has resulted in $35.4 billion worth of damage and losses, based on the NOAA's Severe Weather Data Inventory. Also, drought's impacts may affect major sectors of society (e.g., agriculture, economics, public health, recreation, and water resources) over several years in a row. For these reasons, many organizations and governments pay attention to droughts and effort has been devoted to developing a new drought index or technique for drought analysis and monitoring. A substantial improvement in drought monitoring systems has taken place during the twentieth century around the world, greatly improving the ability to provide relevant and timely drought information in terms of early warning to decision makers.

Historically, it is only since the work of Palmer (1965) that the study of drought index has gained momentum. The Palmer Drought Severity Index (PDSI; Palmer, 1965) is based on the supply and demand concept of the water balance equation which incorporates precipitation, moisture supply, runoff, and evaporation demand at surface level. The PDSI has become a standard index for measuring meteorological drought in the United States. However, the PDSI suffers from some serious weaknesses. Alley (1984) and Karl (1983, 1986) found that the performance of the PDSI was particularly poor in the western United States and its values are not comparable between diverse climate conditions. Similarly, other authors (Akinremi et al., 1996; Weber and Nkemdirim, 1998) showed that the PDSI values are influenced by the calibration period and the empirical constants in the index are derived from a relatively small number of locations. Many problems were solved by Wells et al. (2004), who developed the self-

calibrated PDSI (sc-PDSI) by replacing empirical constants in the index with dynamically calculated values. Nevertheless, the fixed temporal scale of the PDSI, which makes it difficult to use in rapidly evolving drought conditions, still remains. In this respect, the Standardized Precipitation Index (SPI) developed by McKee et al. (1993) can be calculated at different time scales with considerations of groundwater, soil moisture, reservoir storages, snowpack, and river discharges. The SPI can be calculated for any weekly or monthly time scale since it is normalized by the statistical approach of the historical record at every location. The SPI value also places the severity of a current drought into a historical perspective because the frequency of each value is known. This is an important difference between the SPI and the PDSI. To date, several studies confirmed the effectiveness of SPI (Khan et al., 2008; Patel et al., 2007; Sims et al., 2002; Vicente-Serrano et al., 2006), and the index is accepted and recommended by the World Meteorological Organization (WMO) as the primary meteorological drought index. Furthermore, the SPI has a strong correlation with the PDSI at 9- and 12- month time scales (Lloyd-Huges and Saunders, 2002; Redmond, 2002). Despite its success, the SPI suffers from the main criticism that it is based only on precipitation data. The index does not consider other variables that can influence droughts such as temperature, evapotranspiration, and wind speed. As noted by Hu and Willson (2000), the effects of precipitation and temperature on PDSI are almost equal when both have similar magnitude. Similarly, Rebetze et al. (2006) showed that the extremely high temperatures during the summer of 2003 increased evapotranspiration and extended drought. Also, Barriopedro et al. (2011) observed that droughts of 2010 in Europe and Russia were caused by a strong heat wave. More importantly, the empirical study of Vicente-Serrano

et al. (2010) demonstrated that the severity of drought is directly related to the temperature increase, and neither the PDSI nor the SPI indices could identify the drought caused by temperature increase. Overall, these studies clearly indicate that temperature is an important driving factor of drought index.

Taking the effect of temperature into account, the Standardized Precipitation Evapotranspiration Index (SPEI, Vicento-Serrano et al., 2010) was developed using the difference between precipitation and potential evapotranspiration (ETP). Up to now, the SPEI has been used in several studies for drought monitoring (Fuchs et al., 2012; Potop, 2011; Sohn et al., 2013). Abiodun et al. (2013) and Yu et al. (2013) investigated climate change with the SPEI. However, one of the limitations with the SPEI is that the drought of SPEI is not defined when ETP is zero, which is common in many regions of the world during winter. In the same vein, some scholars suggested that the use of actual ET instead of ETP is a better approach when a drought index is defined (Dai, 2011; Joetzjer et al., 2012; Kim and Rhee, 2016). The study conducted by Kim and Rhee (2016) demonstrated that considering actual ET can provide a reliable measure of drought severity compared with PDSI and SPI. The drought index they proposed, the Standardized Evapotranspiration Deficit Index (SEDI), was estimated by combining the actual ET from the Bouchet (1983) hypothesis with a structure of the SPI. They estimated actual ET using the method of Anayah and Kaluarachchi (2014) which was validated by measured ET at 34 global FLUXNET sites, and the wet environment (ETW) is calculated by using the equation of Priestley and Taylor (1972). Then, Kim and Rhee (2016) used ETW minus actual ET to measure drought conditions. As a result, the spatial drought patterns of the SEDI were consistent with the PDSI and SPI over the contiguous United States,

and this index could identify vegetative droughts such as a Vegetation Health Index (VHI). However, this study would have been much more useful if the authors addressed the precipitation and used the accurate ET method. Taking these points into account, this study has focused on developing a drought index with an enhanced ET method including precipitation and remote sensing vegetation data. The specific objective is to evaluate the applicability of the proposed index in this study over the contiguous United States (CONUS) by comparing it with the U.S. Drought Monitor (USDM) which is the most widely used tool in the United State.

Methodology and Data

Methodology

We propose to develop a simple drought index called the Evapotranspiration Water Deficit Drought Index (EWDI), which is derived from precipitation, meteorological data, and vegetation information. EWDI uses the structure of SPI with the monthly difference between ETW and ET. This value represents water deficit using the complementary relationship. The complementary relationship to estimate ET will be addressed in the following sections followed by a non-parametric approach to calculating the probability-based drought index.

Complementary relationship

The first complementary relationship was developed by Bouchet (1963) and hypothesized that the decrease in evapotranspiration is matched with an increase in potential evapotranspiration as the surface dries. The primary advantage of the

complementary relationship is requiring only meteorological data. However, Granger (1989) argued that the symmetric relationship between evapotranspiration and potential evapotranspiration is only true when the temperature is near 6 ˚C, and Granger and Gray (1989) proposed an improved complementary relationship using the psychrometric constant and the slope of the saturation vapor pressure curve (widely known as the GG model). Later, many studies demonstrated the performance of GG model in wide range of surface and atmospheric conditions (Aminzadeh et al., 2016; Han et al., 2011; Hobbins et al., 2001; Kahler and Brutsaert, 2006; Kim and Kaluarachchi, 2017a; 2017b; Szilagyi and Jozsa, 2008). The model of Kim and Kaluarachchi (2017a) was validated using measured ET from 75 AmeriFlux sites and showed the lowest mean Root Mean Square Error (RMSE) compared to the Complementary Relationship Areal Evapotranspiration or commonly known as the CRAE method (Morton, 1983), the Advection-Aridity model (Brutsaert and Stricker, 1979), the modified GG model of Anayah and Kaluarachchi (2014), and recent studies (Han et al., 2011; Mu et al., 2007, 2011; Thompson et al., 2011). Moreover, Kim and Kaluarachchi (2017b) further validated the modified GG model of Anayah and Kaluarachchi (2014) through a direct comparison with a remote sensing methodology, the operational Simplified Surface Energy Balance (SSEBop) model (Senay et al., 2013). This work improved the model to overcome the symmetric behavior assumption of the complementary relationship. These results indicate that the model of Kim and Kaluarachchi (2017b) can be used as an accurate and a reliable method to estimate ET under a variety of climatic and physical conditions including severe arid conditions.

The general form of the complementary relationship is

$$ET = k * ETW - ETP \quad (1)$$

where ET, ETP, and ETW are in mm/day. ETW represents wet environment evaporation (mm/day) which is ET of a surface with unlimited moisture and most often derived from the Priestley-Taylor equation (Priestley and Taylor, 1972). k is assumed to be 2 describing a symmetrical relationship between ET and ETP proposed by Bouchet (1963). Although the complementary relationship has been successfully applied to a wide range of physical and surface conditions for many years (Brutsaert and Stricker, 1979; Granger and Gray, 1989; Hobbins et al. 2001; Morton, 1983; Szilagyu and Jozsa, 2008), there are drawbacks associated with the symmetrical assumption that says the decrease in ET is matched with an increase in ETP as the surface dries. Kahler and Brutsaert (2006) presented that k can be around 5, and Aminzadeh et al. (2016) extended the asymmetric complementary relationship based on the study of Kahler and Brutsaert (2006). Recently, Kim and Kaluarachchi (2017b) proposed the exponential correction function and demonstrated that the inclusion of relative evaporation with the newly proposed correction function greatly improved the performance. The ET model of Kim and Kaluarachchi (2017b) is described in Eq. (2).

$$ET + ETP = 2f(G) * ETW \quad (2)$$

where $f(G)$ is the correction function. The proposed nonlinear correction function was derived from 2772 data of 60 AmeriFlux station (Kim and Kaluarachchi, 2017b) and given by Eq. (3).

$$f(G) = \alpha e^{\beta G} \quad (3)$$

A multiple regression analysis showed the values of α and β to be 0.7895 and

0.9655, respectively. G of Eq. (3) is the relative evaporation parameter, the ratio of actual ET to ETP, proposed by Granger and Gray (1989). Later, Kim and Kaluarachchi (2017a, 2017b) successfully proposed an improve approach to calculate G using the Budyko framework (Li et al., 2013). The updated G parameter is given in Eq. (4).

$$G = \frac{ET}{ETP} = 1 + \frac{P}{ETP} - \left[1 + \left(\frac{P}{ETP}\right)\right]^{1/\omega} \quad (4)$$

where P is precipitation and ETP is estimated using Penman's (1948) equation. Parameter ω is a constant that represents the land surface conditions, especially the vegetation cover (Li et al., 2013). Furthermore, ω is linearly related with the vegetation cover estimated by Normalized Difference Vegetation Index using Eq. (5).

$$\omega = a \times \frac{NDVI - NDVI_{min}}{NDVI_{max} - NDVI_{min}} + b \quad (5)$$

where a and b are constants that are found for each site. An optimal ω value can be derived through a curve fitting method that minimizes the mean squared errors between the Budyko modeled annual evaporation ratios and the measured values (Li et al., 2013). Having found G from Eq. (4) and estimated ETW from the Priestley-Taylor's equation (1972), ET is estimated from Eq. (6).

$$ET = \frac{2G}{G+1} f(G) * ETW \quad (6)$$

The work described in this study uses this ET model and will be referred as GG-NDVI whereas the ET method used by Kim and Rhee (2016) is the modified GG model (Anayah and Kaluarachchi, 2014)

EWDI formulation

With a known value for ET, the difference between ETW and ET for the month i

is calculating using Eq. (7), which provides a simple measure of the water deficit D_i for the particular month i.

$$D_i = ETW_i - ET_i \quad (7)$$

Given the monthly time-series of D_i, EWDI uses a non-parametric approach, in which empirically derived probabilities are obtained through an inverse normal approximation (Abramowitz and Stegun, 1965) because this probabilistic approach allows a consistent comparison between EWDI against other standardized indices (Farahmand and AghaKouchak, 2015; Vicente-Serrano et al., 2010).

The probability distribution function of the D_i, according to the Tukey distribution, is given by Eq. (8).

$$P(D_i) = \frac{i-0.33}{n+0.33} \quad (8)$$

where $P(D_i)$ is the empirical probability of D_i which is aggregated across the period of interest. In this study, we used 12-month duration for accumulating D_i because 9-12 month time-scale is the most useful in estimating the extreme drought conditions (Begueria., 2014; Hobbins et al., 2016). For example, to calculate a 12-month EWDI in December, D_i is summed over the period from January to December. i is the rank of the aggregated D_i in the historical time series ($i = 1$ is the maximum D_i) and n is the number of observations in the series being ranked. EWDI then can be easily derived following the classical approximation of Abramowitz and Stegun (1965),

$$EWDI = W - \frac{C_0+C_1W+C_2W^2}{1+d_1W+d_2W^2+d_3W^3} \quad (9)$$

where

$$W = \sqrt{-2\ln P(D_i)} \text{ for } P(D_i) \leq 0.5 \quad (10)$$

If $P(D_i) > 0.5$, replace $P(D_i)$ with $[1 - P(D_i)]$ and the sign of EWDI is reversed. The constants are $C_0 = 2.515517$, $C_1 = 0.802853$, $C_2 = 0.010328$, $d_1 = 1.432788$, $d_2 = 0.189269$, and $d_3 = 0.001308$. The average value of EWDI is 0, and the standard deviation is 1. A zero EWDI value means that D_i accumulated over the aggregation period in the year of interest is equal to the median value, positive value indicates drought, and negative is wet condition.

Hereafter, drought index EWDI estimated from the modified GG (Anayah and Kaluarachchi, 2014) is called EWDI-*mod*. Similarly, drought index EWDI estimated using GG-NDVI (Kim and Kaluarachchi, 2017b) is called EWDI-*ndvi*.

Data

Required meteorological data to calculate both ET values (modified GG or GG-NDVI) are air temperature, precipitation, elevation (pressure), net radiation, wind speed, and NDVI. Net radiation was estimated using the equations suggested by Allen et al. (2007). Air temperature and precipitation data are from the PRISM (Parameter-elevation Regressions on Independent Slopes Model) climate group (available at http://prism.oregonstate.edu/, last accessed on Nov, 2016) at 4-km resolution for the period 2000 – 2015 covering the CONUS. Wind speed was collected from Climate Monitoring at NOAA's National Centers for Environmental Information (available at https://www.ncdc.noaa.gov/societal-impacts/wind/, last assessed on Nov, 2016). Monthly NDVI data required for the GG-NDVI method are from the NASA Earth Observations (NEO, available at http://neo.sci.gsfc.nasa.gov/, last assessed on Nov, 2016).

To assess the capability of EWDI, we used USDM to compare the differences

between the two indices during the evolution of drought through time and space. USDM is derived from measurements of climatic, hydrologic, and soil conditions as well as expert comments from the region (Anderson et al., 2013; Svoboda et al., 2002). USDM is not a forecast instead it assesses the current drought conditions. USDM divides drought severity into five classes: abnormally dry (D0), moderate drought (D1), severe drought (D2), extreme drought (D3), and exceptional drought (D4). All drought indices used in this study were converted to USDM classes as presented in Table 1. Additionally, we compared EWDI against PDSI and SPI which were retrieved from WestWide Drought Tracker (WWDT, available at http://www.wrcc.dri.edu/wwdt/about.html, last assessed on Jan, 2017). USDM data from 2000 to 2015 were collected from the USDM website (http://droughtmonitor.unl.edu/Home.aspx), and four indices are resampled to match the 4-km resolution of EWDI using bilinear interpolation in ArcMap software.

We also used EC flux tower data (in mm/month) from FLUXNET stations to perform a comparison of modified GG and GG-NDVI ET products. The latent heat flux data were collected from Oak Ridge National Laboratory's AmeriFlux website (http://ameriflux.ornl.gov/, last accessed on Nov 23, 2016). The tower-measured monthly latent heat flux data were calculated using the equation as $ET = \mathrm{LE}/\lambda$, where LE is the latent heat flux (W/m^2) and λ is the latent heat of vaporization (2.45 MJ/kg).

Results and Discussion

Validation of EWDI

The Pearson correlation coefficient was used to determine which ET method is the best estimating drought. Like SPI and other drought indices, EWDI can be estimated

at different time-scales from which specific time aggregated versions are selected. Figure 4-1 provides the results obtained from the correlation coefficient between two EWDI results and USDM for years 2001 to 2015. EWDI using the GG-NDVI ET model generally shows a stronger relationship with UDSM across CONUS. The area-averaged correlation coefficient over all pixels for EWDI from the modified GG model is 0.58, whereas GG-NDVI produced 0.72. Also, correlations between EWDI-*ndvi* and USDM are strongest over much of the Southern and Northern Rockies and Plains of the US climate regions, and highest in Texas ($r > 0.8$). This observation is consistent with the regions where soil moisture on land surfaces makes the largest contributions to ET, referred as "hot spot" of land-atmosphere coupling by Guo et al. (2006) and Koster et al. (2006).

In the same results, the Northeast and Upper Midwest are regions of moderate correlations ($0.4 < r < 0.6$) for EWDI-*ndvi*. It can be clearly seen from Fig. 4-1 that a significant improvement is attributed to the GG-NDVI model in Northwest, Upper Midwest, and Northeast climate regions of the USA. Moreover, the improved performance of EWDI-*ndvi* over the CONUS can be seen from Fig. 4-2. The percent area of CONUS covered by D0 (abnormally dry) and by D4 (exceptional drought) can be compared in Fig. 4-2(a) and 4-2(b), respectively. In Fig. 4-2(a), the drought conditions derived from GG-NDVI are similar to that estimated by USDM. EWDI-*mod* underestimated drought in 2005 and overestimated from 2006 to 2009 and overestimated in 2013 as well. From Fig. 4-2b, EWDI-*ndvi* produced extreme drought conditions (D4, exceptional drought) much better than EWDI-*mod*. It is very much plausible that these improved results are due to the use of an accurate ET method.

To further study these results, the San Bernardino County in California was selected. Figure 4-3 shows the location with the correlation coefficient between EWDI and USDM. The area averaged correlation coefficient over all pixels in California is 0.55 for EWDI-*mod*, and 0.70 for EWDI-*ndvi*. The EWDI-*mod* showed lower correlation (0.4 - 0.6) for most of San Bernardino County and even the northern county values ($r < 0.2$) were much lower than the county area-averaged correlation coefficient of 0.51. However, the correlation coefficients of EWDI-*ndvi* was between 0.6 to 0.8 for most of California and the county area-averaged values increased by 40% compared to EWDI-*mod*.

To compare the temporal drought patterns of EWDI-*mod* and EWDI-*ndvi*, Figure 4-4 presents monthly drought time-series with precipitation over a period of 15 years, and percent area of San Bernardino County covered by abnormally dry (D0) conditions from 2012 to 2015. This time period was selected because observed ET data are only available from 2012 to 2015. The San Bernardino County has a Mediterranean climate with dry summers and mild winters where 70% of precipitation falls from November to March (Fig. 4-4(a)). Heavy precipitation during the winter season has eased drought conditions in this county in 2005, 2010 and 2011.

As shown in Fig. 4-4(b), both EWDI-*mod* and EWDI-*ndvi* produced similar drought conditions until the middle of 2012. Thereafter, EWDI-*mod* overestimated drought until May 2013 and underestimated compared to USDM in 2014 and 2015. It is therefore possible to state that EWDI-*ndvi* estimated the drought condition better than EWDI-*mod*. These results may be explained by comparing the ET values shown in Fig. 4-4(c). The plot shows GG-NDVI ET against observed ET, and the same with the modified GG estimates from 2012 to 2015. The results show that the pattern of ET from

modified GG are much higher than observed ET whereas GG-NDVI shows similar patterns with observed ET. The mean RMSE is 37 mm/month for modified GG, and 7 mm/month for GG-NDVI. The overestimated ET from modified GG, which brings a small water deficit, resulting in a corresponding drought that is underestimated compared to USDM. Taken together, these results indicate that the water deficit derived from the complementary relationship can be used as a drought index and the use of an accurate ET method can improve the performance of EWDI.

Although the present results are significant, it should be noted that EWDI-*ndvi* for Minnesota showed the area-averaged correlation coefficient of 0.56 compared to 0.35 with EWDI-mod and Northeast Minnesota showed a weak correlation in the range of 0.2-0.4 as shown in Fig. 4-5.

For the temporal assessment of EWDI, the Goodhue County, which is showing the highest correlation in Minnesota, was selected. The corresponding monthly drought time-series of EWDI with precipitation are shown in Fig. 4-6(a). According to precipitation data from PRISM, the annual precipitation of 2003 was only 585 mm making it the driest year in the history for the Goodhue County. As a result, USDM showed almost the entire county to be abnormally dry (D0) from March 2003 to May 2004, and both EWDI-*mod* and EWDI-*ndvi* were consistent with USDM during this drought period as shown in Fig. 4-6(b). However, both did not capture drought conditions for the remaining years. According to the National Drought Mitigation Center and National Weather Services, the Goodhue County experienced drought every winter and spring (from December to March) since 2011 and then there was relief in the summer season (June, July, and August). For 2014 and 2015, EWDI-*mod* and EWDI-*ndvi* could

hardly estimate drought conditions. Year 2015 is the second driest year for the Goodhue County but most areas are considered undergoing the moderate drought (D2) condition. Severe drought (D3) conditions were present for few weeks and completely disappeared in a month. Interestingly, both ET methods performed well as shown in Fig. 4-6(c) with mean RMSE of 12 mm/month for modified GG and 10 mm/month for GG-NDVI. In other words, the performance of EWDI in the Goodhue County did not show improvements even though the ET model performed well.

A possible explanation may be that the complementary relationship is not adequate to estimate drought conditions under energy-limited conditions which usually occur when there is enough moisture such as seen in the Goodhue County (Hobbins et al., 2016; Koster et al., 2009; McEvoy et al., 2016). In the last decade, Minnesota had a high occurrence of surplus precipitation, 31% increase in heavy precipitation, and 71% increase in flooding events (Seeley, 2014). Thus, the climate of Goodhue County is becoming wetter and there is a significant difference in annual mean precipitation between the two counties: 155 mm for San Bernardino and 860 mm for Goodhue.

To understand the relationship between precipitation and the performance of EWDI, Figure 4-7 presents the individual monthly correlations between EWDI-*ndvi* and USDM for seven selected states (see Table 4-2), and monthly precipitation as well. The EWDI-*ndvi* correlation values with USDM were area-averaged over all pixels. For California, Nevada, and Utah, strong correlations are observed during the summer season which are the driest months of the year. In contrast, a weak correlation ($r < 0.4$) was found with USDM during the spring season (April – June) for Michigan and Illinois, and this observation is consistent with Koster et al. (2009). The low correlations with USDM

in parts of the East and North Central US including Minnesota may be linked to the behavior of ET. Several studies indicated that these regions have the energy-limited condition (Hobbins et al., 2016; Koster et al., 2009; McEvoy et al., 2016). Under this condition, ET does not only vary in response to the availability of water (precipitation) but also to the availability of energy (as reflect in ETP), and the relationship between ETW and ET in the complementary relationship vary in a parallel trend. This could be the reason that EWDI-*ndvi* may have poor performance in these regions.

While not shown here, we assessed the ability to use ETP in the EWDI model instead of ETW. While the use of ETP in drought calculation showed slightly better results in few regions, the correlation coefficients with USDM over the CONUS were not lower with both EWDI-*ndvi* and EWDI-*mod* because ETP too overestimated when annual precipitation is low.

Historical droughts over COUNS

Capturing the spatial pattern and severity of droughts are important to calculate an accurate drought index. Figure 4-8 presents three historical droughts in the CONUS using USDM, EWDI, SPI and PDSI. EWDI in Fig. 4-8 represents EWDI-*ndvi* because it showed better performance than EWDI-*mod*. The first case shows the drought of 2007. In early August, a historic heat wave arrived across the Southeast. As a result of the intense heat and minimal rainfall, droughts were broadly experienced across the Southeast and lower Central of parts of the USA. For example, more than 98% of Alabama and Tennessee were on the verge of extreme drought (D3) and it was observed that August 2007 is the hottest month in Alabama since 1950 according to the National Weather

Service (http://www.weather.gov/). During this historical drought of 2007, EWDI showed a similar spatial pattern of drought as USDM, whereas SPI indicated less drought in Alabama because SPI only considers precipitation (Kim and Rhee, 2016; McEvoy et al., 2016). Also, dry and hot conditions dominated the Western USA. USDM and EWDI continued to show D2 and D3 over much of California, Nevada, Utah, Idaho and Western Montana, while SPI underrepresented the spatial extent shown by USDM and EWDI, particularly over Utah, Idaho, and Montana. At this time, Idaho continued with the record-breaking heat event. August of 2007 was cooler than average with little showers across much of Washington and Western Oregon, and therefore these states gained relief from abnormally dry (D0). Meanwhile, wildfires remained active across the Northern Rockies and Northern Intermountain West. Many of the uncontained wildfires were located in Western Montana and Central Idaho and wildfires in Idaho burnt 6.5 million acres of vegetation by end of August and this was one of the largest fires to happen in Idaho (National Interagency Fire Center; https://www.nifc.gov/fireInfo/fireInfo_statistics.html). This distinction may be further exemplified using the drought index as a wildfire risk indicator.

The second case focuses on the drought of November 2009. Across Florida, the National Drought Mitigation Center reported that the last few months have been dry and 45% of Florida was abnormally dry (D0), but many areas of Florida were still showing no drought due to heavy rains that took place in May. In the Southern Plains, the area of moderate drought (D1) expanded southward to Texas because annual precipitation deficits were 250 mm below the average across most Southern Texas, and the rest of Texas reduced drought intensity and coverage because of heavy rain over central and

eastern parts of the state (Southern Regional Climate Center, http://www.srcc.lsu.edu/index.html). In the west, severe drought (D2) conditions expanded from Arizona towards California to include D1 to D2 conditions in Southern California as well as Southern Nevada. Drought intensity and spatial patterns derived from EWDI are comparable to that derived by USDM for this case with slight overestimation of drought intensity in Florida, Arizona, and Texas.

Interestingly, additional reassessment of the drought situation in Montana was made by experts in the field. D0 was removed from Western Montana and a small area of D0 was added along the north and eastern borders. However, Montana Drought Status formulated by the Governor's Drought and Water Supply Committee (http://dnrc.mt.gov/divisions/water/drought-management) reported that drought was a little or no concern in Eastern Montana in November 2009 similar to the results of EWDI. Additionally, USDM clearly identified moderate drought (D1) in Northern Minnesota in November 2009 as shown in Fig. 4-9. The reason is temperatures for the month averaged more than 5 °C above normal and precipitation was less than 20 mm across nine counties. USDM produced droughts in places such as Lake of the Woods, Beltrami, Hubbard, Cass, Itasca, Koochiching, St. Louis, Lake, and Cook as shown in Figs. 4-10(a) and 4-10(b). Meanwhile, EWDI produced nearly no drought in these regions. According to the Minnesota Department of Natural Resources (http://dnr.state.mn.us/climate/drought/index.html), November 2009 was ranked as the second warmest statewide, while October 2009 was the fifth wettest on record for Northern Minnesota, along with seventh snowiest. Thus, when there is ample precipitation from the previous month with warmer temperatures helped reduce the

drought conditions in Northern Minnesota in November 2009. In this regard, EWDI captured the precursor signals of water stress developing over few weeks and similar results were produced in Wyoming and Montana too. These results provide further support for the concept of EWDI and that it can be successfully used to monitor drought.

The third case focuses on the critical drought experienced across the Southern USA in 2011. In Texas, rainfall averages were about 280 mm/year, making it the driest year in Texas history and the agriculture losses were estimated at 5.2 billion dollars. Hot and dry conditions prevailed most of Texas and produced a large precipitation deficit. To make matters worse, excessive heat accompanied with hot maximum temperatures (>43 °C) in Texas and D3-D4 drought conditions expanded across Kansas and Oklahoma. At the end of July 2011, many locations recorded one of the driest months on record and all indices agreed and showed a wide spread of D3 and D4 conditions across these states. Farther southeast, despite the above average rains across Louisiana, Mississippi, and Alabama in early July, EWDI and SPI continued to indicate least severe drought condition of D2 because annual rainfall deficits were below the average across the regions based on data from the Southern Regional Climate Center (http://www.srcc.lsu.edu/index.html) and National Oceanic and Atmospheric Administration (NOAA, https://www.ncdc.noaa.gov/cag/). Meanwhile, EWDI estimated that moderate drought (D1) reached Southern Missouri and Tennessee and severe drought condition of D2 prevailed most of Alabama due to the record-setting heat affecting these regions for several weeks. Lastly, Figure 4-11 compares the correlation coefficients between USDM and three drought indices: EWDI, SPI, and PDSI. The area-averaged correlation coefficients over all pixels in the CONUS for USDM, SPI, and PDSI were

0.72, 0.57, and 0.56, respectively. Therefore, it can be concluded that the spatial and temporal distributions of drought derived from EWDI and USDM were more consistent for several major droughts over the CONUS and sometimes EWDI simulated drought conditions better than other indices.

Summary and Conclusions

The results of this work support that ET derived from the complementary relationship is able to capture drought conditions and the key to approach is the use of an accurate ET prediction method. ET from the proposed complementary relationship model, GG-NDVI, represents the current amount of water transferred to the atmosphere and ETW which is ET of a surface with unlimited moisture. Then, the difference between ETW and ET relates to surface water availability which is the important driver producing drought. Taking this into account, this study was designed to build a drought index, EWDI, based on ET by combining the structure of SPI, and to address its applicability by comparison to commonly used drought indices, USDM, SPI, and PDSI. In addition, it is important to test the reliability of a specific ET prediction model that can be accurately used in drought calculations. Thus, this study compared two different ET prediction models to calculate EWDI and then compared with existing drought indices.

The ET models selected for this work are modified GG (Anayah and Kaluarachchi, 2014) and GG-NDVI (Kim and Kaluarachchi, 2017b) and both use the original GG model (Granger and Gray, 1989) with updates. The modified GG model is independent of precipitation. The advantage of using of GG-NDVI is that it considers both precipitation and land surface conditions. Therefore, the GG-NDVI model can

produce comparable or even better ET estimates than other models (Kim and Kaluarachchi, 2017b) and EWDI derived from GG-NDVI showed much higher correlations with USDM than from modified GG. These results confirm that EWDI is able to capture drought conditions. Moreover, the results demonstrate that using an accurate ET model can help to improve drought monitoring performance and the results are consistent with those of Kim and Rhee (2016) who proposed the first ET-based drought index. Furthermore, the regions with high correlation between EWDI-*ndvi* and USDM are consistent with the 'hot spot' regions that are likely to be located between arid and wet areas (Guo et al., 2006; Koster et al., 2004, 2006). One unanticipated finding was that Minnesota was a region of weak correlations for both EWDI-*ndvi* and EWDI-*mod* even with accurate ET estimates from both modified GG and GG-NDVI. A possible reason for this weak correlation across Minnesota is due to the prevailing energy-limited conditions (Han et al., 2014; McEvoy et al., 2016). Within the complementary relationship when energy-limited conditions are present, ET and ETW varies in a parallel trend and ET is closer to ETW with increasing moisture (Kim and Kaluarachchi, 2017b). In other words, the water availability from precipitation controls the ET variability under water-limited conditions, and the strong correlation between precipitation and droughts estimated by EWDI-*ndvi* can be seen from Fig 4-7.

Despite this limitation, EWDI-*ndvi* could identify droughts over CONUS consistent with USDM from the drought incidents of August 2007, November 2009, and July 2011. Specifically, the August 2007 and the summer of 2015 (not shown in this study) showed that EWDI may be used as an indicator of wildfire risk. One of the significant findings to emerge from this study is that USDM required the reassessment of

drought of November 2009 whereas EWDI-*ndvi* produced the drought condition accurately. The unexpected performance of USDM occurred only three states in this study and it is important to understand the possible limitation of the USDM model. As noted by Svoboda et al. (2002) and the National Drought Mitigation Center, USDM requires additional indicators in the Western USA and it is not recommended for specific or local conditions because USDM can only be used to identify likely areas of drought impacts.

This work clearly suggests that EWDI can successfully capture droughts over CONUS, and the use of an accurate ET model can improve the performance of EWDI as a drought index. More importantly, EWDI derived from the GG-NDVI model that include land surface characteristics can uniquely describe drought conditions. Also, EWDI that uses land surface information has a large impact on drought monitoring compared to other drought indices, and EWDI may play an additional role in identifying wildfire risk. EWDI can be computed using data from PRISM and readily available remote sensing data from MODIS with similar or higher performance compared to USDM. In conclusion, the findings from this work have significant importance in understanding how ET can assist in a broader spectrum of decision-making related to water resources planning and drought management.

Literature Cited

Abiodun, B. J., Salami, A. T., Matthew, O. J., and Odedokun, S. (2013). "Potential impacts of afforestation on climate change and extreme events in Nigeria." Clim. Dyn., 41(2), 277 – 293, doi:10.1007/s00382-012-1523-9.

Abramowitz, M., and Stegun, I. A. (1965). *Handbook of Mathematical Functions, with Formulas, Graphs, and Mathematical Tables*, Dover Publications, 1046.

Alley, W. M. (1984). "The Palmer Drought Severity Index: Limitations and assumptions." J. Climate Appl. Meteor., 23, 1100 – 1109.

Akinremi, O. O., McGinm, S. M., and Barr, A. G. (1996). "Evaluation of the Palmer Drought Severity Index on the Canadian prairies." J. Climate, 9, 897 – 905.

Anderson, M. C., Hain, C., Otkin J., Zhan, X., Mo, K., Svoboda, M., Wardlow, B., and Pimstein, A. (2013). "An intercomparison of drought indicators based on thermal remote sensing and NLDAS-2 simulations with U.S. Drought Monitor classifications." J. Hydrometeor., 14, 1035-1056.

Allen, R. G., Tasumi, M., Morse, A., and Trezza, R. (2007). "Satellite-Based Energy Balance for Mapping Evapotranspiration with Internalized Calibration (METRIC): Model." Journal of Irrigation and Drainage Engineering, 133 (4), 380-394.

Anayah, F. M., and Kaluarachchi, J. J. (2014). "Improving the complementary methods to estimate evapotranspiration under diverse climatic and physical conditions." Hydrology and Earth System Sciences, 18, 2049-2064.

Aminzadeh, M., Roderick, M. L., and Or, D. (2016). "A generalized complementary relationship between actual and potential evaporation defined by a reference surface temperature." Water Resour. Res., 52, 385-406.

Barriopedro, D., Fischer, E. M., Luterbacher, J., Trigo, R. M., and Garcia-Herrera, R. (2011). "The hot summer of 2010: Redrawing the temperature record map of Europe." Science, 332(6026), 220 – 224.

Bouchet, R. J. (1963). "Evapotranspiration reelle et potentielle, signification climatique (Actual and Potential Evapotranspiration Climate Service)." Int. Assoc. Sci. Hydrol., 62, 134-142. France.

Brutsaert, W., and Stricker, H. (1979). "An advection-aridity approach to estimate actual regional evapotranspiration." Water Resour. Res., 15 (2), 443-450.

Dai, A. (2011). "Characteristics and trends in various forms of Palmer Drought Severity Index during 1900 – 2008." J. Geophys. Res., 116:D12115.

Farahmand, A., and AghaKouchak, A. (2015). "A generalized framework for deriving nonparametric standardized indicators." Adv. Water Resour., 76, 140-145.

Fuchs, B., Svoboda, M., Nothwehr, J., Poulsen, C., Sorensen, W., and Guttman, N. (2012). "A new National Drought Mitigation Center."

Granger, R. J. (1989). "A complementary relationship approach for evaporation from nonsaturated surfaces." J. Hydrol., 111, 31-38.

Granger, R. J., and Gray, D. M. (1989). "Evaporation from natural nonsaturated surface." J. Hydrol., 111, 21-29.

Guha-Sapir, D. (2011). "Natural disasters in countries with very high human development." CRED Crunch, 24, 1-2.

Guo, Z., Dirmeyer, P. A., Koster, R. D., Bonan, G., Chan, E., Cox, P., Gordon, C. T., Kanae, S., Kowalczyk, E., Lawrence, D., Liu, P., Lu, C. H., Malyshev, S., McAvaney, B., McGregor, J. L., Mitchell, K., Mocko, D., Oki, T., Olseson, K. W., Pitman, A., Sud, Y. C., Taylor, C. M., Verseghy, D., Vasic, R., Xue, Y., and Yamada, T. (2006). "GLACE: The Global Land-Atmosphere Coupling Experiment. Part II: Analysis." J. Hydrometeor., 7, 611-625.

Han, S., Hu, H., and Yang, D. (2011). "A complementary relationship evaporation model referring to the Granger model and the advection aridity model." Hydrol. Processes, 25 (13), 2094–2101.

Han, S, Tian, F., and Hu, H. (2014). "Positive or negative correlation between actual and potential evaporation? Evaluating using a nonlinear complementary relationship model." Water Resour. Res., 50, 1322-1336.

Hobbins, M. T., Ramirez, J. A., Brown, T. C., and Classens, L. H. J. M. (2001). "The complementary relationship in estimation of regional evapotranspiration: The complementary relationship areal evapotranspiration and advection-aridity models." Water Resour. Res., 37 (5), 1367-1387.

Hu, Q., and Willson, G. D. (2000). "Effect of temperature anomalies on the Palmer Drought Severity Index in the central United States." Int. J. Climatol., 20, 1899 – 1911.

Joetzjer, E., Douville, H., Delire, C., Ciais, P., Decharme, B., and Tyteca, S. (2012). "Evaluation of drought indices at interannual to climate change timescales: a case study over the Amazon and Mississippi river basins." Hydrol. Earth Syst. Sci. Discuss., 9, 13231 – 13249.

Karl, T. R. (1983). "Some spatial characteristics of drought duration in the United States." J. Climate Appl. Meteor., 22, 1356 – 1366.

Karl, T. R. (1986). "The sensitivity of the Palmer Drought Severity Index and Plamer's Z-index to their calibration coefficients including potential evapotranspiration." J. Climate Appl. Meteor., 25, 77 – 86.

Khan, S., Gabriel, H. F., and Rana, T. (2008). "Standard precipitation index to track

drought and assess impact of rainfall in water tables in irrigation areas." Irrig. Drain. Syst., 22, 159 – 177.

Kim, D., and Rhee, J. (2016). "A drought index based on actual evapotranspiration from the Bouchet hypothesis." Geophys. Res. Lett., 43, 10277 – 10285.

Kim, H., and Kaluarachchi, J. J. (2017a). "Estimating evapotranspiration using the complementary relationship and the Budyko framework." J. of Water and Climate, doi:10.2166/wcc.2017.148.

Kim, H., and Kaluarachchi, J. J. (2017b). "Complementary relationship for estimating evapotranspiration using the Granger-Gray model: Improvements and comparison with a remote sensing method." Hydrol. Earth Syst. Sci. Discuss., http://doi.org/10.5194/hess-2017-346.

Koster, R. D., Gou, Z., Dirmeyer, P. A., Bonan, G., Chan, E., Cox, P., Davies, H., Gordon, C. T., Kanae, S., Kowalczyk, E., Lawrence, D., Liu, P., Lu, C. H., Malyshev, S., McAvaney, B., Mitchell, K., Mocko, D., Oki, T., Oleson, K., Pitman, A., Sud, Y. C., Taylor, C. M., Verseghy, D., Vasic, R., Xue, Y., and Yamada, T. (2006). "GLACE: The Global Land-Atmosphere Coupling Experiment. Part I: Overview." J. Hydrometeor., 7, 590-610.

Kahler, D. M., and Brutsaert, W. (2006). "Complementary relationship between daily evaporation in the environment and pan evaporation." Water Resources Research, 42, W05413.

Li, D., Pan, M., Cong, Z., Zhang, L., and Wood, E. (2013). "Vegetation control on water and energy balance within the Budyko framework." Water Resour. Res., 49, 969-976.

Lloyd-Huges, B., and Saunders, M. A. (2002). "A drought climatology for Europe." Int. J. Climatol., 22, 1571 – 1592.

McKee, T. B., Doesken, N. J., and Kleist, J. (1993). "The relationship of drought frequency and duration to time scales." Preprints, Eight Conf. on Applied Climatology, Anaheim, CA, Amer. Meteor. Soc., 179 – 184.

Morton, F. I. (1983). "Operational estimates of areal evapotranspiration and their significance to the science and practice of hydrology." J. Hydrol., 66, 1-76.

Mu, Q., Zhao, M., and Running, S. W. (2007). "Development of a global evapotranspiration algorithm based on MODIS and global meteorological data." Remote Sens. Environ., 111(4), 519-536.

Mu, Q., Zhao, M., and Running, S. W. (2011). "Improvements to a MODIS global terrestrial evapotranspiration algorithm." Remote Sens. Environ., 115, 1781-1800.

Palmer, W. C. (1965). "Meteorological drought." U.S. Weather Bureau Research Paper 45, 58.

Patel, N. R., Chopra, P., and Dadhwal, V. K. (2007). "Analysing spatial patterns of meteorological drought using standardized precipitation index." Meteor. Appl., 14, 329 – 336.

Penman, H. L. (1948). "Natural evaporation from open water, bare and grass." Proceedings of the Royal Society A: Mathematical, Physical and Engineering Sciences, 193(1032), 120-145.

Priestley, C. H. B., and Taylor, R. J. (1972). "On the assessment of surface heat fluxes and evaporation using large-scale parameters." Monthly Weather Rev. 100, 81-92.

Potop, V. (2011). "Evolution of drought severity and its impact on corn in the Republic of Moldova." Theor. Appl. Climatol., 105, 469 – 483.

Rebetze, M., Mayer, H., Dupont, O., Schindler, D., Gartner, K., Kropp, J. P., and Menzel, A. (2006). "Heat and drought 2003 in Europe: A climate synthesis." Ann. For. Sci., 63, 569 – 577.

Redmond, K. T. (2002). "The depiction of drought." Bull. Amer. Meteor. Soc., 83, 1143 – 1147.

Seeley, M. (2014). *Weather, climate change, and impacts in Minnesota, Morris Ara Climate Dialogue,* Jefferson Center and IATP, Morris, Minnesota.

Senay, G. B., Bohms, S., Singh, R. K., Gowda, P. H., Velpuri, N.M., Alemu, H., and Verdin, J.P. (2013). "Operational evapotranspiration mapping using remote sensing and weather datasets: A new parameterization for the SSEB approach." Journal of the American Water Resources Association 49, 577–591.

Sims, A. P., Dutta, D., Nigoyi, S., and Raman, S. (2002). "Adopting drought indices for estimating soil moisture: A North Carolina case study." Geophys. Res. Lett., 29, 1183.

Sohn, S. J., Ahn, J. B., and Tam, C. Y. (2013). "Six month-lead downscaling prediction of winter to spring drought in South Korea based on a multiple ensemble." Geophys. Res. Lett., 40, 579 – 583.

Svoboda, M., LeComte, D., Hayes, M., Heim, R., Gleason, K., Angel, J., Rippey, B., Tinker, R., Palecki, M., Stooksbury, D., Miskus, D., and Stephens, S. (2002). "The drought monitor." Bull. Amer. Meteor. Soc., 83, 1181-1190.

Szilagyi, J., and Jozsa, J. (2008). "New findings about the complementary relationship

based evaporation estimation methods." J. Hydrol., 354, 171-186.

Thompson, S. E., Harman, C. J., Konings, A. G., Sivapalan, M., Neal, A., and Troch, P. A. (2011). "Comparative hydrology across AmeriFlux sites: The variable roles of climate, vegetation, and groundwater." Water Resour. Res., 47.

Vicente-Serrano, S. M., Cuadrat-Prats, J. M., and Romo, A. (2006). "Early prediction of crop production using drought indices at different time-scales and remote sensing data: Application in the Ebro Valley (north-east Spain)." Int. J. Remote Sens., 27, 511 – 518.

Vicento-Serrano, S. M., Begueria, S., and Lopez-Moreno, J. I. (2010). "A multiscalar drought index sensitive to global warming: The Standardized Precipitation Evapotranspiration Index." J. Climate, 23, 1696 – 1718.

Weber, L., and Nkemdirim, L. C. (1998). "The Palmer Drought Severity Index revised." Geogr. Ann., 80A, 153 – 172.

Wells, N., Goddard, S., and Hayes, M. J. (2004). "A self-calibrating Palmer Drought Severity Index." Journal of Climate, 17, 2335 – 2351.

Wilhite, D. A. (1993). "Drought assessment, management, and planning: theory and case studies." Natural Resource Management and Policy Series, 2, Kluwer, 293.

Yu, M., Li, G., Hayes, M. J., Svoboda, M., and Heim, R. R. (2013). "Are droughts becoming more frequent or severe in China based on the Standardized Precipitation Evapotranspiration Index:1951-2010." Int. J. Climatol.

Table 4-1. Drought classes of USDM and corresponding threshold value for classifying drought with PDSI, SPI and EWDI. All indices data from 2001 to 2015 were collected.

Drought condition	USDM	PSDI	SPI	EWDI
Abnormally dry	D0	-1.0	-0.5	-0.5
Moderate drought	D1	-2.0	-0.8	-0.8
Severe drought	D2	-3.0	-1.3	-1.3
Extreme drought	D3	-4.0	-1.6	-1.6
Exceptional drought	D4	-5.0 >	-2.0 >	-2.0 >

Table 4-2. Correlation coefficient between EWDI-*ndvi* and USDM, precipitation and temperature for seven selected US States.

	California (CA)	Nevada (NV)	Utah (UT)	Texas (TX)	Wisconsin (WI)	Michigan (MI)	Illinois (IN)
Correlation coefficient, r	0.72	0.73	0.76	0.66	0.64	0.59	0.57
Precipitation (mm/month)	46	20	30	61	71	73	96
Temperature (˚C)	15	10	9	19	7	7	11

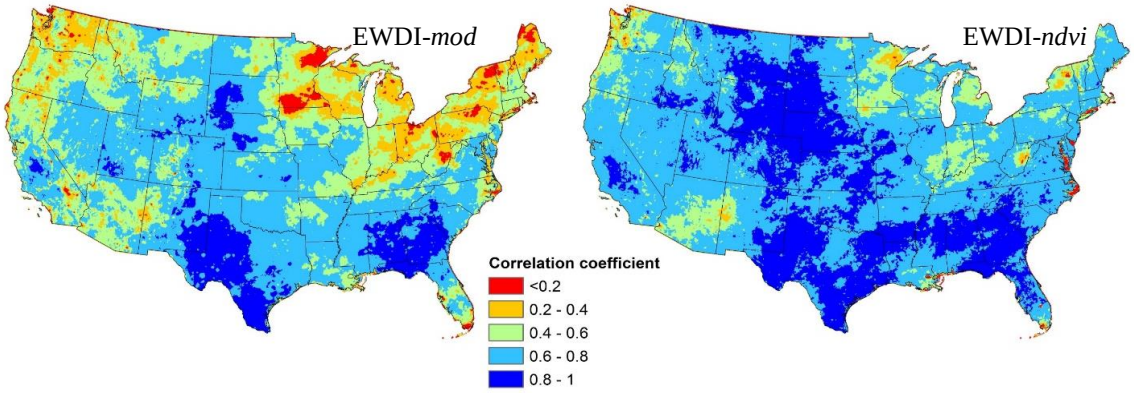

Figure 4-1. Correlation coefficient between EWDI-*mod* and EWDI-*ndvi* and USDM. EWDI-*mod* represents EWDI using the modified GG (Anayah and Kaluarachchi, 2014) and EWDI-*ndvi* represents EWDI using GG-NDVI (Kim and Kaluarachchi, 2017b). The area-averaged correlation coefficient over all pixels for EWDI-*mod* and EWDI-*ndvi* is 0.58 and 0.72.

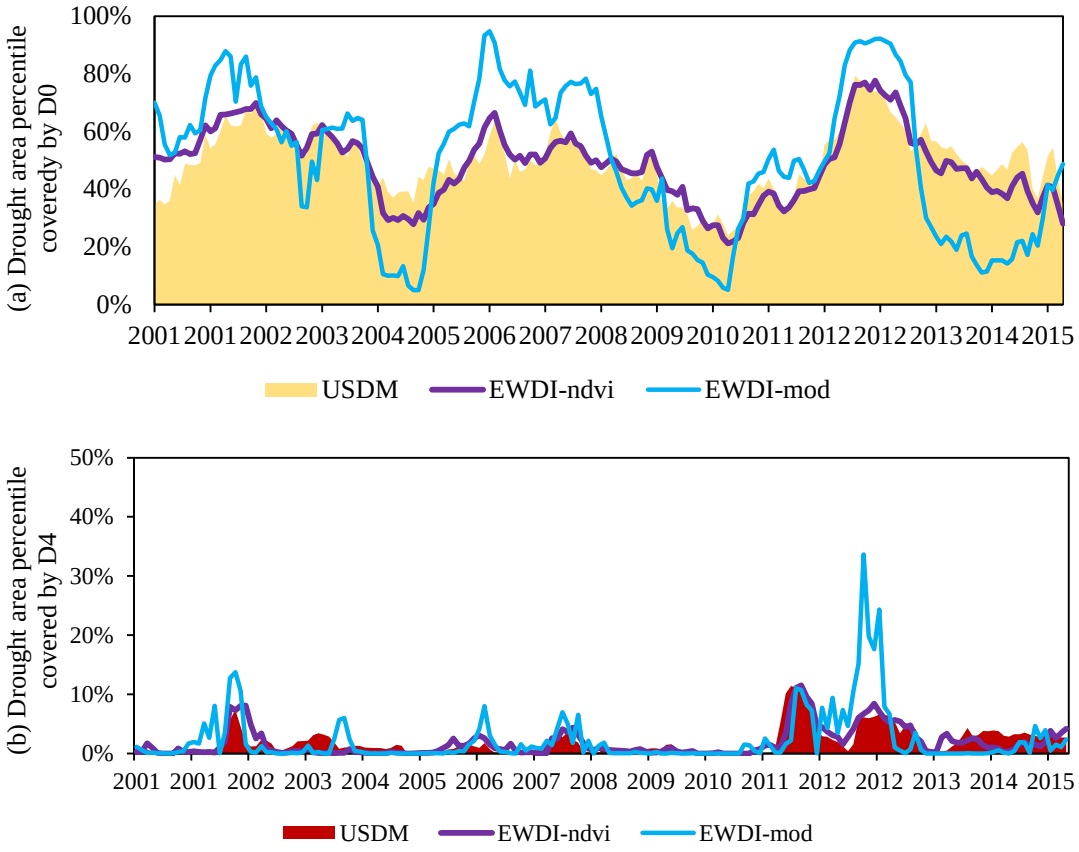

Figure 4-2. Percent area of CONUS (a) covered by D0 (abnormally dry) and (b) covered by D4 (exceptional drought) from 2001 to 2015.

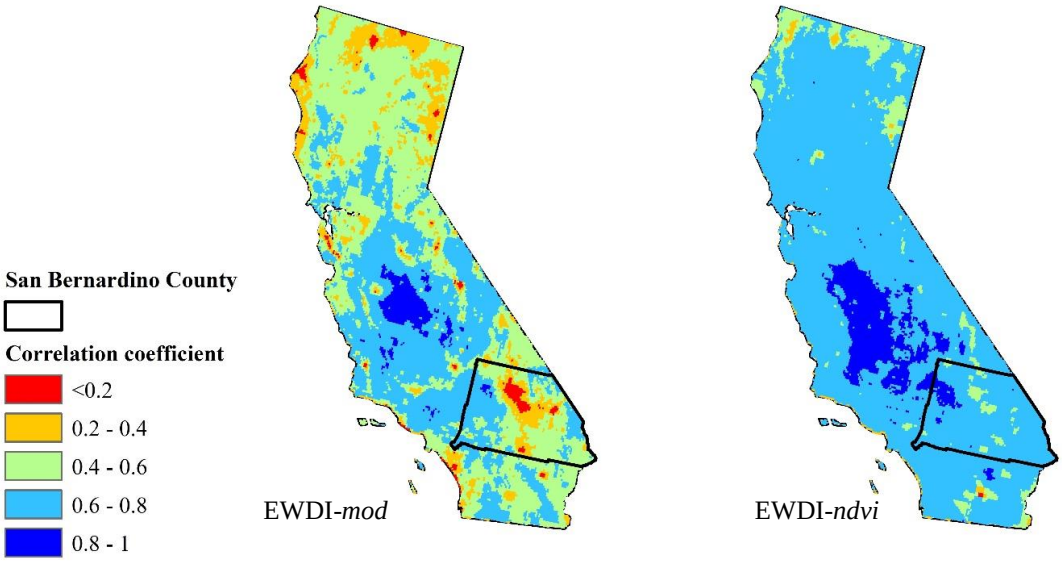

Figure 4-3. Correlation coefficient between EWDI-*mod* and EWDI-*ndvi* and USDM for California and San Bernardino County, CA.

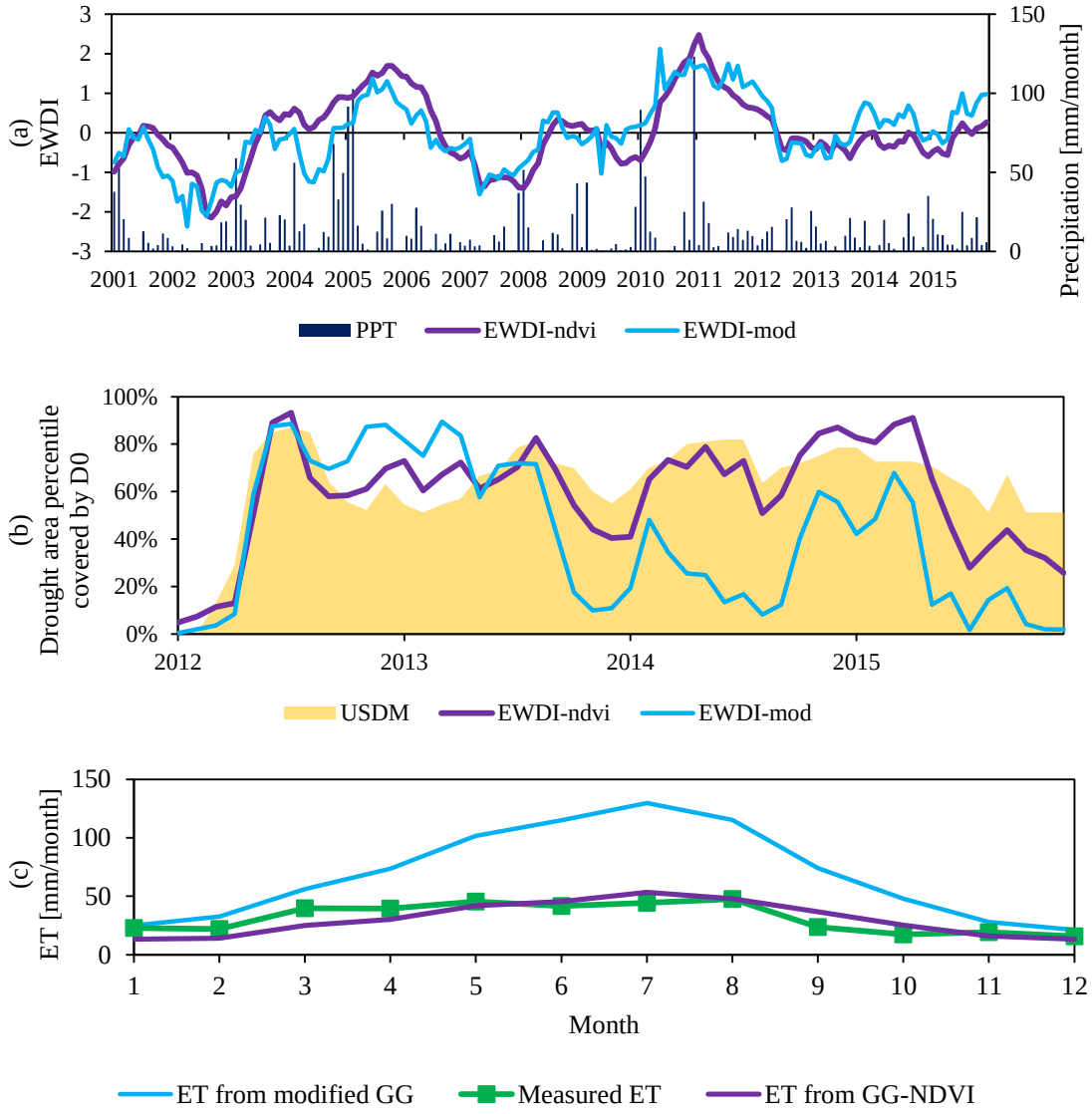

Figure 4-4. (a) Monthly time-series of EWDI-*mod*, EWDI-*ndvi*, and precipitation area-averaged over the San Bernardino county from 2001 to 2015, (b) percent area of San Bernardino County covered by D0, and (c) monthly estimated ET values from modified GG and GG-NDVI and mean monthly observed ET values from 2012 to 2015.

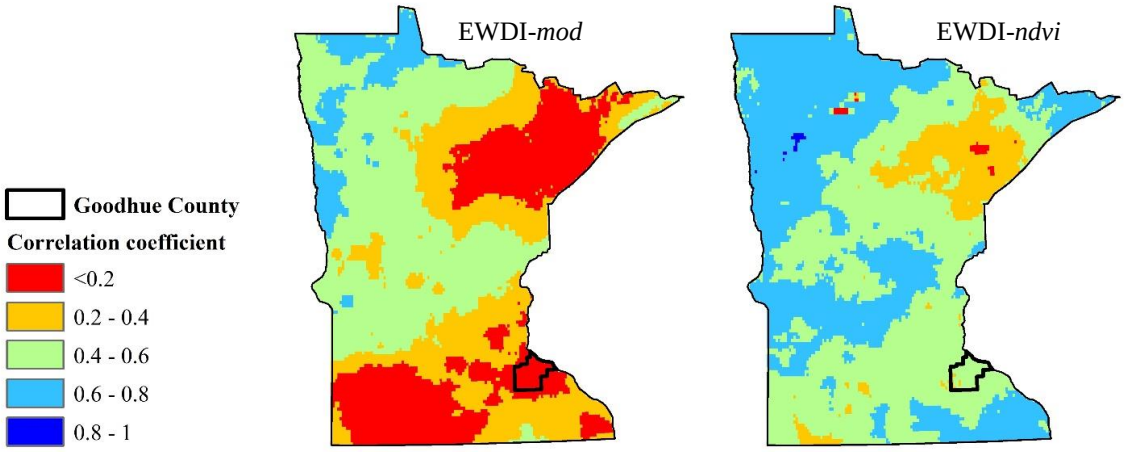

Figure 4-5. Correlation coefficient between EWDI-*mod* and EWDI-*ndvi* and USDM for Minnesota and Goodhue County, MN.

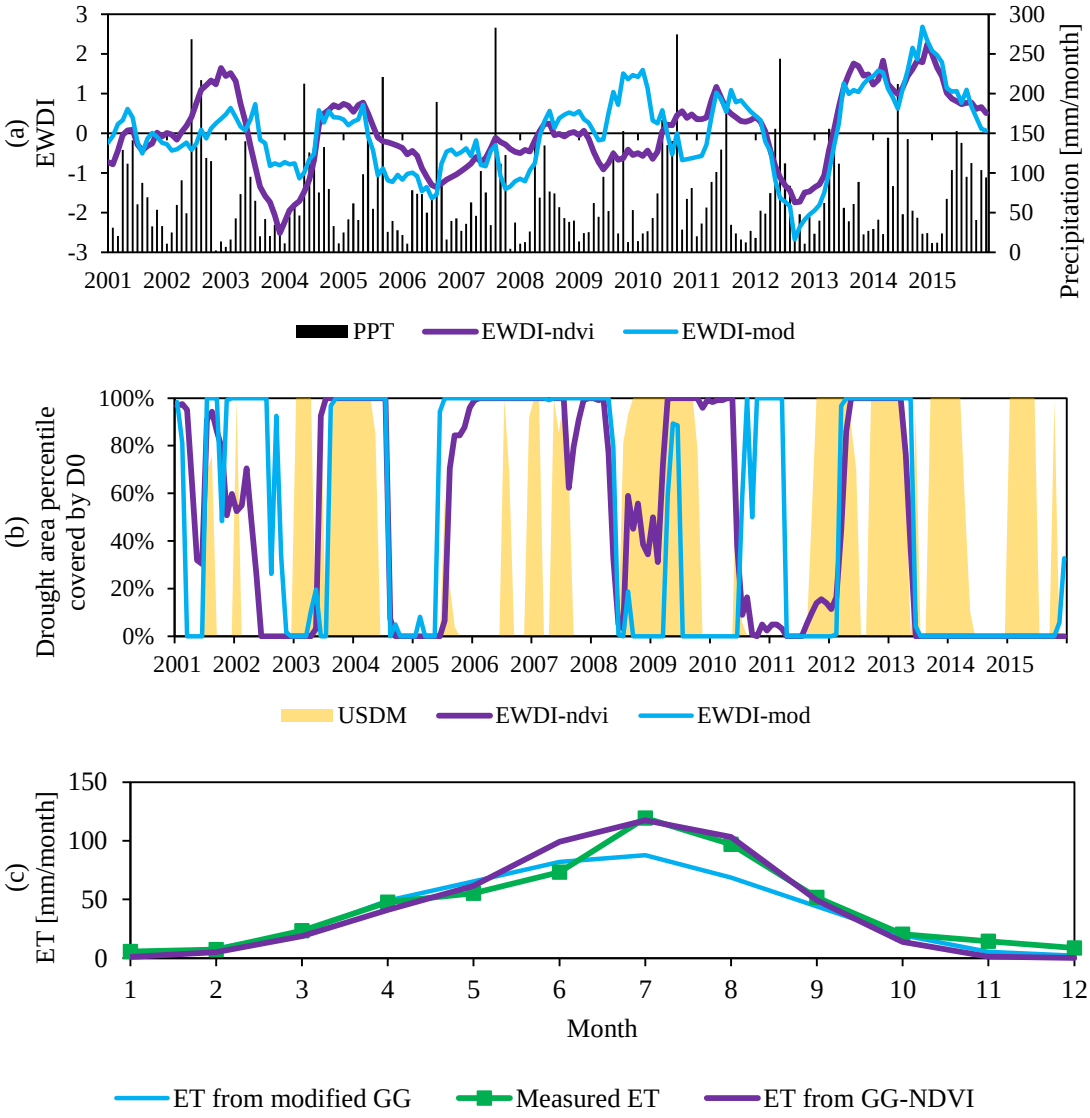

Figure 4-6. (a) Monthly time-series of EWDI-*mod*, EWDI-*ndvi*, and precipitation area-averaged over the Goodhue County from 2001 to 2015, (b) percent area of Goodhue county covered by D0, and (c) mean monthly estimated ET values from modified GG and GG-NDVI and mean monthly observed ET values from 2012 to 2015.

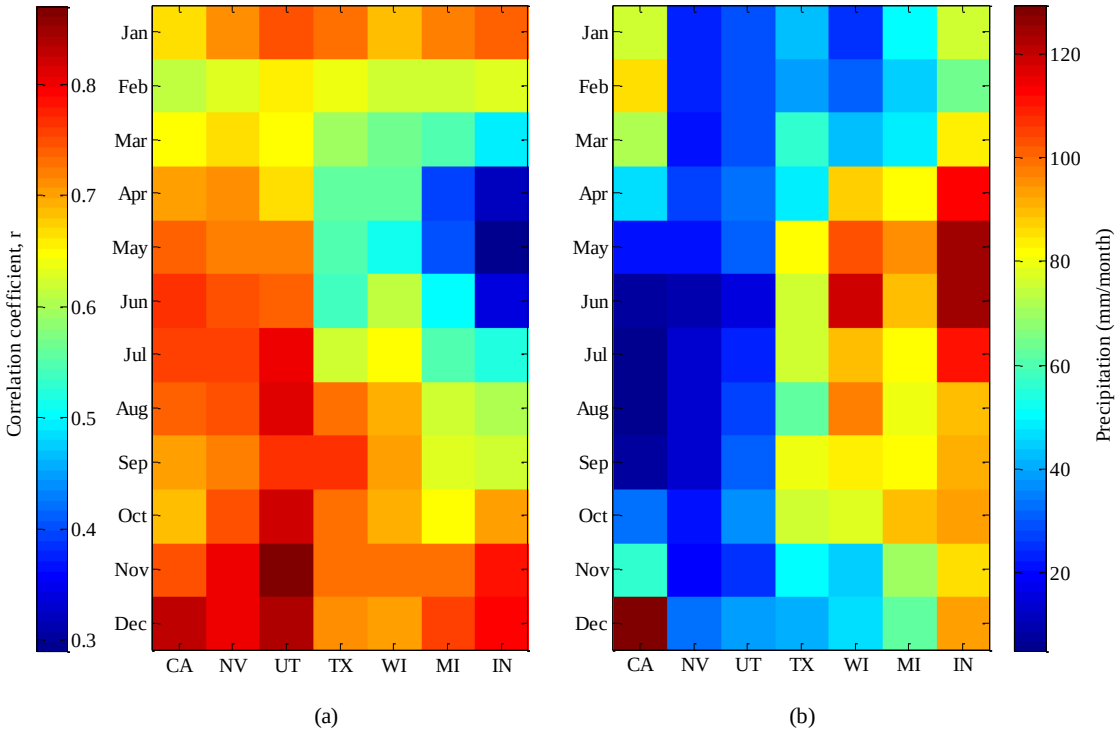

Figure 4-7. (a) Monthly correlations coefficient between EWDI-*ndvi* and USDM and (b) monthly precipitation for seven selected states calculated at each grid point for 2001 to 2015 and then averaged over the state.

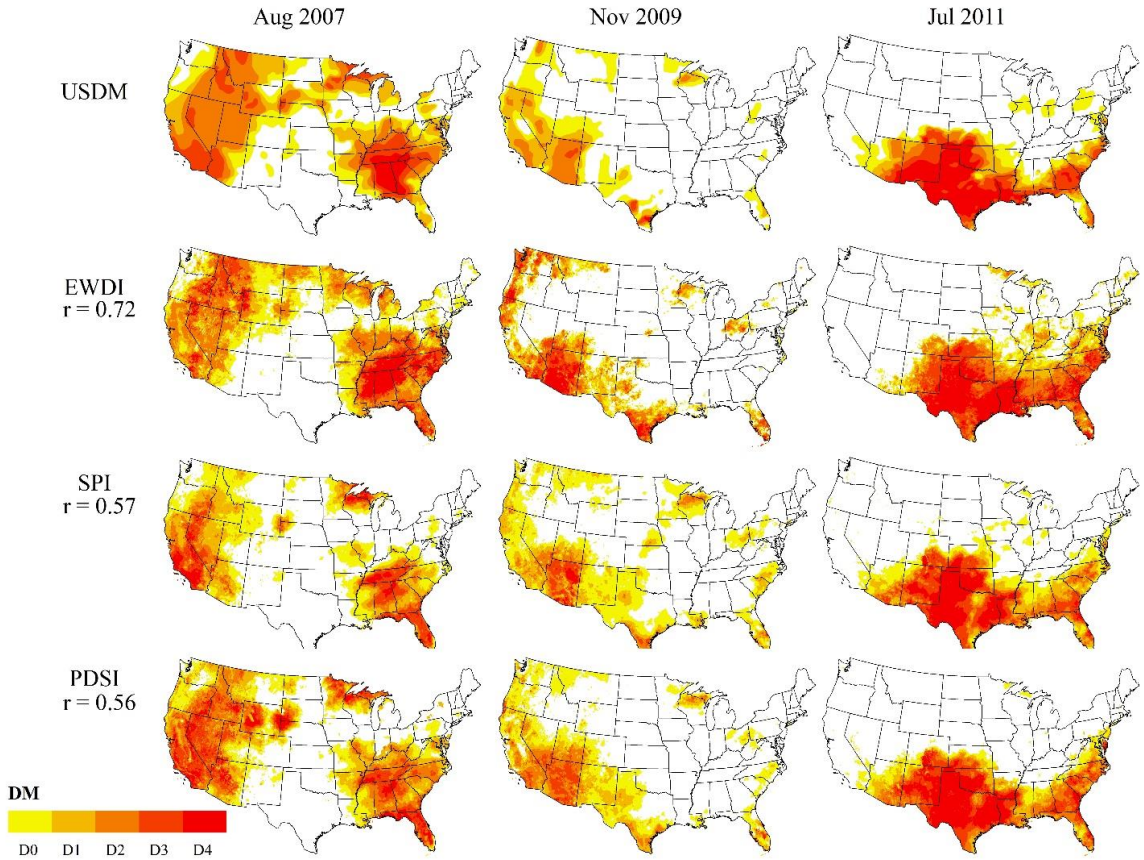

Figure 4-8. Spatial distributions of USDM, EWDI, SPI, and PDSI results for major drought months in the CONUS. The quantity of r shown in figure means the correlation coefficient with USDM from 2001 to 2015.

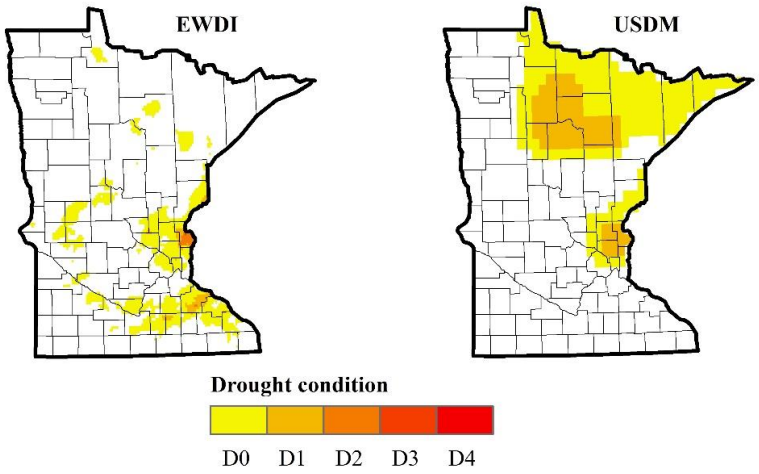

Figure 4-9. Drought conditions of EWDI (left) and USDM (right) in November 2009 for Minnesota.

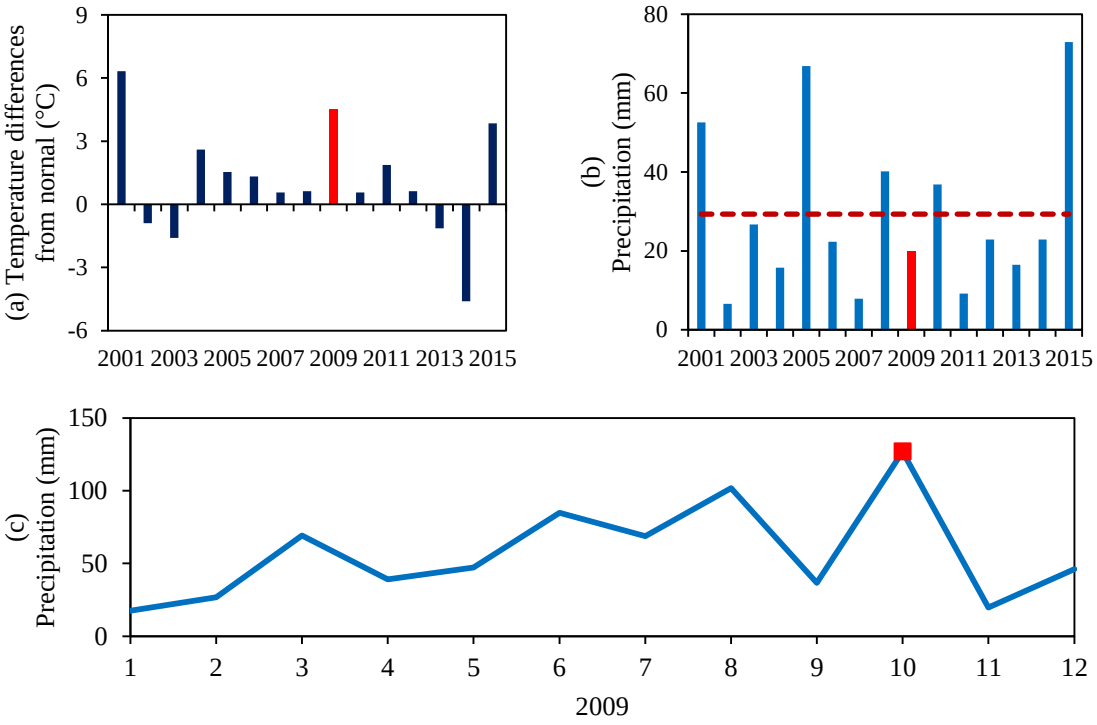

Figure 4-10. (a) Temperature deviations from normal in November, (b) monthly average precipitation in November from 2001 to 2015, and (c) Monthly time-series of precipitation for 2009 for Northern Minnesota.

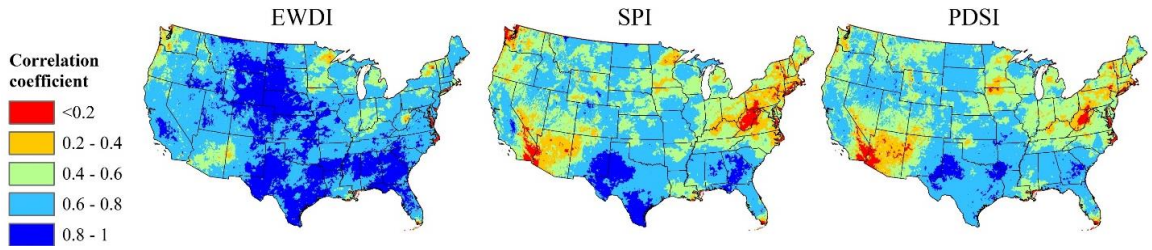

Figure 4-11. Correlation coefficient between USDM and three drought indices: EWDI, SPI, and PDSI.

CHAPTER 5

SUMMARY AND CONCLUSIONS

Summary and conclusions

This dissertation proposed an improved version of the Granger and Gray (1989) using both the complementary relationship and the Budyko framework in Chapter 2. Then, existing limitation of the complementary relationship was identified by comparing remote sensing ET product in Chapter 3. Lastly, the applicability of using accurate ET model as a drought index was addressed in Chapter 4.

In Chapter 2, the modified GG model developed by Anayah and Kaluarachchi (2014) was refined by using the Budyko framework based on the study of Li et al. (2013). The relative evaporation parameter in the original GG model was derived from limited sites under wet conditions in Canada (Granger and Gray, 1989). To overcome this limitation, the Fu equation (Li et al., 2013) was used instead of the relative evaporation parameter on the basis that the Fu equation can support the complementary relationship (Zhang et al., 2004; Yang et al., 2006). This chapter used 75 AmeriFlux eddy covariance tower sites in the United States to retrieve required meteorological data including precipitation. Also, NDVI were from the MODIS Land Subsets. 75 sites were divided into dry and wet climate conditions based on an aridity index from UNEP (Barrow, 1992). The proposed model, denoted as GG-NDVI, showed much lower RMSE in both dry and wet sites compared to the modified GG model (Anayah and Kaluarachchi, 2014), Mu et al. (2011), Han et al. (2011, 2012).

The study in Chapter 3 provided an inherent limitation of the complementary

relationship and validation through a direct comparison with the SSEBop (Operational Simplified Surface Energy Balance, Senay et al., 2013). The SSEBop ET data set retrieved from the USGS Geo Data Portal for the period 2000-2007 covering the United States and 60 AmeriFlux stations were used for validation of ET results from SSEBop and GG-NDVI. The results showed that GG-NDVI can produce similar or better accuracy than SSEBop. More importantly, this study observed that the assumption of symmetric complementary relationship was a deficiency in GG-NDVI that produced poor results under certain condition. Under the symmetric complementary relationship, ET is close to ETW with increasing humidity, but natural surfaces even in the wettest regions will not approach saturation. Therefore, this study proposed a nonlinear correction function to the GG-NDVI to better describe the complementary relationship. This correction function improved the GG-NDVI model significantly especially, under conditions of high humidity and dense vegetation.

In Chapter 4, ET calculated from the latest version of GG-NDVI, denoted as Adjusted GG-NDVI, used to estimate drought conditions across the United State for the period of 2001 to 2015. The proposed drought index, EWDI, was calculated by using the difference between ETW and ET with the probability distribution function of Abramowitz and Stegun (1965) because this probabilistic approach allowed a consistent comparison between EWDI against other standardized indices. Also, the drought severity of EWDI was divided into five classes that is the same classes with the U.S. Drought Monitor (USDM). Required meteorological data were from the PRISM at 4-km resolution covering the CONUS and monthly NDVI data were retrieved from the NASA Earth Observations. The results of this chapter supported that the EWDI could capture

drought conditions and using an accurate ET model can help to improve drought monitoring performance. One unanticipated finding was that within the complementary relationship when energy-limited conditions are present, ET and ETW varied in a parallel trend and ET is closer to ETW, resulting in decreasing EWDI performances such as Minnesota. Despite this limitation, EWDI could identify droughts over CONUS consistent with USDM from the major drought incidents of August 2007, November 2009, and July 2011. It can also potentially use for identifying wildfire risk and future studies will be needed.

Overall, the present dissertation makes several noteworthy contributions to develop ET method. The specific contributions will be as follows:

- ✓ This work is the first study to apply the vegetation cover to the complementary relationship with the Budyko framework. Generally, the complementary relationship showed a regular and periodic ET behavior and is influenced by the principles of the complementary relationship. The complementary relationship assumes a homogeneous surface which assumes a complete mixing of the effects of diverse surface conditions. Thus, the vegetation cover in the complementary relationship plays a role in the fluctuation of estimated ET similar to the observed ET. We, therefore, believe that the Budyko framework provided a significant contribution to improving the performance of the complementary relationship.
- ✓ It was expected that GG-NDVI is a simple and a reliable approach for the prediction of ET since it does not require a calibration process compared

to the crop coefficients in reference ET method (Allen et al., 1998, 2005) and the multiplying factor in the SSEB model.

- ✓ We found empirical evidence of the validity of the complementary relationship through several studies, but this study is the first study to identify an inherent limitation of the complementary relationship, especially in wet conditions. To overcome this limitation, we provided a robust option for the use of the complementary relationship. This change made a significant contribution to the improvement of GG-NDVI ability to estimate ET under various climatic conditions.
- ✓ It is important to test the reliability of ET products that are used for drought monitoring. According to the proposed comprehensive model evaluation of this study, we demonstrated that the use of ET is a better option for drought conditions than considering reference ET. Moreover, this study provided additional evidence with respect to that using land surface information has a large impact on drought monitoring compared to other drought indices. More importantly, the advantage of using GG-NDVI is that it can comprehensively consider both effects of precipitation and vegetation cover. Taken together, this dissertation has extended our knowledge of ET to support water resource management and risk management.

Literature Cited

Abramowitz, M., and Stegun, I. A. (1965). *Handbook of Mathematical Functions, with*

Formulas, Graphs, and Mathematical Tables, National Bureau of Standards Applied Mathematics Series, Washington, D.C.

Anayah, F. M., and Kaluarachchi, J. J. (2014). "Improving the complementary methods to estimate evapotranspiration under diverse climatic and physical conditions." Hydrology and Earth System Sciences, 18, 2049-2064.

Barrow, C. J. (1992). *World atlas of desertification (United Nations Environment Programme)*, edited by N. Middleton and D. S. G. Thomas. Edward Arnold, London.

Granger, R. J., and Gray, D. M. (1989). "Evaporation from natural nonsaturated surface." J. Hydrol., 111, 21-29.

Han, S., Hu, H., and Yang, D. (2011). "A complementary relationship evaporation model referring to the Granger model and the advection-aridity model." Hydrol. Processes, 25(13), 2094–2101.

Han, S., Hu, H., and Tian, F. (2012). "A nonlinear function approach for the normalized complementary relationship evaporation model." Hydrol. Processes, 26(26), 3973–3981.

Li, D., Pan, M., Cong, Z., Zhang, L., and Wood, E. (2013). "Vegetation control on water and energy balance within the Budyko framework." Water Resour. Res., 49, 969-976.

Mu, Q., Zhao, M., and Running, S. W. (2011). "Improvements to a MODIS global terrestrial evapotranspiration algorithm." Remote Sens. Environ., 115, 1781-1800.

Senay, G. B., Bohms, S., Singh, R. K., Gowda, P. H., Velpuri, N.M., Alemu, H., and Verdin, J.P. (2013). "Operational evapotranspiration mapping using remote

sensing and weather datasets: A new parameterization for the SSEB approach." Journal of the American Water Resources Association 49, 577–591.

Yang, D., Sun, F., Liu, Z., Cong, Z., and Lei, Z. (2006). "Interpreting the complementary relationship in non-humid environments based on the Budyko and Penman hypotheses." Geophysical Research Letters, 33, L18402.

Zhang, L., Hickel, K., Dawes, W. R., Chiew, F. H. S., Western, A. W., and Briggs P. R. (2004). "A rational function approach for estimating mean annual evapotranspiration." Water Resour. Res., 40, 02502.

APPENDICES

CURRICULUM VITAE

HOMIN KIM

(September 2017)

Education

Ph.D., Civil and Environmental Engineering, 2017

Utah State University, Logan, Utah, USA

Advisor: Dr. Jagath J. Kaluarachchi

M.Sc., Civil Engineering, 2008

University of Seoul, Seoul, South Korea

Advisor: Dr. Yongjun Cho

B.Sc., Civil Engineering, 2006

University of Seoul, Seoul, South Korea

Professional Experience

Graduate Research Assistant (Jan, 2013 – present), Department of Civil and Environmental Engineering, Utah State University, Logan, Utah

Assistant Manager (Aug, 2010 – Aug, 2011), Department of Coastal Research Institute, Sekwang Engineering Consultants, Seoul, South Korea.

Graduate Research Assistant (Mar, 2006 – July, 2010), Department of Civil Engineering, University of Seoul, Seoul, South Korea

Teaching Experiences

Teaching Assistant, Groundwater Engineering, Fall 2015, Utah State University

Lecturer, Basin Fluid Mechanics, Spring 2008 – Fall 2010, University of Seoul

Publications

Kim, H, and Kaluarachchi, J. J., 2017. Complementary relationship for estimating evapotranspiration using the Granger-Gray model: Improvements and comparison with a remote sensing method, Hydrolo. Earth Syst. Sci. Discuss, http://doi.org/10.5194/hess-2017-346.

Kim, H., and Kaluarachchi, J. J., 2017. Estimating evapotranspiration using the complementary relationship and the Budyko framework, Journal of Water and Climate Change, doi:10.2166/wcc.2017.148.

Cho, Y., and Kim, H., 2008. On the hydraulic characteristics of efficient long wave energy Absorber-Eco-Breaker 2. Journal of the Korean Society of Civil Engineers, 28, 5B.

Presentations at professional meetings

Presentations

Kim, H., and Kaluarachchi, J. J., 2017. Estimating drought conditions across the United States using and evapotranspiration-based Drought Index, presented at Student Research Symposium, Utah State University Research Week Showcase, Logan, Utah.

Kim, H., and Kaluarachchi, J. J., 2016. Evaluating and enhancing the complementary relationship to estimate evapotranspiration with a remote sensing method, presented at the December 2016 Graduate Virtual Poster Showcase, AGU showcase, Washington, DC.

Kim, H., and Cho, Y., 2010. Development of FLB – Flexible Floating Breaker-As effective suppressor of frequently occurring waves, Conference of the Korean Association of Ocean Science and Technology Societies, KAOSTS, South Korea.

Posters

Kim, H., and Kaluarachchi, J. J., 2015. Application of the Budyko framework and the complementary relationship to estimate evapotranspiration, AGU Fall Meeting, San Francisco, CA, 2015.

Kim, H., Lim, C., Kim, M., and Cho, Y., 2007. Development of long period waves energy absorber, Proceeding of the 33th KSCE Annual Conference, Korean Society of Civil Engineers, South Korea.

Affiliations

American Geophysical Union (since 2014)

American Water Resources Association (since 2017)

Licenses

EIT, passed the Fundamentals of Engineering Civil Exam, Utah Division of Occupational and professional Licensing, July, 2017.

Civil Engineer, issued on June 2006, by Human Resources Development Service, South Korea.

Awards and Scholarship

Research and Graduate Studies Travel Award, Utah State University, 2015

College of Engineering Travel Grants, Utah State University, 2015

Hi-Seoul Scholarship Fellowship, 2008-2009.